UNIVERSITÀ DEGLI STUDI DI UDINE
hic sunt futura

www.uniud.it

Doctor of Philosophy in:

"ENVIRONMENTAL AND ENERGY ENGINEERING SCIENCE"

XXXI Cycle

Title of the thesis

"Development of sustainable methodologies for homogeneous gold catalysis"

Mattia Gatto

Prof. Daniele Zuccaccia - Supervisor
Prof. Alessandro Del Zotto - Co-supervisor

Anno 2019

List of abbreviations

X	general counterion
BAr^{F-}	tetrakis(pentafluorophenyl)borate
BF_4^-	tetrafluoroborate
SbF_6^-	hexafluoroantimonate
NTf_2^-	bis(trifluoromethanesulfonyl)imide
OAc^-	acetate
OTf^-	trifluoromethanesulfonate
OTs^-	p-toluenesulfonate
TFA^-	trifluoroacetate
ClO_4^-	perchlorate
PTC	Phase Transfer Catalyst
NBu_4OTf	tetra-butylammonium trifluoromethanesulfonate
[BMIM]OTf	1-butyl-3-methylimidazolium trifluoromethanesulfonate
Aliquat-OTf	tri-octylmathylammonium trifluoromethanesulfonate
$(Bu_2)NH_2OTf$	di-butylammonium trifluoromethanesulfonate
$(Me_2)(Et)(Dec)NOTf$	dodecylethyldimethylammonium trifluoromethanesulfonate
ε_r	dielectric costant
DMF	dimethylformamide
DMPU	N,N'-dimethylpropyleneurea
GVL	γ-valerolactone
MIBK	methylisobutylketone
DMSO	dimethylsulfoxide
DMU	N,N'-dimehtylurea
chOTf	choline trifluoromethanesulfonate
PC	propylenecarbonate
NM	nitromethane
Cit.ac.	citric acid
SDS	aodium dodecylsoulfate
L	general ligand
NAC	Nitrogen Acyclic Carben, wen not otherwise specified it is referring to bis(tert-butylamino)methylidene
NHC	Nitrogen Heterocyclic Carben
NHC^{iPr}	1,3-bis(2,6-di-isopropyl-phenyl)imidazol-2-ylidene
NHC^{CH2}	1,3-bis(2,6-di-isopropyl-phenyl)dihydroimidazol-2-ylidene
BIAN	bis(imino)acenaphtene
JPhos	2-(di-tert-butylphosphino)biphenyl
$(RO)_3P$	tris(2,4-ditert-butylphenyl) phosphite
PAr^F	tris(3,5-bis(trifluoromethyl)phenyl) phosphine
PPh_3	triphenylphosphine
PCy_3	tri-cyclohexyl phosphine
THT	tetrahydrothiophene
TOF	turnover frequency
TON	turnover number
EMY	Effective Mass Yield
E-factor	Environmental factor
VOS	Volatile Organic Solvent
GS	Green Solvent
IL	Ionic Liquid
DES	Deep Eutectic Solvent
KIE	Kinetic Isotopic Effect
RDS	Rate-Determining Step
DFT	Density Functional Theory
NOE	Nuclear Overhauser Effect
PGSE	Pulsed-field Gradient Spin Echo
DOSY	Diffusion order spectroscopy

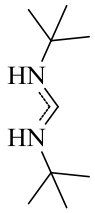

NAC

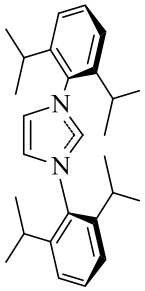

NHC^{iPr}

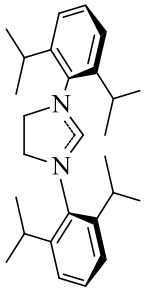

NHC^{CH2}

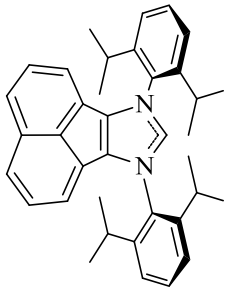

BIAN

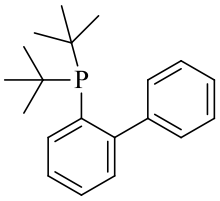

JPhos

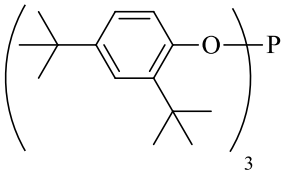

$(RO)_3P$

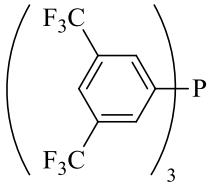

PArF

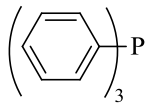

PPh_3

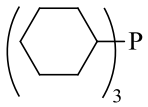

PCy_3

THT

Abstract

In the last two decades, homogeneous gold(I) catalysis has become a useful tool for chemical transformation of organic compounds, and great efforts have been made in the understandings of the catalytic cycle and other variables like structure of the catalyst, nature of the ligand, effect of the additives, etc. Even if a large number of information on the ligand effects is present in the literature on homogeneous gold catalysis, the engineering of new L-Au-X catalysts and reactions is still based on trial and error, sometimes with an unpredictable outcome. Recently, it appears that the anion has an active participation in each single step of the catalysis and this depends both on its nature (co-ordination ability and basicity) and position. Surely, the effect of the anion also depends on the type of reaction as well as the RDS of the catalytic cycle. In this thesis, thanks to a complete rationalization of the counterion effect, resulting from experimental and theoretical studies, highly efficient sustainable methodologies have been developed. Thus, reactions can be conveniently run at room or mild temperature, using neoteric solvents or working in solvent-, silver-, and acid-free conditions. The main reactions studied were the hydration and alkoxylation of alkynes, that generally require large amounts of acidic additives and/or high temperature. Here is reported for the first time an innovative and green method for carrying out these reactions. Lastly, this work demonstrates that the interplay between the ligand, the counterion, the additive and the solvent is crucial in order to obtain good results in terms of efficiency of the reaction.

Summary

In the last few years, the chemistry of gold is reborn following the development of homogeneous catalysts showing outstanding activity in numerous transformations involving the activation of carbon-carbon π-systems towards the nucleophilic attack of a large variety of nucleophiles. Gold shows high alkynophilicity and a notable part of research has been focused on the exploration of the mechanism and kinetic of alkyne activation on the metal center. Although there is plenty informations about the ligand effects on homogeneous gold catalysis, there is still a "trial and error" approach in the development of new [L-Au-X] catalysts for the reactions, and the outcome is often unpredictable and unsatisfactory. This is mainly due to the underestimation of the effect of the nature of the anion X^-. The mechanistic understanding of all the single steps in the nucleophilic addition of water or alcohols to a co-ordinate alkyne, when gold(I) complexes are used as catalysts, is the main focus of this thesis.

In chapter 2.1 are presented and discussed the results of the study of the hydration of alkynes. A green and sustainable protocol for this reaction promoted by NHC gold catalysts, in solvent-, silver-, and acid-free conditions at room temperature has been developed. In optimized conditions, it is possible to strongly reduce the catalyst loading, thus obtaining a very low E-factor and high Effective Mass Yield. Furthermore, it was possible to separate the reaction product by distillation, thanks to the solvent-free condition, obtaining the product with high purity. In addition, it was possible to reuse the catalytic system.

The study of the hydration of 3-hexyne was then extended trying to improve the activity of the [L-Au-X] catalysts by changing the nature of the ligand L (from phosphine to NAC and NHC), and the results of this investigation are reported in chapter 2.2. The generation in-situ of the pre-catalyst, using silver salts as chlorine scavenger, did not appear as a good strategy owing to the negative influence of silver on the reaction. A screening of ionic additives was also made and the best conditions were used for the hydration of deactivated diphenylacetylene.

In chapter 2.3 are presented the results of an investigation focused on the use of neoteric solvents in the alkoxylation and hydration of alkynes, using gold(I) complexes with NHC as ligand and OTf^- as counterion. Relatively to the formation of ion pairs, a good correlation was found between the dielectric constant of the solvent and the Turnover Frequency (TOF). The solvents having suitable functional groups, which show hydrogen bond property and a right basicity, could help the reaction in the crucial steps of the catalytic cycle (nucleophilic attach and proton shuttle). Conversely, those possessing high dielectric constant or able to co-ordinate to the metal center, were found to decrease the reaction rate. γ-Valerolactone was found the most promising solvent and it was explored in the hydration of diphenylacetylene.

This deep study on counterion, ligand, additives, and solvent effects in homogeneous gold(I) catalysis, based on both experimental and computational studies, allowed us to develop for the first time a green and sustainable methodology for the hydration of alkynes. This study opens new directions to better understand and rationalize the mechanism in homogeneous gold catalysis. At the same time, it has been demonstrated that the 12 principles of green chemistry could be fruitfully introduced in gold(I) catalyzed organic reactions.

Index

1

Introduction

1.1. General aspects

Gold is a precious metal and for centuries has interested humanity due to its shiny color and physical characteristics that gave it importance, more than other metals, for the creating of ornamental objects, from the ancients to more recent times. Due to its high resistance to corrosion, it is possible to find very old historical artefacts; in fact in a recent discovery in Bulgaria,[1] a gold ring was found dating from the middle copper age, around 4500-4650 BC. More famous were all the Greek and Central-South American populations who worked this metal, creating ornamental objects. Gold also became a unit measure in the monetary system, it started war[2] and provoked intense mining during the discovery of America. It has been estimated that 186,000 tons of gold had already been mined by 2015 and world consumption is divided into 50% in jewelry, 40% in investments and only 10% in industry.[3] The quantity of gold mined is equal to a cube with 21-meter sides.

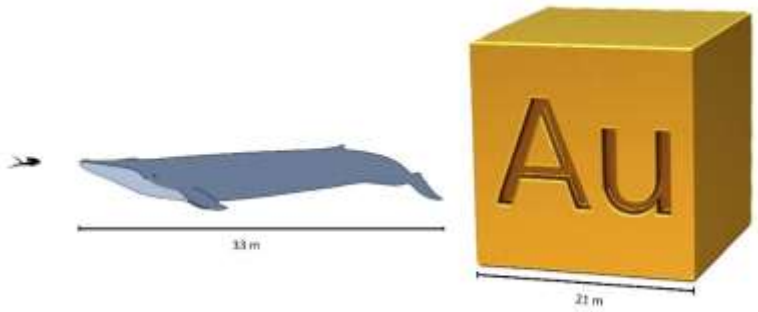

***Figure 1**: Comparison between the gold mined, a blue whale and a human*

In the last century, it was discovered that it has peculiar physical properties and it has been used in electronic engineering. The first application in medicine was in dental surgery but the idea started to grow that gold has high potential for other biomedical applications. Kean et al.[4] documented the use of gold in ancient medicine by shamans or alchemists, from the first Chinese document in 2550 BC to the more recent discovery of Dr. Jacques Forestier in 1929, who tested gold as an anti-arthritic and opened the door to using gold in medicine even as an anticancer agent.[5]

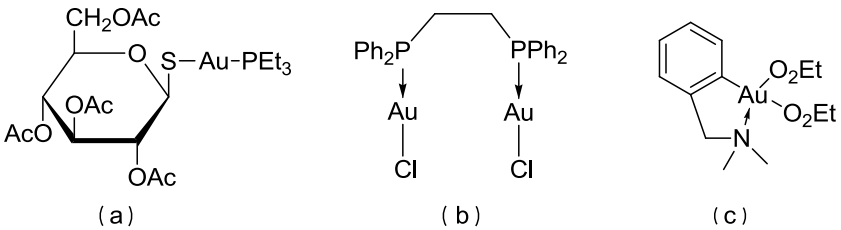

***Figure 2**: Structure of (a) gold(I) "auranofin" use for rheumatoid arthritis (b) anticancer gold(I) di-phosphine complex (c) antitumor and antibacterial gold (III) N-C complex*

From a chemical point of view, gold was continuously studied in stoichiometric chemistry and wasn't expanded in catalysis perhaps because the false belief in the inertness of the metal that is highly resistant to

acid attack and dissolves only in aqua regia or strong ligands such as cyanide, discouraged the scientific community. The second reason for a low interest in gold is that, in comparison with other precious metals used in catalysis, this metal has a high value (**Figure 3**) and was thus probably considered not suitable to be employed in catalysis. But even if gold is expensive, we have to bear in mind that the cost of the catalyst is often dominated by the price of the ligand rather than by the metal center.[6]

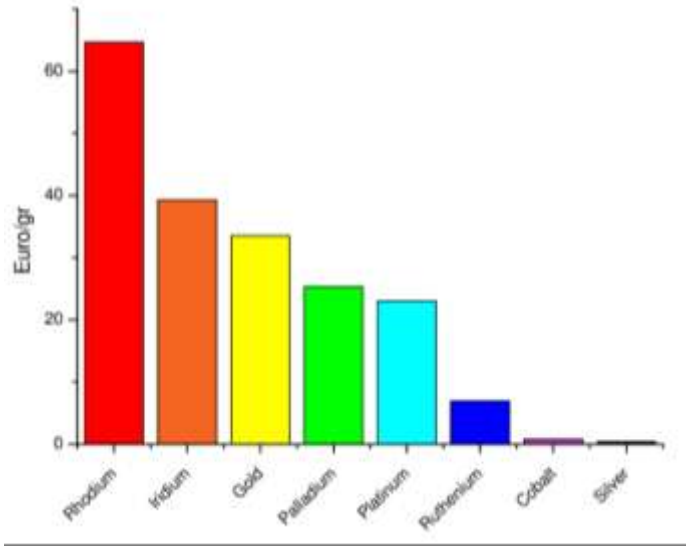

***Figure 3**: Costs of precious metals (Euro/gram)[7]*

The first hint that gold could be used in a catalytic process was discovered by Bond and Sermon[8,9], in the 1970s. This was the first example of the application of heterogeneous gold catalysis in the reaction of hydrogenation of alkenes and alkynes using gold nanoparticles supported on silica. Heterogeneous gold catalysis later found applications in industry for oxidation on carbon monoxide and hydrochlorination of ethyne to vinyl chloride (**Scheme 1**) at low temperature, replacing the more dangerous mercury catalyst.[10]

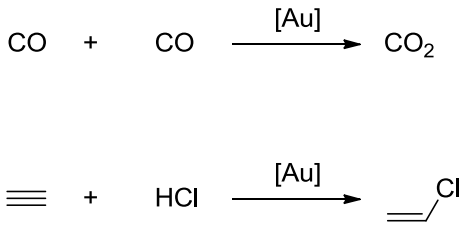

***Scheme 1**: Reaction catalysed by heterogeneous gold catalyst*

The activity of gold encouraged the scientific community to apply it in homogeneous catalysis, due to its good air-, moisture- and oxygen-tolerance. Gold acts as a Lewis acid toward C-C π-bonds, activating unsaturated bonds to nucleophilic attack.

A Lewis acid can be described as "any species with a reactive vacant orbital or available lowest unoccupied molecular orbital", which means that the frontier orbital of a compound (metal) controls the activation of

substrates rich in electrons. The structural aspect of the bonding between a metal and a π-system can be expressed by the Dewar-Chatt-Duncanson model (**Figure 4**).[11]

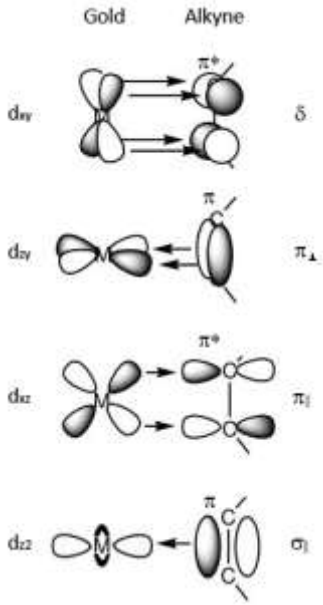

***Figure 4**: Orbital diagram shows interaction between the gold metal center and the alkyne*

Gold is a transition metal of the 11th group with the atomic number 79, it's electronic configuration is [Xe] $4f^{14}$ $5d^{10}$ $6s^1$ and the main oxidation states are Au(I) (d^{10}) and Au(III) (d^8). As shown in **Figure 4**, the σ bond is formed with the overlap of the π-bond of the ligand with an empty d orbital of the metal with the right symmetry, there is also the back-donation from a full d-orbital of the metal to an anti-bonding π* orbital of the alkene or alkyne. It also has to take into account the relativistic effect present in gold complexes.

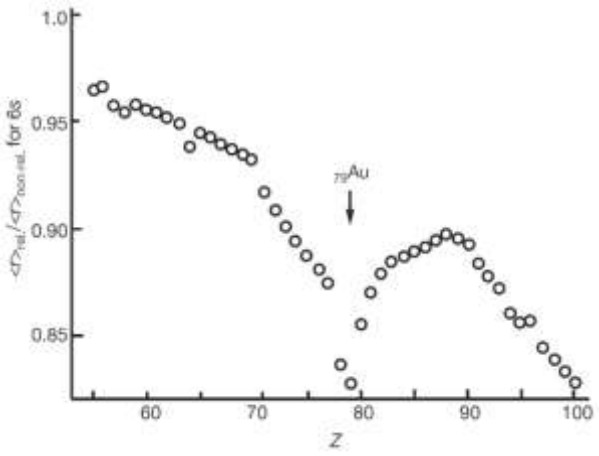

***Figure 5**: Calculated relativistic contraction of the 6s orbital*

This particular property occurs with the increasing of the atomic number (protons), so the more shielding orbitals are contracted to the nucleus, bringing the electrons speed to approximately the speed of light, so relativistic effects have to be taken into account. The direct results are: i) stabilization of orbital energies, thanks to the contraction of s and p orbitals, with a direct consequence that the electrons closer to the

nucleus gain a greater ionization energy, ii) the electrons in d and f orbitals have a weaker nuclear attraction, due to the shielding of contracted s and p orbitals, so the expansion of those orbitals leads to a destabilization of their energy and iii) spin-orbit splitting. For gold(I) indeed there is a contraction of the 6s orbital that stabilizes energetically (decreasing energy values for LUMO) and an expansion of 5d orbital that destabilizes energetically (increasing energy value of HOMO).

Gold(I) complexes have the electronic configuration of [Xe] $4f^{14}$ $5d^{10}$ $6s^{0}$ with a linear geometry (L-Au-X).[12] In line with Pearson's "*Hard and Soft Acids and Bases*" (HSAB),[13] gold(I) is classified as a soft acid and easily bonds with soft bases, so the main ligands present in the literature are carbenes, phosphines, thiolates, thioesthers and selenates.[14] Last but not least, it is important to mention that gold presents "aurophilicity", i.e. the strong interaction between gold atoms, a peculiar property that does not follow the classic bonding theory.[15]

1.2. Gold in catalysis

Gold catalysis has been studied since the 1970s when Bond and Sermon[8,9] identified the activity of gold in the reaction of halogenation of alkenes in heterogeneous catalysis and after that the idea of using gold as a catalyst started to grow. In the past 30 years a lot of papers have been published using heterogeneous gold but it has only been used as homogeneous catalyst in the last 18 years.

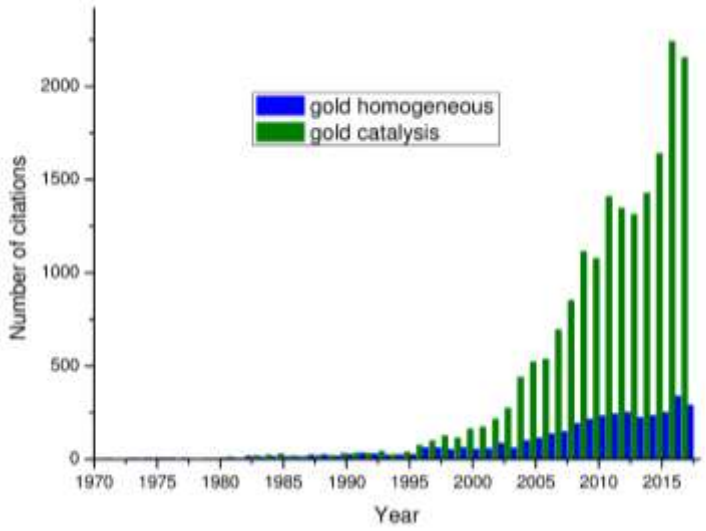

***Figure 6**: Number of citations using Web of Science as search engine*

As shown in **Figure 6**, the scientific community has increased its attention on heterogeneous gold but there are still few studies on homogeneous catalysis with respect to the total citations on gold catalysis.

The most common activity for gold complexes is as a Lewis acid for the activation of C-C multiple bonds (alkyne, alkenes, allenes, etc.), possible for its peculiar properties, described in the previous section. Even if

the substrate and the nucleophile can differ, the catalytic cycle for gold(I) can be represented in a similar way and the reaction proceeds through an inner-sphere or outer-sphere mechanism.[16]

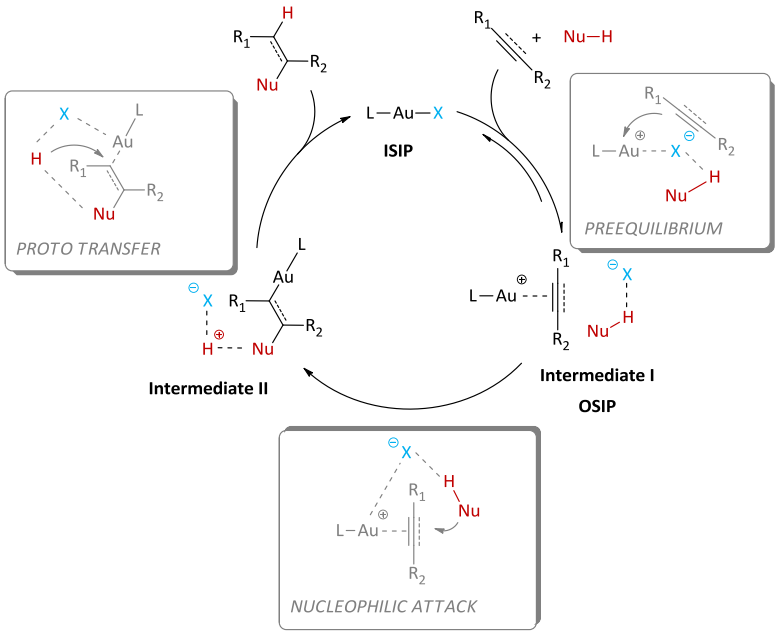

***Figure 7**: General mechanism for gold catalysis*

Using a general gold catalyst L-Au-X, where L is a ligand (phosphine, carbene, etc.) and X is the anion (TFA^-, OTf^-, BF_4^-, etc.), there is a pre-equilibrium where the substrate co-ordinates with the metal generating a η^2 complex (**Figure 7** , **Intermediate I**). At this stage the gold complex acts like a Lewis acid activating the substrate and, in the presence of a nucleophile (Nu-H), a nucleophilic attack can occur, generating an organo-compound with a σ-bond Au-C (**Figure 7**, **Intermediate II**). In the presence of protons, proto-deauration occur, with release of the product and regeneration of the pre-catalyst.

During the last 20 years, various efforts were made to understand the mechanism and optimize the catalysis, changing ligand, anion and catalytic conditions.

1.2.1. Ligand effect in homogeneous gold(I) catalysis

In 1991 Fukuda and Utimoto[17] first reported the use of sodium tetrachloroaurate for the hydration and methoxylation of different terminal alkynes, using 2% of catalyst with respect to the substrate. The disadvantage of this reaction was the rapid death of the catalyst, turning gold(III) into reduced metallic gold that is inactive for this reaction.

Teles et al.[18] raised attention on the more stable phosphine gold(I) species, which were tested for the reaction of methoxylation of 1-propyne (**Scheme 2**) that provided the expected Markovnikov addition to the triple bond.

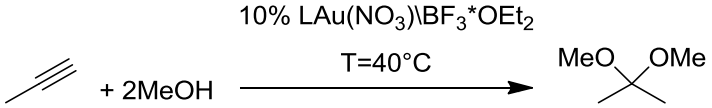

***Scheme 2**: methoxilation of 1-propyne*

The parameter used to understand the activity of the reaction was the Turn Over Frequency (TOF, h^{-1}) and the influence of the ligand was very prominent for this reaction: $P(OPh)_3$ (1500) > $P(OMe)_3$ (1200) > $P(4\text{-}F\text{-}C_6H_4)_3$ (640) > PPh_3 (610) > PEt_3 (550) > $AsPh_3$ (430). The activity was inversely correlated to the Lewis basicity of the ligand: the more electron-poor ligand gave the best TOF results but decreased the stability. In fact, for $P(OPh)_3$ there was full deactivation after 2500 TON while its homologous PPh_3 catalyst was working even over 5000 TON. Tanaka et al.[19] and Schmidbaur et al.[20] tested the efficiency of phosphine gold(I) complexes, underlining the importance of using additives for preservation of the catalyst and using different anions to obtain higher TOF. In 2012 Hammond et al.[21] published a paper on the ligand effect and ligand design in homogeneous gold(I) catalysis. They took different reactions testing a group of phosphino-gold(I) complexes, finding that there is no universal ligand that works better than others, but a clear understanding of the ligand effect allowed the design of suitable ligands for each reaction. This study explained: i) the electrophilic activation of alkynes promoted by the electron-deficient ligand, ii) the protodeauration promoted by electron-donating ligand and iii) the deactivation of the catalyst after co-ordination of the substrate or deactivation of the catalyst after protodeauration that is related to the nature of the ligand.

In 2003 Hermann et al.[22] first used a NHC gold(I) acetate complex as catalyst for hydration reaction.

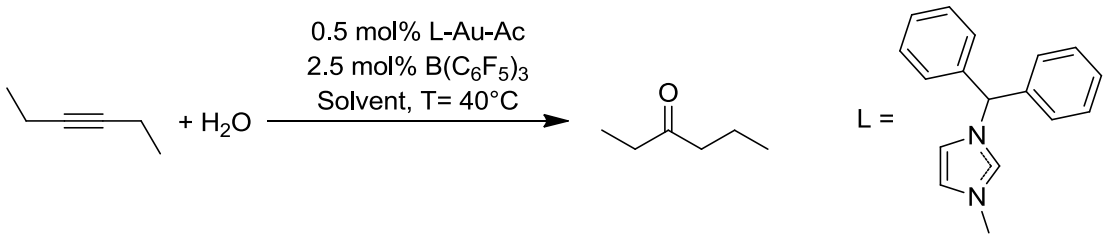

***Scheme 3**: hydration of alkynes using a nitrogen heterocyclic carbene as ligand*

The reaction was run in the presence of solvent, showing the best activity using tetrahydrofurane instead of methanol. The NHC gold(I) chloride species was completely inactive for this reaction, and the presence of a Lewis acid was necessary in order to increase the TON and TOF values, but no full conversion was obtained. The most remarkable result was achieved by Nolan and co-workers,[23] when the hydration of alkyne was conducted at 120 °C in a mixture of dioxane\water or methanol\water. They generated the active species *in situ* with silver tetrafluoroborate and tested many gold complexes with different NHC, finding that the best result was obtained using a gold complex bearing NHC^{iPr} as ligand. That allowed them to operate with a catalyst loading between 0.1 and 0.001% with respect to the substrate, obtaining an impressive result for homogeneous gold catalysis that usually works from 5 to 1% of catalyst loading.

Gold complexes are also active for the addition of other heteroatoms to unsaturated substrates.[24] The first evidence was found by Utimoto et al. in 1987[25] when they were able to obtain an intramolecular hydroamination of alkyne using gold(III).

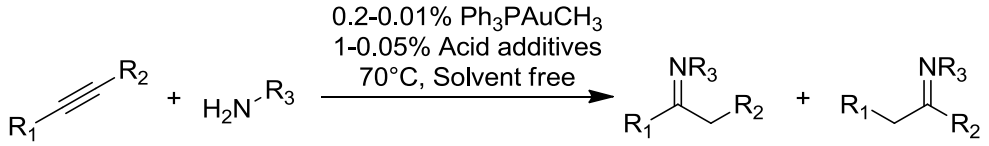

***Scheme 4**: intramolecular hydroamination of alkyne using gold (III)*

In 2003 Tanaka et al.,[26] using the catalyst proposed by Teles et al. for the hydration reaction of alkynes, developed the hydroamination reaction of alkynes using acidic additives to promote the reaction (**Scheme 4**). They found that with a polyoxometallated salt it was possible to achieve complete conversion, at low catalyst loading and in neat condition.

A real breakthrough in this reaction was made by Bertrand et al.,[27] who used a new series of cyclic alkyl amino carbene (CAAC) for the hydroamination reaction of alkynes.

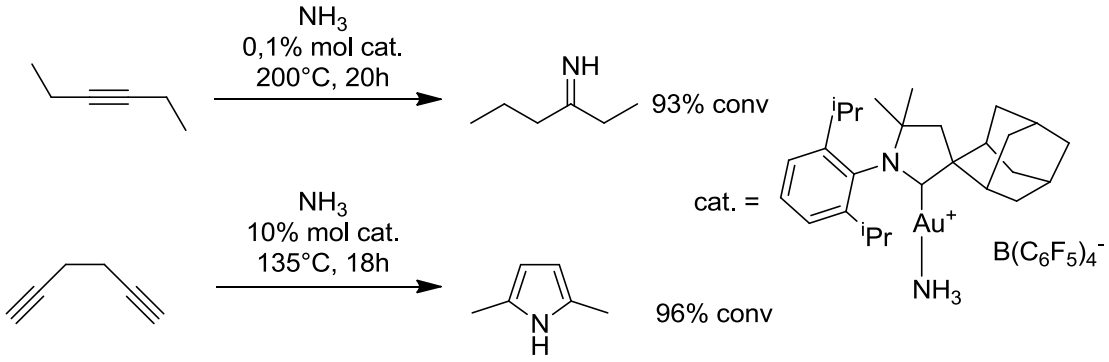

***Scheme 5**: reaction of hydroamination of alkynes*

The reaction was performed in NMR tubes with deuterated benzene, the temperature was kept from 160 to 200 °C, with catalyst loading 5 to 0.1% with respect to the substrate, obtaining almost full conversion with

the exception of the chlorine complex. The catalyst was also active for the hydroamination of both terminal and internal alkynes, with multiple triple bond, giving the possibility of a tandem hydroamination/cyclization with the formation of heterocycles. The reaction was also tested for allenes, obtaining a mono-, di- or tri-substituted amine product, and this was possible changing the molar ratio between catalyst and ammonia. The results highlighted the possibility that gold(I) complexes work even for non-activated alkynes or allenes.

1.2.2. Anion effect in homogeneous gold(I) catalysis

Not only the ligand but also the anion influences the activity of gold in catalysis, so it is important to take this into consideration. In fact, a lot of gold complexes are active in catalysis after halide extraction by silver salt, and show different behavior in the activity of reactions depending on the nature of the anion. In the optimization of gold catalysis 86% of studies focus just on the design of the ligand or optimization of the catalytic system (temperature, solvents, catalyst loading). The remaining 14% are focused on the anion.

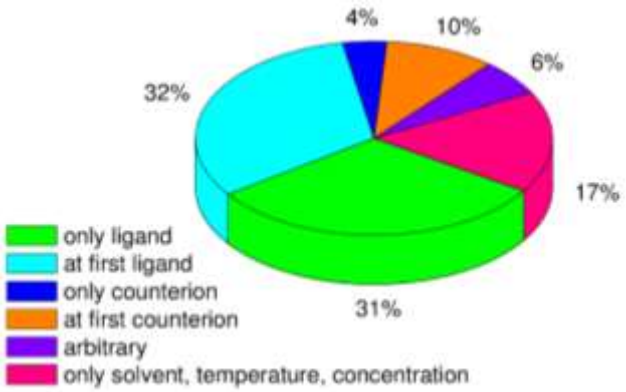

Figure 8: *Subdivision in % of the research topic on gold catalysis*

In the first uses of gold as catalyst, in particular gold(III), only $NaAuCl_4$ or $HAuCl_4$ was used but after 2002, anions different from chloride were tested with success, giving more active species. As a general trend, during optimization of the reaction parameters, monoanionic and differently co-ordinating counterions are generated by using halide scavengers based on silver salts. However, in many cases a co-catalysis by silver-based contaminants is present, proving active participation in the reaction.[28] The "silver effect" on gold(I) catalysis was also discussed in a study by Shi and co-workers in 2012.[29]

In 2006 Brouwer and He,[30] showed how anions gave different activity in the reaction of hydroamination of 1,3-dienes.

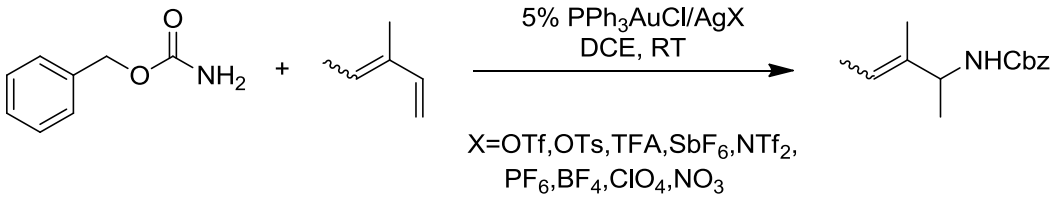

Scheme 6*: reaction of hydroamination of 1,3-dienes*

The full conversion was achieved with low co-ordinating anions (OTf^-, ClO_4^-) and no product formation was observed for other anions (Cl^-, OTs^-, NO_3^- and CF_3COO^-) due to their high affinity to gold(I) ion. The co-ordination abilities of these anions were calculated[31] and measured[32] years later, confirming the co-ordination order found by Brouwer and He.

Anna Homs et al. [33] found an anion influence even for the [2+2]cycloaddition reaction of alkynes with alkenes, developing a new methodology using NHC^{iPr} or JPhos as the ligand.

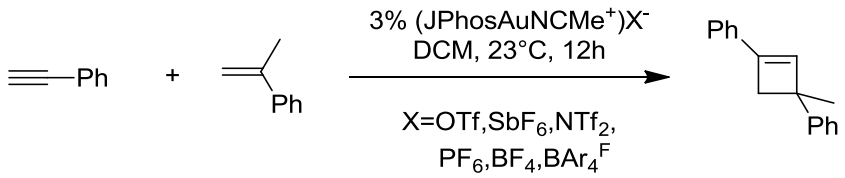

***Scheme 7**: reaction of [2+2]cycloaddition of alkynes with alkenes*

The activity was greater with JPhos, so it was taken as primary ligand. A strong anion influence was noticed, with an increase of 10-30% in the yield of the products when SbF_6^- and BAr^{F-} are used. With kinetic and theoretical calculations, they were able to explain that the determining step is the first ligand exchange (proprionitrile), forming the active η^2-species that is more stable with non co-ordinating counterions.

In the intramolecular hydroamination of allenes, Toste et al.[34] designed a different dinuclear gold(I) phosphine complex. Despite the ligand employed, this work showed that the use of achiral anions with different size and with different electron-withdrawing group, changed the catalytic activity in terms of yield and enantiomeric excess.

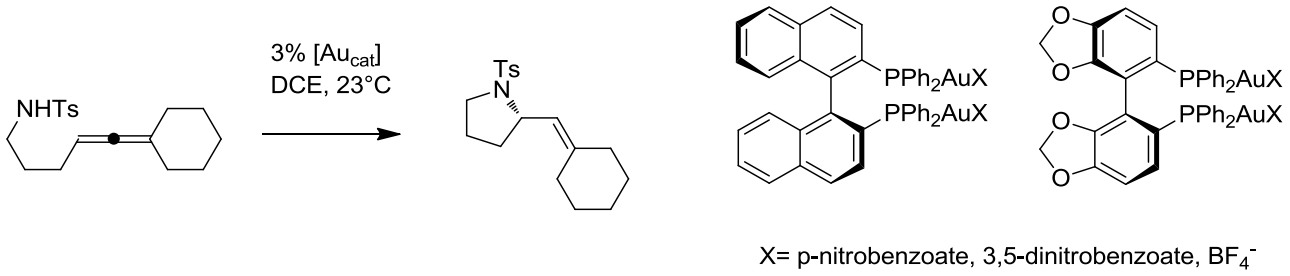

***Scheme 8:** reaction of intramolecular hydroamination of allenes*

Li et al.[35] studied cycloisomerization of bromoallenyl ketones by 1,3-Br migration. The mechanism was followed also by DFT calculations and it was found that cationic Au(I) bearing low co-ordinating anion, produces prevalently one product by 1,3-Br migration. Contrary with a more co-ordinating anion the mechanism change and no 1,3-Br migration was observed with the formation of another product.

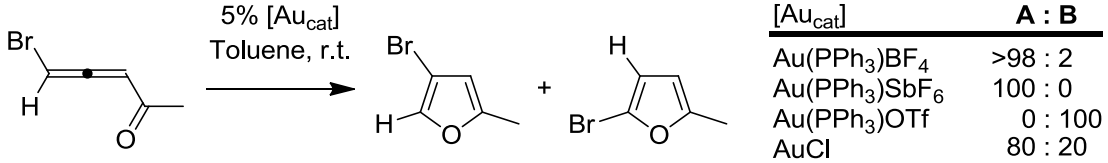

[Au$_{cat}$]	A : B
Au(PPh$_3$)BF$_4$	>98 : 2
Au(PPh$_3$)SbF$_6$	100 : 0
Au(PPh$_3$)OTf	0 : 100
AuCl	80 : 20

***Scheme 9**: cycloisomerization of bromoallenyl ketones*

In 2014 Zuccaccia et al.[36] studied the anion effect in the alkoxylation of alkynes catalyzed by gold(I) catalysts bearing N-heterocyclic carbene ligands (**Scheme 10**). They demonstrated that the anion properties, both

basicity and co-ordination ability, have a notable impact on the catalytic performance of gold complexes, and the commonly used non-co-ordinating anions (such as SbF_6^- and BF_4^-) may not be the best choice in some cases.

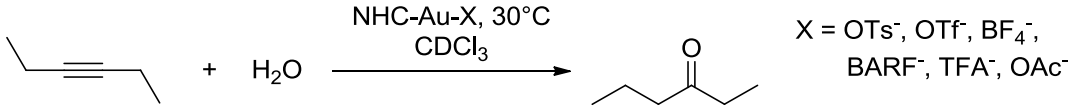

***Scheme 10**: reaction of alkoxylation\hydration of alkynes using NHC-Au-X as catalyst*

For this reaction, the right balance between basicity and co-ordinating ability of the anion OTs^- gives the best result: the pre-equilibrium with this anion is shifted towards the OSIP, its basicity promotes the nucleophilic attack (see **Figure 7**) and the deactivation of catalyst to a gold–methoxide is prevented. The research was extended to testing other ligands for this reaction and also for the cycloisomerization of N-(prop-2-ynyl)benzamide.[37] It was evident that, depending on the substrate, a correct choice of the anion X^- to improve the performances of L-Au-X complexes in catalysis strongly depends on the nature of the ligand and viceversa.

A recent review by Bandini and Jia[38] summarized the importance of the anion for homogeneous gold catalysis. It is largely accepted that weakly co-ordinating anions (i.e., SbF_6^-, OTf^-, $BArF^-$, and BF_4^-) generate more-electrophilic gold centers with consequent stronger metal–π system interactions,[37] more co-ordinating anions can positively affect late-stage catalytic events, such as sequestering the metal center from the catalyst resting state or favoring the frequently occurring protodeauration stage. In addition, basic anions (i.e., benzoates, tosylate, and acetates) can also directly interact with the reaction partners through hydrogen-bond contacts, determining optimal structural geometries for a given transformation or controlling multiple chemo-, regio-, or stereo-selective channels.

Very recently, Hashmi et al.[39] conducted a screening on the reactivity of various gold catalysts with different combination of ligands. The catalytic activity was strongly affected by the counterion, mostly more marked than the corresponding influence of the ligand. It appears clear that the counterion influence is still underestimated in homogeneous gold catalysis and it was pointed out that no general perfect catalyst exists for a specific reaction.

1.3. Green chemistry in gold catalysis

The prevention of environmental pollution is one of the major goal for chemists and during the 1990s many governments enacted laws to prevent or limit the wastes from industries. Within this perspective, in the early 1990s Trost[40] introduced the concept of "Atom Economy" (AE) and years later the scientific community contributed[41] to creating the 12 principles of green chemistry (**Table 1**).[42] Since those principles were created, chemists have been interested in engineering more efficient and environmentally friendly chemical reactions.

Table 1: *The 12 principles of Green Chemistry*

1- Prevent Waste	7- Use Renewable Feedstocks
2- Atom Economy	8- Reduce Derivatives
3- Less Hazardous Synthesis	9- Catalytic rather Stoichiometric Reagents
4- Design Benign Chemicals	10- Design for degradation
5- Benign Solvents & Auxiliaries	11- Real-Time Analysis for pollution Prevention
6- Design for Energy Efficiency	12- Inherently safer processes

The pillar of these principles (**Table 1**) is waste prevention (1), because it is easier to not produce wastes rather than treat or clean up pollution, so it is important to work with substances that are innocuous or with low toxicity (3, 4, 5, 10) wherever possible. Chemicals must be chosen in order to minimize possible accidents (12, e.g. explosion, fire, environmental release) with a real-time monitoring during the reaction (11). The chemical process must be environmentally and economically accessible (6), using renewable feedstocks (7) and all parts of the reaction should be designed for easy degradation (10). Catalytic reactions are energetically favorable with respect to stoichiometric reagents (9) and synthetic methods should be designed to maximize incorporation of all materials used in the process into the final product (2). In order to understand "how green a chemical reaction is" many chemists contributed to writing equations that are now considered as green chemistry metrics.[43]

$$\mathbf{AE} = \frac{\text{mass of desired product}}{\text{mass of all products}} \qquad \mathbf{E\text{-}factor} = \frac{\text{mass of waste}}{\text{mass of desired product}}$$

$$\mathbf{EMY} = \frac{\text{mass of desired product}}{\text{total mass of material used}} \times 100$$

As mentioned before, the AE was introduced by Trost[40] defined as the ratio between the mass of desired product to the total mass generated in the reaction, expressed in percentage. The E-factor, introduced by Sheldon,[44] is the ratio between the mass of total wastes and mass of the desired product. This value also

takes into account the not converted reagent, additive and solvent losses and even the energy needed for the reaction (if data is accessible); water is not included in this equation because it is considered innocuous. The Effective Mass Yield, introduced by Hudlicky et al.[45] represents the ratio between the mass of desired product with respect to all the compounds introduced in the process, with the exception of water, alcohol, acetone, acetic acid and sodium chloride, or compounds that are not considered hazardous wastes. With all of these criteria it is possible to evaluate a chemical process, in order to understand if it is safe and environmentally friendly. If a process does not respect these twelve principles, the reaction conditions must be converted into a better ones.

The use of a catalyst is highly desirable in a green chemistry context; thus, concepts such as Turn-Over Number (TON) and TOF have been shown to be useful in describing the efficiency and sustainability of catalytic reactions. An additional target of green chemistry is to minimize the use of auxiliary substances and to perform the process under mild conditions, possibly at room temperature and without the use of inert atmosphere. In this context, the development of solvent-free reactions has greatly contributed to reducing the environmental impact of chemical processes.[46] In addition, the use of recyclable catalysts can greatly improve the sustainability of the whole process.

However, in the Handbook of Green Chemistry edited by P. T. Anastas,[47] the term 'gold' refers only to heterogeneous/nanoparticle catalysis; there are no examples with gold used for green processes referring to homogeneous gold catalysis.

In fact, thanks to the electronic similarities between gold and mercury, it was possible to slowly replace mercury salts in industrial processes.[48] Mercury was used until the discovery of the well-known toxicity of its compounds, that are responsible for ataxia, hearing and speaking damage and in extreme cases paralysis, coma, insanity and death.[49] The most dramatic case of mercury pollution was called Minamata disease, after the Chisso Minamata industry in Japan released methylmercury into the environment with wastewater, causing the illness of 2265 people with a 79% death rate.[50]

During the last 10 years, gold has become a powerful tool in organic chemistry.[51] However, most of the gold-catalyzed transformations proceed under unsustainable (from a green chemistry point of view) conditions, requiring relatively high catalyst loading (1−5 mol %) and affording low TONs (in the range 20−100). Moreover, the use of volatile organic solvents and/or silver salts as halide scavengers also represents a drawback. To date, protocols describing the use of low catalyst loading, room/low temperature, solvent- and silver-free conditions, and recyclable catalysts are limited.[52] The design of new, efficient and sustainable processes therefore represents a fundamental challenge in the future of gold-based catalysis.

The hydration of alkynes is an important reaction in organic chemistry and is one of the most straightforward and environmentally friendly methods to form a carbon−oxygen bond.[53] This reaction is also noteworthy

from a sustainability standpoint, as it satisfies both carbon efficiency and atom economy rules. For alkyne hydration[54], toxic mercury salts were initially used as catalysts. Many other metals were subsequently tested in order to avoid the use of Hg(II) salts, but Au(III),[55] Pt(II),[56] Ag(I),[57] and Ru(II)[58] were shown to be less efficient. A few years later, an important breakthrough was made by Teles et al., who introduced the use of gold(I) catalysts.[18] Afterward, Tanaka later extended this preliminary work by testing several alkynes, both terminal and internal, and different acids (**Table 2**).[19] TON and TOF values of 1000 and 1000 h^{-1}, respectively, were obtained under optimized conditions (methanol as solvent, 70 °C, 50 mol % of strong Brønsted acid as co-catalyst) using PPh_3-Au^+ as catalyst.[59] E-factor and EMY values were around 22 and 5, respectively. Later on, Nolan was able to further optimize the reaction conditions, reducing the catalyst loading to 10 ppm using 1,4-dioxane, high temperature, and an NHC ligand instead of phosphane (**Table 2**).[23] The decrease of catalyst loading and the use of acid-free conditions were of great eco-friendly impact, but unfortunately, the use of 1,4- dioxane and silver salt combined with high temperature (up to 120 °C) made this effort partially fruitless, with E factor and EMY values of 8 and 15, respectively. Several other papers appeared to deal with the use of both Au(I) and Au(III) catalysts for the hydration of alkynes, but to the best of our knowledge, a complete rationalization and optimization of this reaction using greener conditions is still lacking in the literature.[60] Hu and Wu[61] made a first effort in this direction, performing the hydration of several terminal alkynes at room temperature under both acid- and silver-free conditions (E-factor and EMY were around 17 and 10, respectively). Even though most of their trials were run using methanol as solvent, they succeeded in achieving a conversion of 57% under neat conditions after 24 h using an ionic additive ($KB(C_6F_5)_4$). Unfortunately, the TON and TOF values were both very low, although an appreciable EMY value of 67 was reached (**Table 2**).

Table 2: Principal parameters for hydration of alkynes						
	Tanaka[19]	Nolan[23]	Wu[61]		Li[63]	
Solvent	MeOH	Dioxane	MeOH	***neat***	MeOH	MeOH[a]
TON	***1000***	***84000***	20	11	200	***1200***
TOF (h^{-1})	***1000***	***4500***	1	0.5	10	10
T (C°)	70	120	***RT***	***RT***	120	120
Ag^+ Additives	***NO***	YES	***NO***	***NO***	***NO***	***NO***
H^+ Additives	YES	***NO***	***NO***	***NO***	***NO***	***NO***
Reusable catalysts	NO	NO	NO	NO	***YES***	***YES***
E-factor	22	8	17	5	***2***	***2***
EMY	5	15	10	67	34	35

[a] after 6 recycles

In gold-catalyzed hydration of alkynes the recycling of the catalyst has been poorly investigated.[62] In a recent work,[63] AuNHC@porous organic polymers were used with the aim of catalyst recycling. Although the system was shown to be moderately active (TON in the order of 10^2–10^3, E-factor around 2, and EMY around 35) the use of high temperature (120 °C) and the large amount of diethyl ether (around 30 times the volume of the product) necessary to separate the product from the catalyst made the process poorly sustainable (**Table 2**).

As far as the mechanistic aspects are concerned, some theoretical papers have appeared in the literature aimed at understanding the mechanism of action of the gold catalyst in protic solvents and under acidic conditions. Summarizing, it was found that (i) the water attack can proceed via an inner-sphere mechanism (*syn* attack) but the presence of additional water (or alcohol) molecules favors the outer-sphere mechanism (*anti* attack); (ii) the first proton transfer can be performed by the gold atom[64] or by additional water[65] or alcohol[66] molecules (the energy barrier is lower when the attack is assisted by water even when compared with the anion-assisted one); (iii) the second proton transfer needs the assistance of an additional water molecule and/or the co-ordination of vinyl alcohol, through the oxygen atom.[61] It is generally accepted that the rate determining step (RDS) is the proton transfer, but the presence of a proper solvent and/or acidic media may promote the proton shuttle, leading to a switch of the RDS. Overall, the lack of a unique mechanism for the gold-catalyzed hydration of alkynes has emerged. However, a common characteristic conclusion from the theoretical studies can be pointed out, namely, that additional explicit water molecules (two, three, or even a large network of water molecules) are needed in order to lower the calculated energy

barriers for both proton transfer steps, the second proton transfer being the most difficult to computationally rationalize. In the strictly related methoxylation of alkynes, it has been found that the role of the counterion[67] is crucial during both nucleophilic attack[68] and the protodeauration steps. [37] The intermediate co-ordination ability and basicity of a sulfonated counterion gave the best results under our conditions.[69]

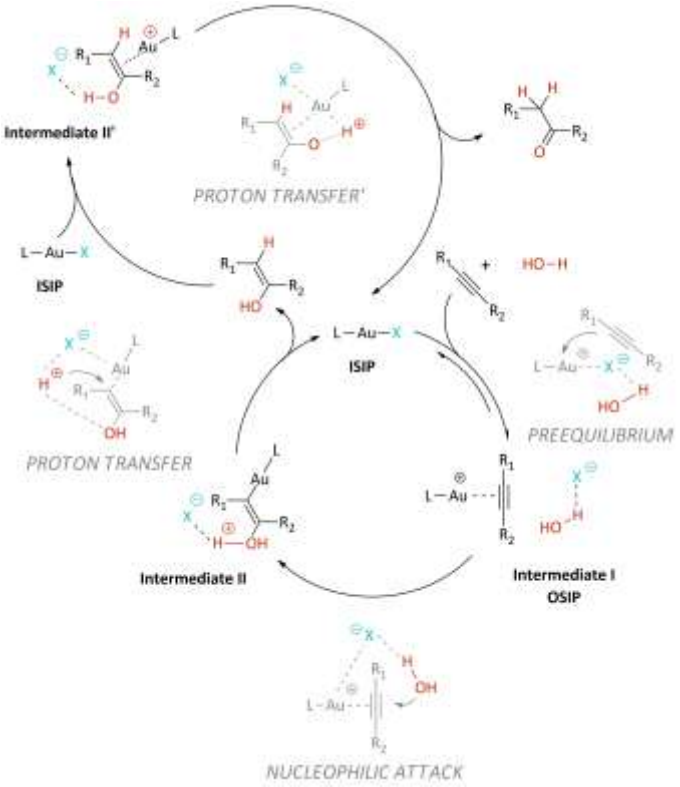

***Scheme 11**: Mechanism of gold(I) homogeneous catalysis in the nucleophilic attack*

It was observed that a proper neutral (such as DMF and DMPU) or ionic additive (such as $NBut_4OTf$) could increase the reaction rate of alkoxylation and hydration of alkynes.[70] Moreover, for solid and/or viscous reagents a solvent is needed because of the immiscibility of the reagents. According to the twelve principles of Green Chemistry[42] (**Table 1**) the use of green solvents, with suitable functionalities, seems to be a step towards new, efficient and sustainable gold catalyzed reactions.

A key topic in organic synthesis is the replacement of VOS with green solvents [71], and bio-based solvents[72] are used in many transition metal catalyzed reactions, for example: water[73], γ-valerolactone[74], glycerol[75], lactic acid and its derivatives[76], D-limonene and *p*-cymene[77] are largely employed. Other examples of green solvents are biodiesel[78], $scCO_2$[79], perfluorinated hydrocarbons[80], polyethylene glycol[81], Deep Eutectic Solvent[82] and ionic liquid[83], frequently used in organic synthesis.

Examples for gold catalysis with neoteric solvents, instead of VOS, are lacking in the literature. Recently, the group of García-Álvarez, using an iminophosphorane Au(I) complex, reported the use of DES in the tandem reaction cycloisomerisation/Diels–Alder.[84] The same catalyst, used in aqueous or eutectic-mixture solutions,

was used in the cycloisomerization of alkynyl amides.[85] Another example of green chemistry in gold catalysis is the use of PPh_3-Au-Cl in PEG for the formation of amides, starting from aldehydes and amines.[86]

1.4. Aim and future prospects

The aim of this paper is the full understanding of chemical transformations using gold(I) complexes ranging from the synthesis of the catalytic precursors and structural characterization of the species, to the kinetics evaluation of the catalytic reactions and their theoretical calculations. A full understanding of the mechanistic and theoretical foundations of this chemistry, with a complete rationalization of the role of ligand, counterion, solvent and additives is still rare in the literature but has started to grow in recent years.

In order to make gold homogeneous catalysis scalable to the industrial level, efforts are needed to make it sustainable and environmentally friendly. Working with low catalyst loadings, green/alternative solvents or neat conditions without silver additives, at room temperature and under air, recyclable catalysts with a simple work-up of the reaction and recovery of the gold, appears to be very difficult; in fact, there are few protocols in the literature showing all these characteristics.

The intention is to develop sustainable conditions for the hydration of alkynes and related alkoxylation, catalysed by homogeneous gold(I) catalysts. Both are important environmentally friendly reactions in the field of organic chemistry that satisfy both the atom economy and carbon efficiency.

In order to obtain good results, research must focus on the following topics: 1) Synthesis and structural characterization of gold(I) catalysts and possible reaction intermediates; 2) Evaluation of molecular kinetics for the catalytic reactions with a clear understanding of the structural properties of the catalysts and rationalization of the role of solvents and other additives; 3) Computational studies with a full rationalization of computed structural and reactive properties, corroborated by experimental data.

2

Results and Discussion

2.1. Hydration of alkynes in solvent-, silver- and acid-free conditions using NHC gold(I) catalysts

This work started by studying the reaction of hydration of alkynes in neat condition, avoiding the use of silver salts and acid additives, at low to mild temperature. With the knowledge about the stability and the reactivity of NHC gold catalysts, the compounds NHC^{iPr}-Au-X [X^- = TFA^-, BF_4^-, NTf_2^-, SbF_6^-, OTs^-, ClO_4^-, $BArF^-$] were initially chosen as catalysts for the hydration of alkynes in neat condition. They were synthesized according to literature procedures (experimental part, page 66). In order not to use any silver additive, even for the synthesis of the gold catalyst, the complex NHC-Au-OTf was synthesized according to the procedure developed by Nolan and co-workers[87], with the addition of HOTf to the acetonyl complex NHC^{iPr}-Au-CH_2-(C=O)CH_3 (see the experimental part). Complexes NHC^{iPr}-Au-X have been tested in the hydration of terminal and internal alkynes (**Table 3**-**Table 6**).

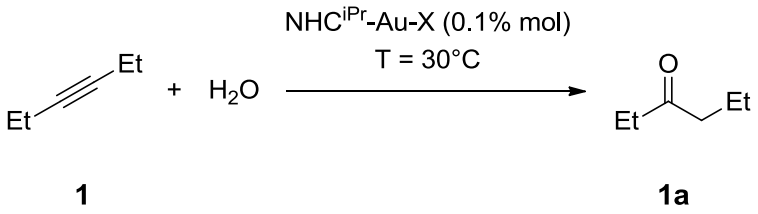

***Scheme 12**: hydration of 3-hexyne in NEAT condition*

***Table 3:** NHC^{iPr}-Au-X catalysed hydration of 3-hexyne[a]*

Entry	Loading (mol%)[b]	T (°C)	X^-	Conv. (%)[c]	Time[d] (h) (TOF[e])
1	0.1	30	BF_4^-	<1	24
2	0.1	30	SbF_6^-	<1	24
3	0.1	30	ClO_4^-	<1	24
4	0.1	30	OTf^-	>99	16 (64)
5	0.1	30	NTf_2^-	>99	16 (64)
6	0.1	30	OTs^-	<1	24
7	0.1	30	TFA^-	<1	24
8	0.1	30	$BArF^-$	<1	24
9	0.1	50	$BF4^-$	<1	24
10	0.1	50	OTs^-	<1	24

[a] Catalysis conditions: 3-hexyne (1.75 mmol, 200 µL) and H2O (1.92 mmol, 35 µL). [b] (moles of catalyst / moles of alkyne) x 100. [c] Determined by ^{1}H NMR; averaged value of three measurements. [d] Time necessary to reach the reported conversion. [e] TOF = ($n_{product}$ / $n_{catalyst}$) / t(h) at the reported conversion.

The standard catalytic run was conducted by mixing the relative alkyne and 1.1 equiv. of water in the presence of the catalyst (from 0.01 to 0.5 mol% with respect to the alkyne) and a proper additive (from 0.5 to 10 mol% with respect to the alkyne) at different temperatures (30, 40, 50, 60 and 70 °C) (**Table 4**, **Table 6**). Two phases are present at the beginning of the reaction (owing to the non-miscibility between alkynes and water) while a single phase only is observed during the reaction, thanks to the formation of the relative ketone that increases the miscibility of the reagents. The conversion and the progress of the reaction were monitored by NMR spectroscopy (**Table S1**). Complexes bearing SbF_6^-, BF_4^-, $BArF^-$, ClO_4^-, TFA^-, and OTs^- as counterion gave no reaction at 30 °C, showing no products after 24 h (**Table 3**, entries 1, 2, 3, 6, 7 and 8). Full conversions (>99%) of 3-hexyne (**1**) into 3-hexanone (**1a**) was reached within 16 h using NHC^{iPr}-Au-NTf_2 and NHC^{iPr}-Au-OTf (**Table 3**, entries 4 and 5).

The TOF value (**Table 5**) was taken into account for comparing the catalytic activity in different conditions. The TOF obtained using NHC^{iPr}-Au-NTf_2 and NHC^{iPr}-Au-OTf is 64 h^{-1}, a higher value with respect to those reported in the literature at room temperature in neat condition.[61] The catalysts with OTs^- and BF_4^- anions did not promote the reaction even increasing the temperature up to 50° C (**Table 3**, entries 9 and 10). This important and unexpected finding suggests that the anion during the reaction has a specific role. This is particularly surprising for OTs^- because it is the best counterion combined with the NHC ligand in the related methoxylation of alkynes.[68] It seems also that the moderately basic nature of SbF_6^-, $BArF^-$, BF_4^- and ClO_4^- is not able to promote the nucleophilic attack and the proton shuttle, even if in the pre-equilibrium step the catalyst is in the active form (OSIP, **Scheme 11**). That result confirms the previously theoretical and experimental observation in the methoxylation of alkynes: when poor basic and poor co-ordinating anions are used, it is guessed that in the mechanism a second methanol molecule is involved.[69]

We have already observed from DFT calculations and NMR experiments that in the absence of a proton donor like methanol, OTs^- is too much co-ordinating for the NHC-Au^+ fragment.[68] With NMR experiments, is possible to see that OTs^- is not co-ordinated to the metal during the methoxylation of 3-hexyne, with the presence of the active form (OSIP). Since we observed by NMR that in the absence of methanol the pre-equilibrium is completely unbalanced to the ISIP, we have reason to infer that methanol may work for the de-co-ordination of OTs^-. For the neat hydration of alkynes using OTs^- as counterion, it is possible that in the pre-equilibrium the catalyst is shifted towards the inactive form (ISIP, **Scheme 11**). Moreover, DFT calculations reported in

this chapter show the formation of a water-gold complex[32a] stabilized by OTs^- that made difficult the co-ordination of the alkyne (**Figure S9** and **Figure S10**).

The intermediate basicity and co-ordinating ability of OTf^- and NTf_2^- (the OSIP is generated with or without the presence of proton donor molecules[68]), are characteristic requested in order to promote the solvent-free hydration of alkynes in these conditions.

In gold catalysis, ionic additives (in particular NBu_4OTf) can improve some catalytic processes, such as: methoxylation of 3-hexyne, cyclization of 4-pentynoic acid, the synthesis of α-pyrone, cycloisomerization of N-(prop-2-ynyl)benzamide to 2-phenyl-5-vinylidene-2-oxazoline, intermolecular hydroamination of alkynes and cycloisomerization of allenone.[70a] Anyway, in order to increase the catalytic performances of gold catalysts, only acidic additives are used for the hydration of alkynes[19] and no information are available for the ionic additives.

Table 4: *NHC^{iPr}-Au-OTf catalyzed hydration of 3-hexyne[a]*

entry	Loading (mol%)[b]	T (°C)	Additives (mol%)[c]	Conv.[d] (%)	Time[e] (h) (TOF[f])
1	0.1	30	[BMIM]OTf (5)	<1	24
2	0.1	30	NH_4OTf (5)	>99	16 (64)
3	0.1	30	NBu_4OTf (5)	>99	2 (495)
4[g]	0.1	30	NBu_4OTf (5)	>99	2 (493)
5	0.1	30	NBu_4OTf (2.5)	>99	2.5 (396)
6	0.1	30	NBu_4OTf (1)	>99	3 (323)
7	0.1	30	NBu_4OTf (0.5)	>99	6 (162)
8	0.2	30	NBu_4OTf (5)	>99	1 (490)
9	0.05	40	NBu_4OTf (5)	93	3 (620)
10	0.05	50	NBu_4OTf (5)	95	1.5 (1267)
11	0.025	50	NBu_4OTf (5)	>99	4 (1000)
12[h]	0.01	60	NBu_4OTf (5)	>99	7 (1414)
13[h]	0.01	60	NBu_4OTf (10)	>99	6 (1668)
14[h]	0.005	70	NBu_4OTf (5)	<1	48

[a] Catalysis conditions: 3-hexyne (1.75 mmol, 200 µL) and H_2O (1.92 mmol, 35 µL). [b] (moles of catalyst / mole of alkyne) x 100. [c] (moles of additive / moles of alkyne) x 100. [d] Determined by ^1H NMR; averaged value of three measurements. [e] Time necessary to reach the reported conversion. [f] TOF = ($n_{product}$ / $n_{catalyst}$) / t(h) at the reported conversion. [g] In the presence of 0.26 mmol of 3-hexanone. [h] 3-Hexyne (3.5 mmol, 400 µL) and H_2O (3.84 mmol, 70 µL).

The results of the catalysis using NHC^{iPr}-Au-OTf with some triflate salts as additive are reported in **Table 4**. By comparison with the results obtained without using additives (**Table 3**, entry 4), it can be seen that the addition of [BMIM]OTf (**Table 4**, entry 1) stops the reaction, while the use of NH_4OTf does not affect the reaction rate with the complete conversion in 16 h (compare entry 2 in **Table 4** with entry 4 in **Table 3**). On the contrary, the use of NBu_4OTf successfully increases the reaction rate and full conversion is obtained in 2h (compare entry 3 in **Table 4** with entry 4 in **Table 3**), the gain of TOF is about an order of magnitude: from 64 to 495 h^{-1}.

The presence of a cationic organic fragment (NBu_4^+) can provide the increase of solubility of the salt in 3-hexyne, increasing the amount of water in organic phase and favoring the reaction (**Figure 9**). This behavior is similar to the well-known PTC catalysts (phase transfer catalyst)[88], used for gold nanoparticles catalysists for a long time.[89]

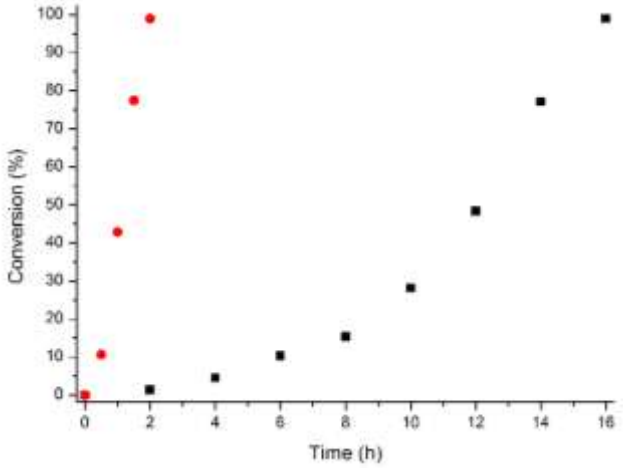

Figure 9: *Hydration of 3-hexyne with 0.1% of NHC^{iPr}-Au-OTf with (red circle) or without (black square) the 5% of NBu_4OTf.*

As expected, the reaction takes place in the organic phase and the use of a water-soluble NH_4^+ salt does not increase the reaction rate. On the contrary the use of [BMIM]OTf, a ionic liquid immiscible with 3-hexyne, can seize the water distributed in the organic phase arresting the reaction. Changing the amount of NBu_4OTf, a clear trend was observed from 0 to 5 mol%: from 2.5 to 5 mol% there is only a slight increase of TOF (from 396 to 495 h^{-1}) while 2.5 mol% to lower values a substantial decrease was detected (**Figure 10**). As a matter of fact, at room temperature, 5 mol% of NBu_4OTf represents the best choice.

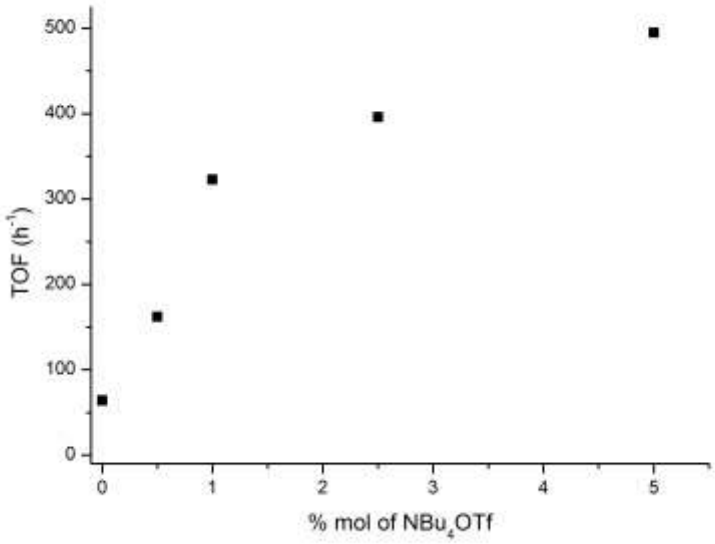

Figure 10: *Hydration of 3-hexyne with 0.1% of NHC-Au-OTf with different amount of $NBut_4OTf$.*

It was also checked if there was a potential benefit of the product (3-hexanone) during the catalysis, adding 15 mol% of 3-hexanone directly from the beginning (entry 4, **Table 4**), but no substantial variation of the reaction rate was observed, that demonstrates the stronger effect of ionic additives.[70]

In order to verify the applicability of this methodology, it was studied the effect of temperature and catalyst loading. When NBu_4OTf (5 mol%) is employed as the additive and 3-hexyne as the substrate, increasing the temperature by 10 °C (from 30 to 40 and 50 °C) entails a decrease of the reaction times of 1.5 h, with an increase of TOF from 620 to 1267 h^{-1} (entries 9 and 10, **Table 4**). As expected, the beneficial effect of increasing the temperature allowed us to decrease the catalyst loading down to 0.01 mol% with a TOF of 1668 h^{-1} in the presence of NBu_4OTf (10 mol%) at 60 °C (entry 13, **Table 4**). No reaction was observed at 70 °C using a 0.005 mol% catalyst loading (entry 14, **Table 4**). It should be point out, however, that the catalyst loading and TOF obtained in neat condition are in line with those reported in the literature using protic solvents, high temperature, and with Brönsted acids added.[19]

Moreover, we were able to separate NHC^{iPr}-Au-OTf/NBu_4OTf from 3-hexanone by distillation under reduced pressure, thanks to the absence of the solvent, obtaining a high purity product without metal contamination (see the Experimental part). Usually, in homogeneous gold catalysis, expensive chromatographic procedure is required for the separation of the products but with our method we obtained very high EMY and low E-factor values. In fact, in the hydration of 3-hexyne at 30 °C with 0.1 mol% of NHC^{iPr}-Au-OTf and 5 mol% of NBu_4OTf we obtained EMY equal to 87 and E-factor equal to 0.15, and at 60 °C with 0.01 mol% of NHC^{iPr}-Au-OTf and 5 mol% of NBu_4OTf, EMY increased to 94 and E-factor decreased to 0.06 (**Table 4**, entry 3 and 12).

Later, the effect of catalyst concentration was determined. In the presence of 5 mol% NBu_4OTf, the catalyst (NHC^{iPr}-Au-OTf) loading was changed and the reaction time halved when the catalyst amount was doubled, from 0.1 to 0.2 mol% (**Table 4**, entries 3 and 8).[90] This behavior suggests a 1st order dependence on the catalyst, as recently reported in the literature in the methoxylation of alkynes using NHC-gold complexes.[70b] It can be proved that in the rate determining step of the reaction only one gold atom is involved.

Nevertheless, the RDS can be also the protodeauration or the nucleophilic attack (**Scheme 11**, page 17). In different catalytic conditions the kinetic Isotopic Effect (KIE)[91] was measured. When D_2O was used instead of H_2O, a reduction of TOF was observed, from 64 to 17 h^{-1} (**Table 5** entry 3 vs. 1,[92] **Figure 11a**), giving a KIE of 3.8. In the presence of NBu_4OTf (5 mol%), the TOF decreased from 495 to 198 h^{-1} and the reaction decelerate when D_2O was used instead of H_2O (**Table 5** entry 2 vs. 4, **Figure 11b**), giving a KIE of 2.6. These KIE values clearly indicate that the turnover-limiting step is the proton transfer (**Scheme 11**, page 17) in both conditions. When an ionic additive is used, there is a small decrease of the KIE and this may indicate that during the proton transfer steps, NBu_4OTf has a specific role. In a work of Straub and co-workers[93] for the hydration of terminal alkynes in methanol, a KIE of 3-5 was obtained and the authors pointed out that the turnover-

limiting step was the protonolysis of the gold-carbon bond. In order to further confirm that the rate determining step is the proton transfer, the effect of Brönsted acids was tested in our solvent-free conditions. The reaction speeds up with the addition of HOTf, as expected, and TOF of 330 h^{-1} was obtained (**Table 5** entry 1 vs. 5,[92] **Figure 11c**). On the contrary, the KIE value is close to one in those acidic conditions (**Table 5**, entry 5 vs. 6), which indicates that the RDS becomes the nucleophilic attack. In order to confirm this finding, the Brönsted acid was changed ($HClO_4$ instead of HOTf) but a complete inhibition of the catalyst was observed due to the specific role of the anion.

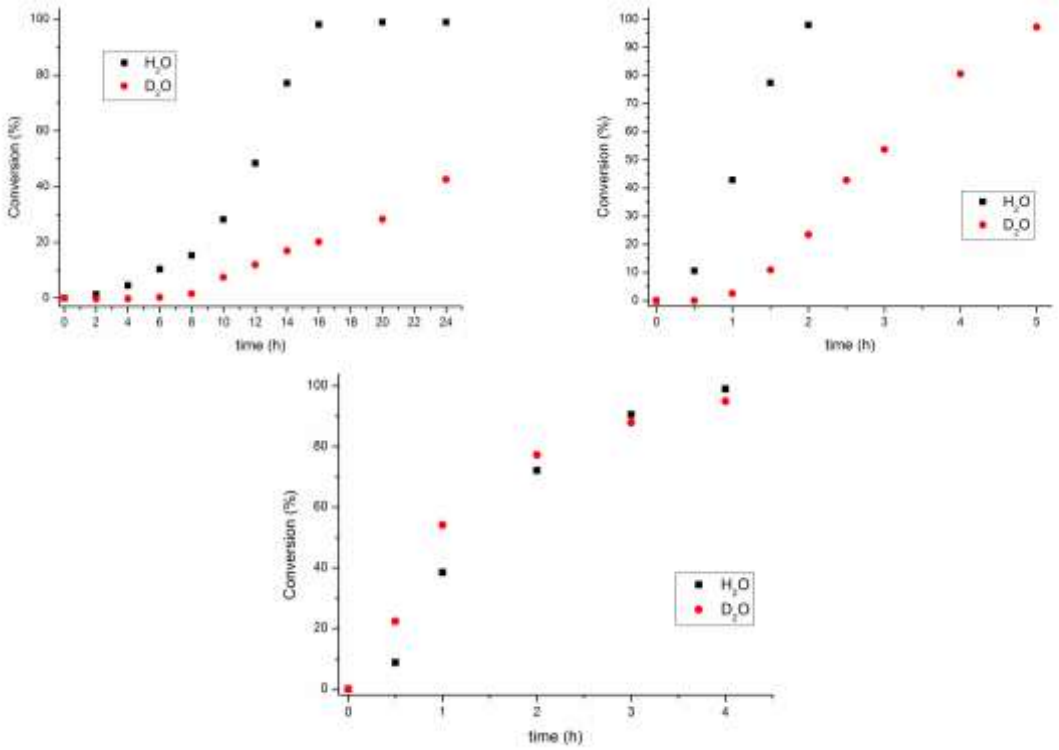

Figure 11: *Hydration of 3-hexyne with 0.1% of NHC^{iPr}-Au-OTf a) with water (black square) or deuterated water (red circle), b) in the presence of 5% of $NBut_4OTf$, c) in the presence of 5% of HOTf .*

To the best of our knowledge, for the first time in the hydration of alkynes the addition of Brönsted acids has a negative effect on kinetic. A clear picture begins to take shape: in aprotic and neutral conditions (in the presence of ionic additives or not) the proton transfer is the RDS of the reaction (high KIE value), it was assisted by the metal center instead of traces of H^+ (**Scheme 11**, page 17). In fact, the presence of H^+ ions accelerates the proton transfer, under solvent-free acidic conditions, allowing the dissociation of the product with a common enol-ketone tautomerization. The RDS becomes the nucleophilic attack (KIE equal to one).

In these conditions, the contribution of the anion is crucial and a poor basic anion (ClO_4^-) inhibits the nucleophilic attack and the reaction is stopped (**Scheme 11**, page 17) even in acidic conditions.

Table 5: *NHC^{iPr}-Au-OTf catalyzed hydration of 3-hexyne[a], acidic additives and KIE effect*

entry	Loading (mol%)[b]	Nucl.	Additives (mol%) [c]	Conv.[d] (%)	Time[e] (h) (TOF[f])
1	0.1	H_2O	NBu_4OTf (0)	>99	16 (64)
2	0.1	D_2O	NBu_4OTf (0)	42	24 (17)
3	0.1	H_2O	NBu_4OTf (5)	>99	2 (495)
4	0.1	D_2O	NBu_4OTf (5)	>99	5 (198)
5	0.1	H_2O	HOTf (5)	>99	3 (330)
6	0.1	D_2O	HOTf (5)	>99	3 (330)
7	0.1	H_2O	$HClO_4$ (5)	<1	24

[a] Catalysis conditions: 3-hexyne (1.75 mmol, 200 µL) and nucleophile (1.92 mmol, 35 µL). [b] (moles of catalyst / moles of alkyne) x 100. [c] (moles of additive / moles of alkyne) x 100.d Determined by 1H NMR; average value of three measurements. [e] Time necessary to reach the reported conversion. [f] TOF = ($n_{product}$ / $n_{catalyst}$) / t(h) at the reported conversion.[92]

Therefore, in all the reaction steps the role of the NHC^{iPr}-Au-X catalyst would be important (**Scheme 11**) even for the second proton transfer, which leads to the formation of the ketone from the enol intermediate. For the complete understanding of these results, DFT calculations were performed (Experimental part). The complex [NHC'-Au-OTf] (NHC' = 1,3-dimethylimidazol-2-ylidene), H_2O and 2-butyne have been chosen for the calculations. In all the steps of the reaction pathway the role of the anion OTf^- is emphasized, which are: pre-equilibrium, nucleophilic attack of water to the Au–butyne complex and the two proton transfers to the unsaturated carbon atom (**Scheme 11**: proton transfer and proton transfer').

The counterion substitution with the alkyne, in the initial complex, is the first step of the catalysis (ICOTf, **Figure 12**). The metal centre co-ordinates the 2-butyne generating different conformations. For the nucleophilic attack step two conformations are interesting: the conformation denoted as ICsub in **Figure 12** (where the most stable hydrogen-bonded $[OTf(H_2O)]^-$ group is located above the gold) and the conformation denoted RC (Reactants Complex) in **Figure 12** (where the $[OTf(H_2O)]^-$ group occupies opposite site of the Au center and around the alkyne). Its energy is little higher of 3.5 kcal/mol with respect to that of ICsub. In the nuchleophilic attack of the water to the C-C triple bond in the OSIP mechanism (anti-periplanar) the reactants complex is represented by the RC conformation. An energy barrier of 7.4 kcal/mol is required for the formation of the ICsub and RC adducts from the initial complex ICOTf and it is thermodynamically favored, in line with the relatively weak co-ordinating ability of OTf^-. As already observed in the NHC-gold(I)-catalyzed alkoxylation of alkynes,[69] in the RC complex one basic atom weakly interacts with the metal center (Au…O =

3.294 Å) while an hydrogen bond (HB) is formed between the counterion and water. This typical anion role, namely "it acts as a template", has two functions: i) to enhance the nucleophilicity of the water acting like hydrogen-bond acceptor and ii) to hold the water in the right position for the outer-sphere attack. In that moment the oxygen atom of water is far 3.202 Å from the closest carbon atom of the co-ordinated butyne. In the absence of the anion, the transition state for the nucleophilic attack was not found, thus pointing out that the water alone is not enough nucleophilic to attack the substrate and the presence of OTf^- is needed. Moreover, endeavors to calculate a nucleophilic attack by an inner-sphere mechanism starting from ICsub complex gave the RC complex, hence supporting an outer-sphere nucleophilic attack in the presence of the counterion OTf^-.

The transition state structure (TSI in **Figure 12**) of the outer-sphere nucleophilic attack has an activation barrier of 17.4 kcal/mol and the formation of the intermediate I is endothermic by 5.7 kcal/mol. An abstraction of one hydrogen from water by OTf^-, in the TSI, can be observed (HO-H = 1.031 Å, HOH….O(OTf^-) = 1.549 Å). The H-O(OTf) distance is 1.058 Å and the HO…H is 1.486 Å in the intermediate complex I, as a result of the abstraction of the hydrogen of water by OTf^-. In the transition state TSII for the first proton transfer, the proton is found between C2 (H…C2 = 1.563 Å) and the oxygen of OTf^- (H…O = 1.154 Å). In the intermediate II C2 in the trans position, with respect to the hydroxyl group, is bonded to the hydrogen and the product is η^2-co-ordinated to the gold with its unsaturated double bond (Au…C2 = 2.209 Å, Au…C1 = 2.491 Å). Very interestingly, there is a weak interaction of the anion with the gold center also in the trans position with respect to the hydroxyl of the formed enol. A calculated energy barrier of 1.4 kcal/mol, for the hydrogen transfer to the carbon, was found and the intermediate complex II is stabilized by 23.1 kcal/mol with respect to the intermediate I. At this stage, an α-auro ketone compound can be formed.[87] An different path to proton transfer (step II) has been considered, in order to analyze the possible role of α-auro ketone as off-cycle or on-cycle intermediate. The vinyl gold intermediate I (see **Figure 12**) could generate an α-auro ketone instead of enol complex II, once HOTf is formed. Results of our calculations, reported in the Experimental section (**Figure S11**, pag. 104), show the high activation barrier (45.9 kcal/mol), excluding the formation of this kind of intermediate during the reaction. Similarities were found in the counterion effect in the nucleophilic attack (step I) and protodeauration (step II) for the hydration of alkynes compared to the alkoxylation of alkynes using methanol as nucleophile with NHC gold (I)-catalyst.[69]

The breaking of the O-H bond, and the following proton transfer, has been experimentally found to be the rate determining step of the reaction (in aprotic and neutral conditions, KIE values much higher than 1).

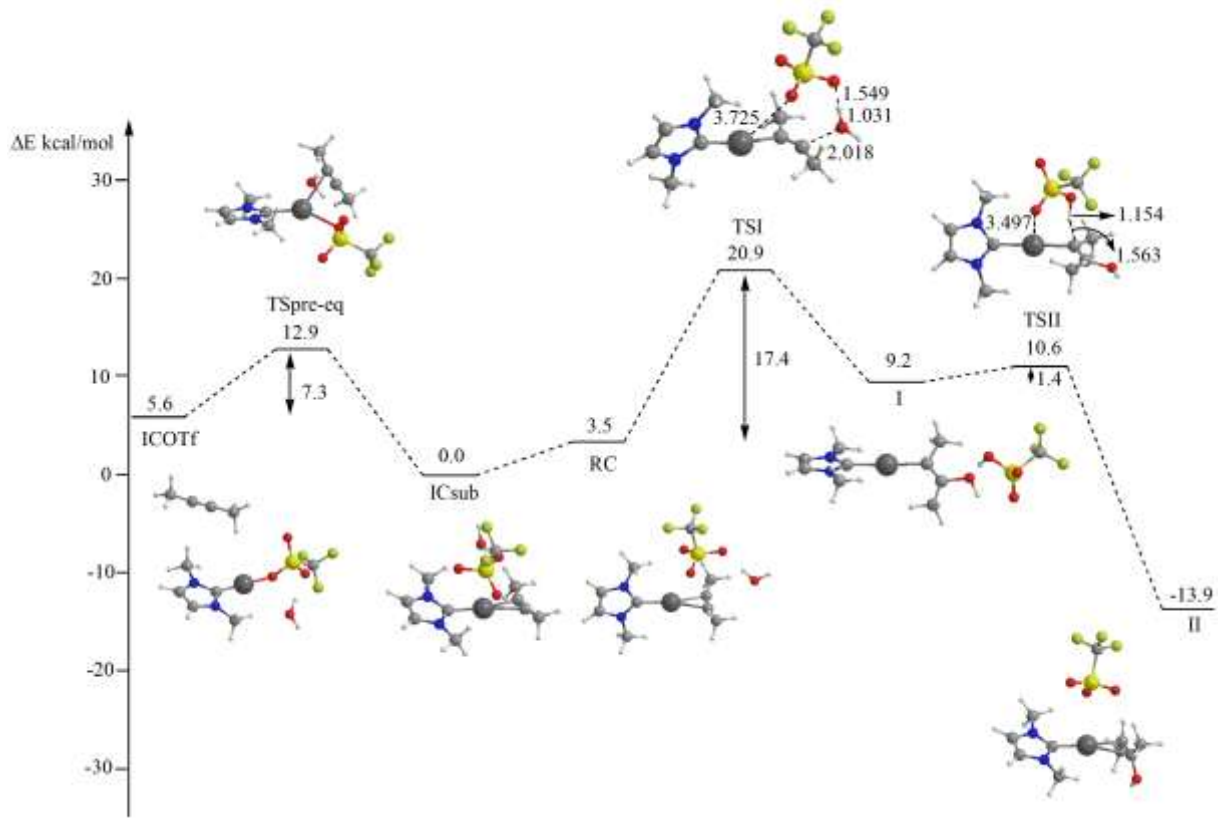

***Figure 12**: DFT calculated energy profile for the pre-equilibrium, nucleophilic attack (step I) and proton transfer (step II) for the reaction between 2-butyne and water, catalyzed by (NHC')-Au-OTf. The structures of the involved species are also shown. Geometric structure of TSI and TSII with relevant distances (in Å). Energy values (kcal/mol) refer to ICsub taken as zero.*

The intermediate III (**Figure 13**) structure is peculiar, because the gold atom exhibits a square-planar geometry. The Au-H bond is 1.555 Å, the organic moiety is η^1–coordinated to gold via the C2 carbon atom (Au-C2 = 2.096 Å) and the anion is bound to the metal centre via one oxygen atom (O(OTf^-)-Au = 2.206 Å) in trans position with respect to the hydrogen. The C1-C2 bond length is longer (1.518 Å), while the C-O bond length is shortened (1.225 Å). One example of the unusual square-planar geometry with a d^{10} gold(I) configuration has already observed for [AuCl(diphosphanylborane)] complexes having short Au-B distances. Interestingly, in intermediate III the OTf^- stabilizes the gold-hydrogen interaction via trans co-ordination, which would formally likewise the Au-B bonding situation in [AuCl(diphosphanylborane)], with the counterion acting as a σ-donor ligand (in place of Cl^-) and H^+ as Lewis acid (probably a much stronger Lewis acid than the borane moiety).

The next hydrogen shift to C2 from gold and it corresponds to a lower activation barrier of 10.9 kcal/mol through the transition state TSIV (**Figure 13**). In the latter, the distance Au-H increases to 1.608 Å, while the H-C2 distance is 1.601 Å. At the same time, both the O(OTf^-)-Au distance (2.441 Å) and Au-C2 bond length (2.192 Å) increase. The product IV (see **Figure 13**) is stabilized by 19.5 kcal/mol with respect to TSIV and 8.6 kcal/mol with respect to intermediate species III. In IV the counterion is located above gold, with a weak interaction, the Au-C2 distance increased up to 2.438 Å, and the hydrogen is nearly completely migrated

towards C2 (H-C2 = 1.145 Å, Au-H = 1.917 Å). The release of the product (ketone) and the regeneration of the catalyst is without energy barrier with the formation of the product complex PC, highly stabilized with respect to IV (-25.5 kcal/mol). The global energy for the catalytic addition of water to 2-butyne process is exothermic by -28.0 kcal/mol.

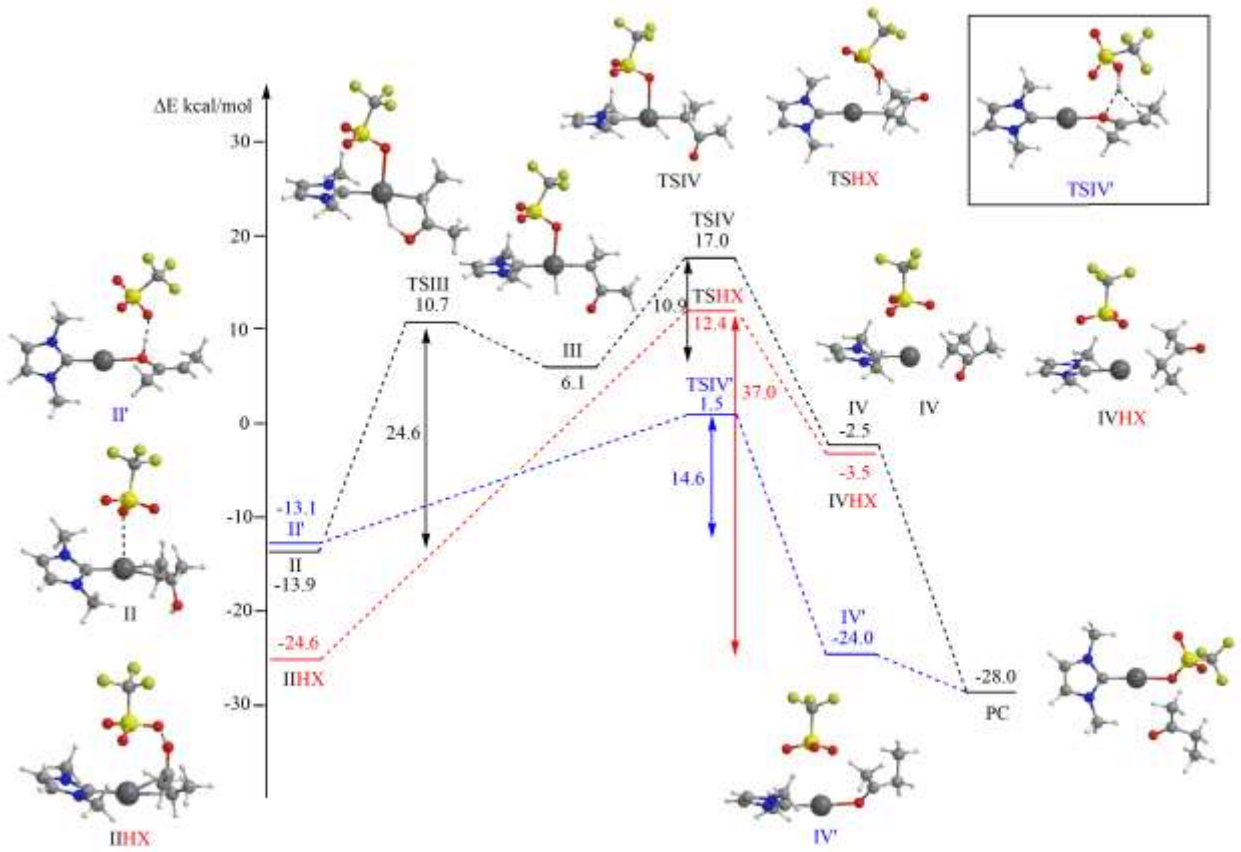

***Figure 13**: DFT calculated energy profile for the proton transfer' (step III) for the reaction between 2-butyne and water, catalyzed by (NHC')-Au-OTf. Energy profiles in black and in blue describe gold/anion- mediated processes, the one in red describes an only anion-mediated process. The structures of the involved species are also shown. Energy values (kcal/mol) refer to ICsub taken as zero.*

As underlined above, the counterion could play also a role as proton shuttle in the proton transfer step, without gold assistance for the migration of hydrogen. Calculation of the energy profiles for the reaction occurring mediated by only OTf^- has been made, in order to evaluate which is the most favorable pathway for the hydrogen migration from oxygen between: i) gold/anion-assisted and ii) only anion-assisted. However, a different structure for intermediate II should be considered. In the numerous conformations resulting from the position of the anion with respect to the gold-enol complex, one conformation is in line for our purpose, where OTf^- is positioned above gold but in cis position with respect to the hydroxyl group of the enol, in cis position. We named it as structure IIHX, shown in **Figure 13**. The IIHX species is more stable than intermediate II by 10.7 kcal/mol, due to hydrogen bond between OTf^- and the hydroxyl group of the organic portion ((OTf^-)O-HO = 1.503 Å and H-O = 1.042 Å) with a different resonance structure of the alkenol (see **Figure 13**). The substrate in fact is η^2-co-ordinated to gold in a more asymmetric way (Au…C2 = 2.181 Å, Au….C1 = 2.569 Å), with a longer C1-C2 bond length (1.414 Å) and a shorter C1-O distance (1.312 Å) in

comparison with intermediate II. The geometric parameters of the co-ordinated enol indicate a charge separation, with a δ^- on C2 and a δ^+ on the oxygen of the hydroxyl atom. The reactants complex corresponds to the conformation IIHX in our searching for an anion-assisted hydrogen migration in the process of proton transfer'. A transition state calculation gives the structure TSHX in (**Figure 13**), with an activation barrier of 37.0 kcal/mol (with respect to initial IIHX), and this result suggests that the basicity and the hydrogen bond ability of OTf^- is too much weak to abstract the second proton from oxygen. We note here that the energy profile in **Figure 13**, describing the proton transfer' anion-mediated from IIHX to IVHX, is the deprotonation of intermediate II to give the α-auro ketone. In the transition state TSHX, the substrate is η^1-co-ordinated to gold with a C-C bond length of 1.523 Å, a C-O bond length of 1.221 Å and an Au-Cα bond length of 2.232 Å, which can be indeed considered an α-auro ketone. The calculated TSHX energy of 37.0 kcal/mol is relatively high and the structure is not a minimum so at this stage any role of α-auro ketone as in-/off-cycle could be excluded. Moreover, the intermediate IIHX is more stable than intermediate II by 10.7 kcal/mol, the global energy activation barrier increases to 35.3 kcal/mol instead of 24.6 kcal/mol for intermediate III formation.

Finally, a plausible alternative conformation of the gold-enol complex has been considered by the interaction of gold with the oxygen atom of the enol OH,[61] indicate as structure II' in **Figure 13**. The II' species is less stable than intermediate II by only 0.8 kcal/mol (respect to IIHX by 11.5 kcal/mol) and it is represented by a strong hydrogen bond between the hydroxyl group of the substrate and the counterion ($(OTf^-)O$-HO = 1.394 Å and H-O = 1.082 Å). A calculation produces the transition state TSIV' (**Figure 13**), with the lowest calculated activation barrier of 14.6 kcal/mol (26.1 kcal/mol with respect to IIHX), and thus suggests that the gold complex stabilizes the forming enolate in a concerted process, with an enhancing of the weak proton acceptor ability of OTf^-.

Looking at the whole reaction energy profile, it appears clear that the hydrogen migration step in proton transfer' (step III) has a higher energy barrier (in a range between 37.0 and 26.1 kcal/mol for the three investigated pathways) in comparison with the initial nucleophile attack step of 17.4 kcal/mol (see **Figure 12** and **Figure 13**). It is important to notice that this result corroborates the experimental observation that the breaking of the enol hydrogen-oxygen bond is the RDS (see experimental KIE value larger than one) with a low activation barrier supporting the hydration of alkynes, with no assisting water molecules or any acid promoter.

However, in gold catalysis the presence and the function of H_2O or H^+ can be important. For this reason we also studied the conversion of enol to ketone, in two different scenarios in the presence of ii) traces of water or iii) acid.

In the presence of traces of water, it can be predicted that the OTf^- counterion releases the enol from the gold catalyst and after that a classical enol-ketone tautomerization occurs with the assistance of a water

molecule for the proton shuttle, of a water molecule. As shown on top of **Figure 14** , the enol/OTf^- exchange in intermediate II is a possible process with a relatively low activation barrier of 9.3 kcal/mol.

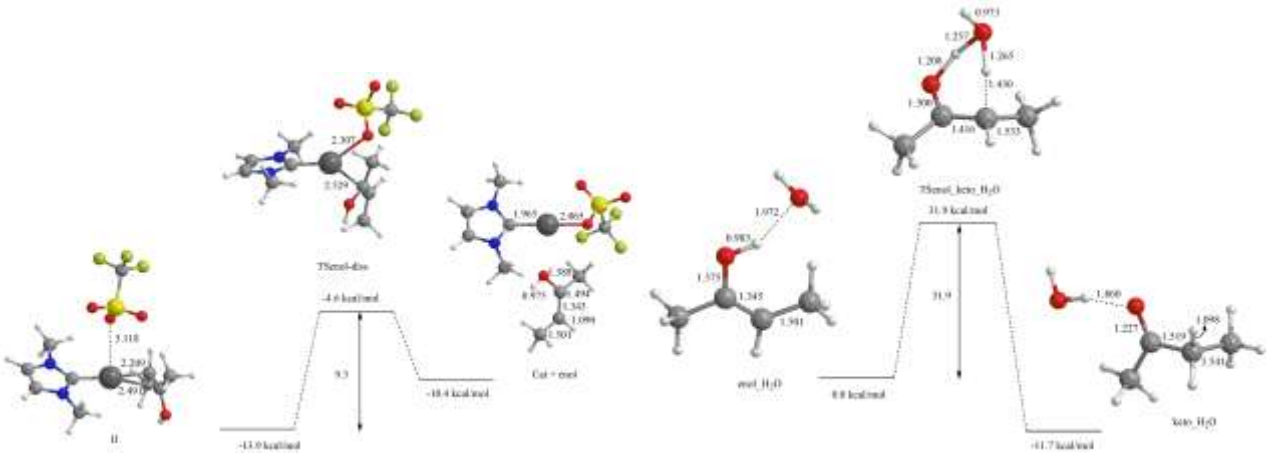

Figure 14*: Energy profile and corresponding geometries of the species involved in the enol substitution by OTf- in intermediate II (top) and in the enol-ketone tautomerization mediated by one water molecule (bottom). Energies (with respect to ICsub as in Figure 3, top), and with respect to enol_H2O taken as zero point energy, bottom)) in kcal/mol and distances in Å.*

The similar hydrogen abstraction from the enolic OH and the hydrogen transfer to carbon assisted by one H_2O molecule requires a relatively high activation energy of 31.9 kcal/mol. Of course, this hydrogen transfer chain would lower the barrier with additional water molecules, but in this case it cannot be included in the computational study due to the experimental conditions employed. Nevertheless, the experimental data are in agreement with this result that the enol to ketone step is the RDS (see experimental KIE value).

According to experimental results, in gold(I)-catalysis the use of HOTf significantly increases the rate of the reaction. The measured KIE values suggest that, under these conditions (in the presence of the acid), the RDS of the alkyne hydration is the nucleophilic attack. We re-investigated the process of enol to ketone transformation in the presence of HOTf, in order to explore the mechanism through which the activation barrier of the proton transfer' (**Scheme 11**) could be lowered. High activation barriers (larger than 40 kcal/mol) are obtained attempting to perform proton transfer from HOTf to the gold co-ordinate substrate. This result suggested that if the substrate is not co-ordinated to the catalyst, the proton transfer could be easier through a classical enol-ketone tautomerization. In **Figure 15** the energy profile for the substitution of the substrate by OTf^- and the subsequent proton transfer by HOTf to the substrate and the H-abstraction by the formed OTf^- from the substrate to give the products complex is reported.

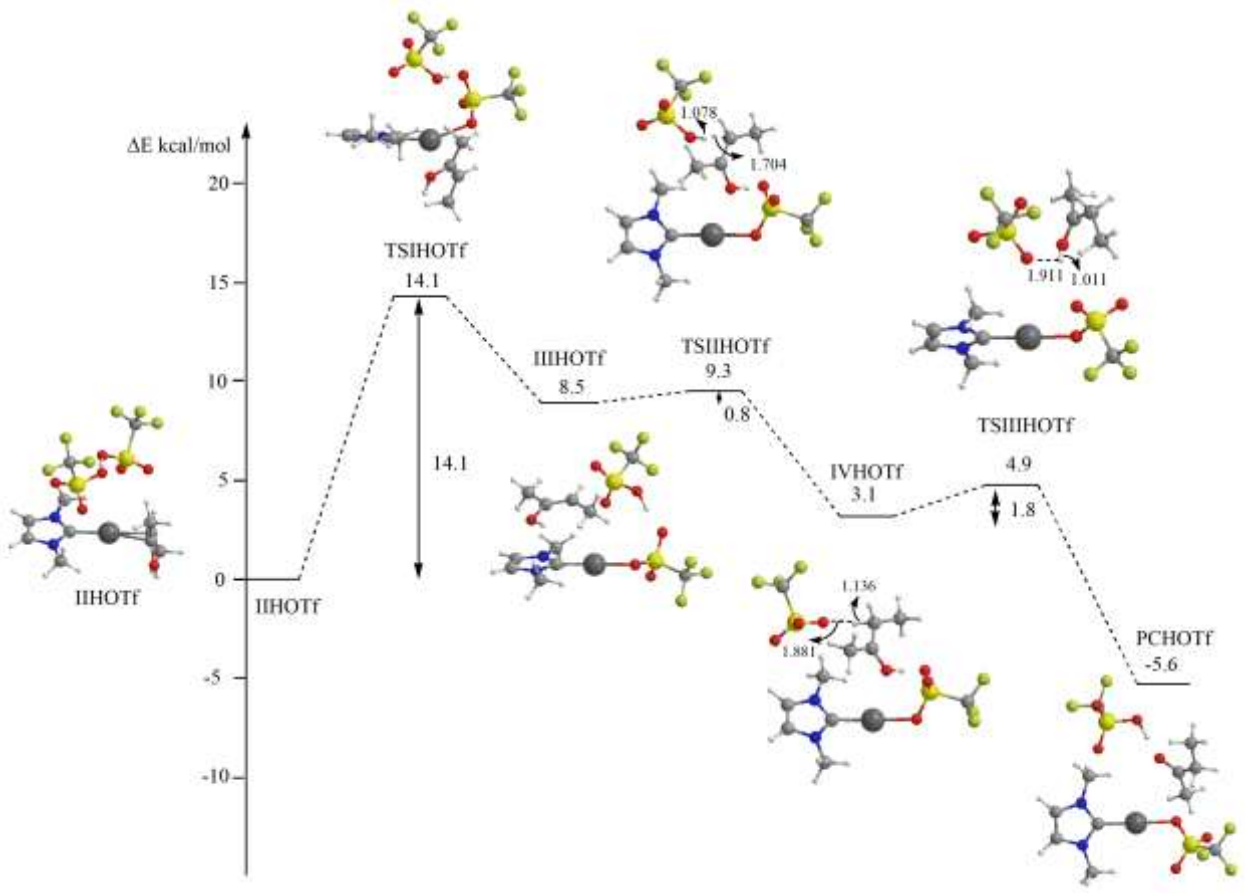

***Figure 15**: DFT calculated energy profile for the proton transfer' (step III) for the reaction between 2-butyne and water, catalyzed by (NHC')-Au-OTf, in the presence of HOTf. The structures of the involved species are also shown. Geometric structure of TSIIHOTf, IVHOTf and TSIIIHOTf with relevant distances (in Å). Energy values (kcal/mol) refer to IIHOTf taken as zero.*

In **Figure 15** there are all the optimized geometries of the species involved in this path. The activation barrier for the substrate substitution by OTf^- in IIHOTf has a value of 14.1 kcal/mol. This is the highest activation barrier for this path, in fact the proton transfer from HOTf to the Cα of the substrate (from the structure IIIHOTf to IVHOTf) occurs with a very low energy barrier (0.8 kcal/mol). To conclude the pathway, the proton transfer from the substrate to the OTf^- previously formed (from the structure IVHOTf to PCHOTf) takes place also with a very low energy barrier (1.8 kcal/mol), in line with the well-known acid-catalyzed enol-ketone tautomerization. We conclude that using the acid (HOTf) the activation barrier for proton transfer' effectively decreases (step III), with only 14.1 kcal/mol calculated, and which concerns to the product de-co-ordination from the gold(I) catalyst. In this acidic condition for this reaction, the nucleophilic attack step with an activation energy barrier of 17.4 kcal/mol shown in **Figure 12** becomes the RDS.

The mechanism in **Scheme 13** occurs when enol became a ketone in the presence of traces of HOTf. However, the KIE value expected is equal to one since the RDS is not the enol O-H breaking, in contrast with the experimentally measured KIE (much larger than one). The theoretical mechanisms proposed for the global reaction of alkynes hydration, with $[NHC'\text{-}Au]^+$ catalyst in the presence of the OTf^- as anion, under the three different experimental conditions are summarized in **Scheme 13**.

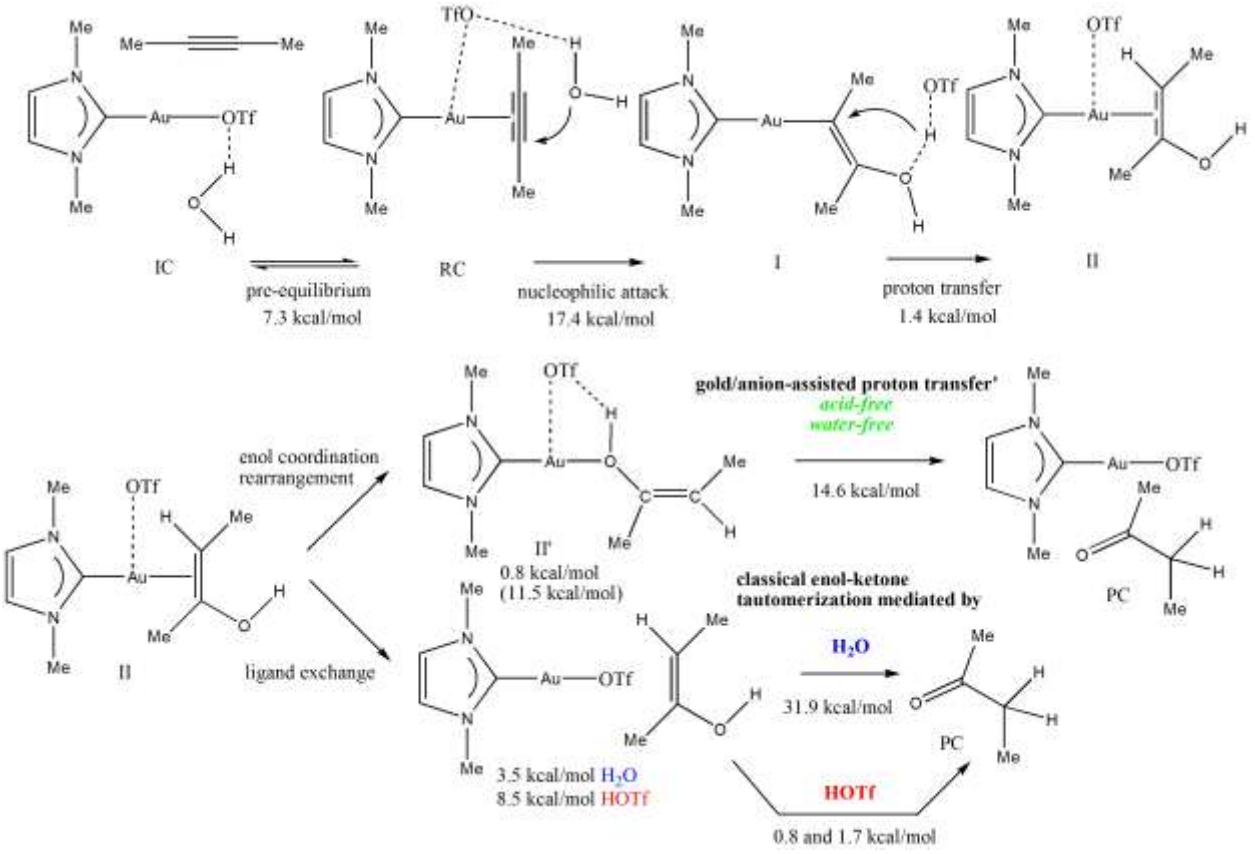

***Scheme 13**: Reaction mechanism between 2-butyne and water catalyzed by the (NHC)'-Au-OTf complex showing the role of anion OTf^-. The two steps, following the pre-equilibrium, are (step I) nucleophilic attack of water to butyne via OTf^- anion template effect and activation of water by anion OTf^- proton acceptor properties, and (step II) proton shift to substrate mediated by the anion OTf^- acting as a proton shuttle (proton transfer). For the gold-enol to ketone conversion (step III): i) in acid- and water-free conditions, proton transfer' via a gold/anion mediated hydrogen transfer process; ii) in traces of water and iii) traces of acid conditions, ligand exchange followed by a classical water- or acid-assisted enol- ketone tautomerization.*

The energies of intermediates (in kcal/mol) are reported with respect to intermediate II in **Scheme 13** (the energy of intermediate II' with respect to the most stable gold-enol complex IIHX is also indicated in parenthesis). The energy barriers (in kcal/mol) are indicated for each step of the total mechanism.

On the basis of these findings, we conclude that the gold/anion-assisted enol to ketone conversion is certainly feasible without inclusion of adventitious acid promoter or water molecules and is consistent with the measured KIE value in the experimental neutral and aprotic conditions. With a mechanistic DFT rationalization of the reaction in hands and once optimized the reaction conditions, (**Table 4**, **Scheme 13**) this methodology was applied to alkynes showing different functional groups, both terminal and internal, and running the reaction in solvent-free conditions, even if they are less active than 3-hexyne (**Chart 1**). The internal aliphatic alkynes with a higher molecular weight, like 4-octyne, (**Table 6**, entry 6), could have low activity due to the lower solubility in water. For aromatic internal alkynes (such as 1-phenyl-1-propyne, entry 5, **Table 6**, entry 5) the behavior is similar, even if they are more inactive compared to aliphatic alkynes.[23] With terminal alkynes, compared to internal ones, (phenylacetylene, 3-phenyl-1-propyne, 1-octyne, 1-hexyne, **Table 6**) it is known that in the nucleophilic attack they are less active in aprotic solvents.[23] Other

deactivated alkynes were tested, like 1-trimethylsilyl-1-hexyne, methyl-2-hexynoate, 1,4-dimethoxy-2-butyne, and diethylacetylenedicarboxylate, observing high conversion after few hours with the expected regio- and chemo-selectivity (**Table 6**, entries 7-10,).[94] 3-Pentyl-1-ol reacts promptly with water, giving 5-hydroxy-2-pentanone (**Table 6**, entry 11), and such a high rate could be attributed to the enhanced solubility of water in the organic phase. Both terminal and internal alkynes with different combination of aryl and alkyl substituents and different functional groups (silyl, alcohol, ether, ester) were suitable substrate in this solvent-, silver-, acid- free catalytic condition.

Table 6: *NHC^{iPr}-Au-OTf catalyzed hydration of alkynes[a] and substrate scope*

entry	Loading (mol%)[b]	Substrate	Conv.[c] (%)	Timed (h) (TOF[e])
1	0.5	1-hexyne (2)	>99 (**2a**)	6 (34)
2	0.5	1-octyne (3)	>99 (**3a**)	6 (34)
3	0.5	3-phenyl-1-propyne (4)	>99 (**4a**)	6 (34)
4	0.5	Phenylacetylene (5)	>99 (**5a**)	8 (25)
5	0.5	1-phenyl-1-propyne (6)	>99 (90 (**6a**), 10 (**6b**))	2 (100)
6	0.1	4-octyne (7)	80 (**7a**)	6 (133)
7	0.5	1,4-dimethoxy-2-butyne (8)	>99 (**8a**)	2 (100)
8	0.5	methyl-2-hexynoate (9)	>99 (90 (**9a**) , 10 (**9b**))	6 (34)
9	0.5	1-trimethylsilyl-1-hexyne (10)	54 (**10a**)	7 (15)
10	0.5	Diethylacetylenedicarboxylate (11)	71 (47 (**11a**) , 53 (**11b**))	2 (71)
11	0.5	3-pentyl-1-ol (12)	>99 (**12a**)	2 (100)

[a] Catalysis conditions: 50°C, alkyne (1.75 mmol) and water (1.92 mmol, 35 µL), 5% NBu4OTf (0,0875 mmol, 34 mg). [b] (moles of catalyst / moles of alkyne) x 100. [c] Determined by ^{1}H NMR; average value of three measurements; in brackets the products obtained (see below) with their molar ratio. [d] Time necessary to reach the reported conversion. [e] TOF = ($n_{product}$ / $n_{catalyst}$) / t(h) at the reported conversion.

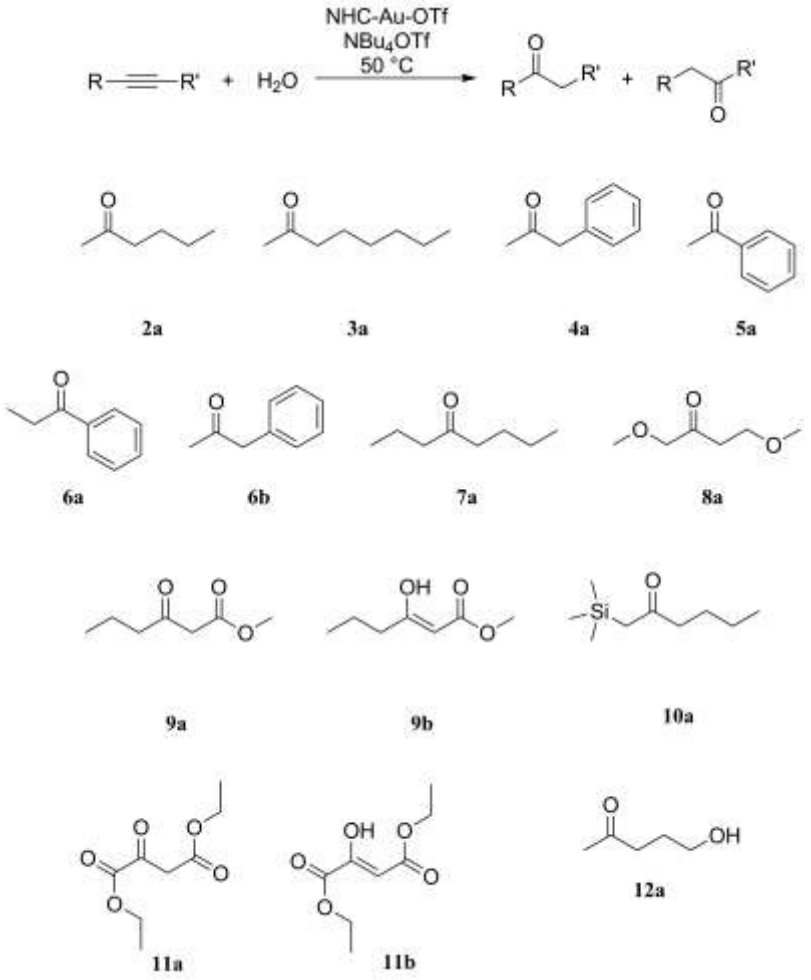

***Chart 1**: The complete set of ketones synthetized by testing our methodology.*

As already mentioned above, it is possible to separate the ketone by distillation under reduced pressure, re-adding the alkyne and the water to the catalyst/additive solid mixture. In case of 3-hexyne, it was possible to reuse the catalytic system up to 4 times, obtaining a final TON of 5000, without appreciable loss of activity (**Figure 16**).

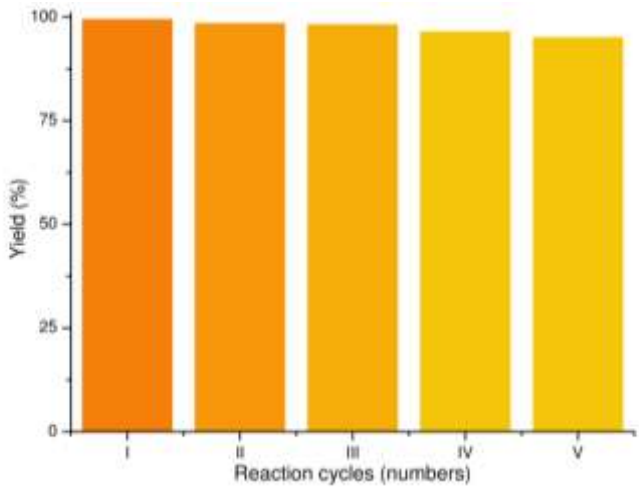

***Figure 16**: Recyclability test of NHC^{iPr}-Au-OTf (0.1 mol%) in the hydration of 3-hexyne with 5 mol% of NBu_4OTf at 30°C (**Table 4**, entry 3).*

This TON value is lower respect that reported Nolan and co-workers[23] who conducted the reaction at 120 °C in 1,4-dioxane/water with NHC-gold catalyst, but it is however a superb result in solvent-, acid- and silver-free condition for the hydration of alkynes at room temperature.[95] Moreover, we were able to obtain E-factor of 0.03 and EMY of 97 that are exceptional if compared with those reported in the literature.[66] It was also possible to work in a gram-scale amount, with an easy recover of the product.

2.2. Hydration of alkynes in solvent-, silver- and acid-free conditions using L-gold(I) catalysts

In this section a complete screening of catalysts was performed for the reaction of hydration of alkynes in neat condition, avoiding the use of silver salts and acid additives at low to mild temperature. The optimized protocol was applied to deactivated substrates as such phenylacetylene and diphenylacetylene. The compounds L-Au-X [L = {NHC^{iPr}}, {PArF}, {BIAN}, {NHC^{CH2}}, {NAC}, {JPhos}, {PCy_3}, {PPh_3}, and {POR_3}, X^- = Cl^-, OTf^-, and OTs^-] were synthesized according to literature procedures (Experimental part) or generated in situ during the catalytic tests (**Table 7**).

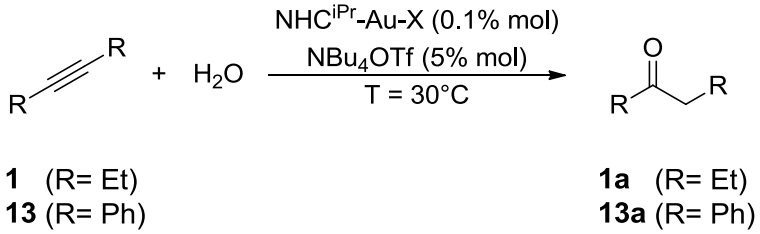

***Figure 17**: Hydration of 3-hexyne and diphenyl acetylene*

For those complexes, neutral ligands with a considerably variation on the stereo and electronic character were used. They were tested as catalysts in the hydration of 3-hexyne (**1**) to form 3-hexanone (**1a**) and diphenylacetylene (**13**) to form 1,2-diphenylethanone (**13a**) (**Table 7** and **Table 8**) in solvent- and acid-free conditions, extending and completing the previous investigation. The role of silver salts (**Table 7**) and ionic additives, other than NBu_4OTf (Experimental part, **Table S5**), were also evaluated.

***Table 7**: L-Au-X (0.1 mol%) catalyzed hydration of 3-hexyne at 30 °C in the presence of NBu_4OTf [a,b]*

Entry	L [c]	X^-	AgOTf (mol%)	Conv. (%)[d]	Timee (h) (TOF[f])
1 [g]	NHC^{iPr}	OTf^-	-	>99	2 (495)
2	NHC^{iPr}	Cl^-	0.1	70	2 (350)
3	BIAN	Cl^-	0.1	76	2 (380)
4	NHC^{CH2}	Cl^-	0.1	76	2 (380)
5	NAC	Cl^-	0.1	0	24
6	JPhos	Cl^-	0.1	75	4 (188)
7	PCy_3	Cl^-	0.1	0	24

8	PArF	Cl^-	0.1	0	24
9	PPh_3	Cl^-	0.1	0	24
10	POR_3	Cl^-	0.1	0	24
11	NHC^{iPr}	OTs^-	-	>99	3.5 (285)
12	BIAN	OTs^-	-	>99	4 (248)
13	NHC^{CH2}	OTs^-	-	98	8 (122)
14	NAC	OTs^-	-	9	24 (4)
15	JPhos	OTs^-	-	74	5 (148)
16	PCy_3	OTs^-	-	6	24 (3)
17	PArF	OTs^-	-	0	24
18	PPh_3	OTs^-	-	3	24 (1)
19	POR_3	OTs^-	-	17	24 (7)
20	BIAN	OTf^-	-	>99	2 (495)
21	NHC^{CH2}	OTf^-	-	>99	4 (248)

[a] Catalytic conditions: 3-hexyne (1.75 mmol, 200 µL), 5% NBu_4OTf (0.087 mmol, 34.3 mg), H_2O (1.92 mmol, 35 µL), L-Au-X (0.00175 mmol) and AgOTf (0.00175 mmol, 0,45 mg) when indicated. [b] mol% = (moles of catalyst / moles of alkyne) x 100. [c] see text. [d] Determined by ^1H NMR; averaged value of three measurements. [e] Time necessary to reach the reported conversion. [f] TOF = ($n_{product}$ / $n_{catalyst}$) / t(h) at the reported conversion. [g] entry 3 **Table 4** page 23.

The common catalytic run was performed by using the alkyne and 1.1 equiv. of H_2O with the catalyst (from 0.1 to 0.01 mol% with respect to the alkyne), AgOTf (when L-Au-Cl precatalysts were used), and an additive (up to 5 mol% with respect to the alkyne), in the temperature range 30-120 °C (**Table 7** and **Table 8**). In order to compare more easily the catalytic results with those reported in previous chapter, the complex NHC^{iPr}-Au-OTf has been included in **Table 7**. The evolution of the reaction was monitored by NMR spectroscopy (Experimental part, **Table S1**). To evaluate the catalytic activity of the catalysts in different conditions, the TOF value, (**Table 7** and **Table 8**) was calculated.

First, the chlorine complexes were tested in the presence of one equivalent of AgOTf (**Table 7**, entries 2-10). Gold complexes bearing PArF, NAC, PCy_3, PPh_3, and POR_3 ligands were catalytically inefficient, and after 24 h no conversion was observed (**Table 7**, entries 5 and 7-10). On the contrary, high but not quantitative conversion (around 75%) of **1** into **1a,** was reached in 2h using NHC^{iPr}, BIAN and NHC^{CH2} as ligands (**Table 7**,

entries 2-4, **Figure 18**), or 4h using the JPhos complex (**Table 7**, entry 6). The yields did not increase even after 24 h of reaction.

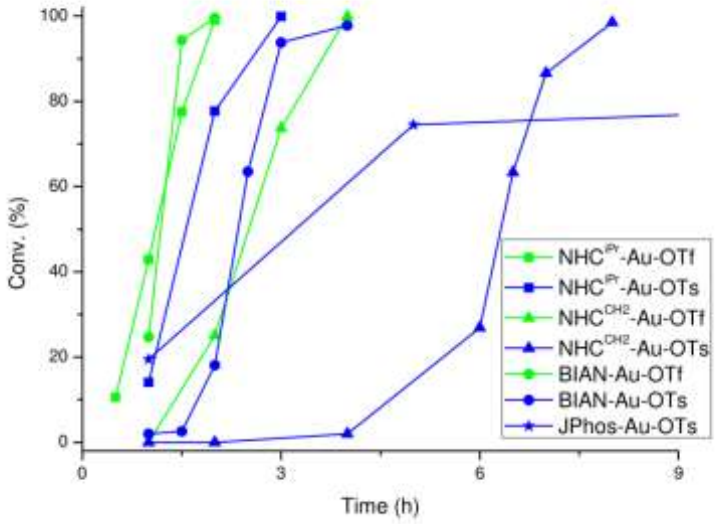

***Figure 18**:Hydration of 3-hexyne with 0.1% of L-Au-X in the presence of 5% NBu4OTf*

Notably, the TOF obtained by generating *in situ* the pre-catalyst with NHC^{iPr}-Au-Cl/AgOTf is 350 h^{-1}, a lower value with respect to that found in silver-free condition (495 h^{-1}, see **Table 7**, entry 1 vs. entry 2).

As mentioned before, for the systems bearing ligands such PCy_3, PArF, POR_3, PPh_3, and NAC (**Table 7**, entries 5 and 7-10) there is not formation of any product in 24 h. Hydration of 3-hexyne promoted by PPh_3-Au-Cl/AgOTf was studied by ^{31}P NMR spectroscopy (**Table 7**, entry 9) in order to understand the stability of gold complexes. The spectra were recorded at the end of the reaction (Experimental part) with a formation of a signal at δ 41.9 ppm due to the presence of $[(PPh_3)_2Au]OTf$[70b,96,97]. The decomposition of the catalyst takes place working in neat conditions. Moreover, the formation of a thin layer of gold on the walls of the reaction vessel was observed, a behavior already known in the literature.[98]

The decomposition process seems to be present, even when the more stable complex with NHC^{iPr} is used and induced by the silver salt giving no quantitative conversion of **1** into **1a** even after 24 h(**Table 7**, entry 1 vs. entry 2) after 24 h (Experimental part, **Table S4**). In gold catalysis the active role of silver additives is frequently discussed[99] and both positive and negative influence has been highlighted.[100]

In order to get over the decomposition of the gold catalyst, induced by silver, and compare different ligands, L-Au-OTs catalysts were tested because some catalyst with OTf ion are unstable and not isolable with all the ligands here employed.[32a,101] Unfortunately, even in these conditions, the deactivation or decomposition of catalysts with phosphines, was observed during the catalysis (**Table 7**, entries 16-19) with the exception of JPhos-Au-OTs, that gave a conversion of 74% after 5 h with a TOF of 148 h^{-1} (**Table 7**, entry 15), similarly to that obtained with the JPhos-Au-Cl/AgOTf system (**Table 7**, entry 6).[102] The catalytic activity of NHC^{iPr}-Au-

OTs when compared to that of NHC^{iPr}-Au-OTf shows the better performance of the latter (**Table 7**, entry 1 vs. entry 11). In fact, a full conversion of **1** into **1a** was observed with both species, but it was reached after 2 h using NHC^{iPr}-Au-OTf and 3.5 h using NHC^{iPr}-Au-OTs (see also **Figure 18**). A possible explanation of such a difference could be ascribed to the higher co-ordinating ability of OTs^-, when compared to OTf^-, toward the gold fragment. We have already reported above that OTs^- inhibited the hydration of 3-hexyne in neat conditions. It is likely that the non-active form NHC-Au-OTs is slowly converted into the most active species NHC-Au-OTf, during the reaction, due to the presence of the excess of NBu_4OTf.

On the bases of the following considerations: a) gold catalysts with phosphines are poorly active, b) catalysts can be deactivated by silver salts, c) L-Au-OTf species are more active than L-Au-OTs ones, the investigation to other gold catalysts with different NHC ligands and using OTf^- as the counterion was extend. Therefore, NHC^{CH2}-Au-OTf and BIAN-Au-OTf were tested and the results were compared with that obtained with NHC^{iPr}-Au-OTf. Full conversion of **1** into **1a** was reached in 2 h using BIAN-Au-OTf (**Table 7**, entry 20), whose activity was identical to that shown by NHC^{iPr}-Au-OTf (**Table 7**, entry 1). Much less efficiently, NHC^{CH2}-Au-OTf needed twice the time to promote the quantitative formation of **1a** (**Table 7**, entry 21).

The results demonstrate that the best performances, in the hydration of 3-hexyne in neat conditions, can be obtained avoiding the use of silver salts using L-Au-X complexes, where L is a NHC type ligand.

As previously reported (**Table 4**) regarding the use of ionic additives, NBu_4OTf acts like a PTC (phase transfer catalysis)[88] improving the speed of the reaction, while NH_4OTf does not show any effect and [BMIM]OTf even stops the reaction.

Different ammonium triflate salts were tested in order to understand the beneficial role of the ionic additive, varying the number and length of alkyl chains. Thus, we deeply investigated the effect using 5% of Bn_3NHOTf, Bu_2NH_2OTf, $Me_2(Et)(Dec)NOTf$, $(Cy)NH_3OTf$, and Aliquat-OTf in the catalytic performances of NHC^{iPr}-Au-OTf. Summarizing, we found that NBu_4OTf remains the best additive (Experimental part, **Table S5**), as previously observed.

The best system for the hydration of 3-hexyne was again NHC^{iPr}-Au-OTf/NBu_4OTf (5%), which was then applied to the hydration of diphenylacetylene (**13**), a very inactive solid alkyne that can be hydrated in neat conditions above its temperature of melting point (62° C), to afford 1,2-diphenylethanone (**13a**). The most salient results are summarized in **Table 8** and shown in **Figure 19**. The hydration of diphenylacetylene is a challenging reaction, frequently studied in the literature but using solvent and additives, such as silver salts and acids.[103] However, its optimization is far from being done and especially from a green point of view.

Table 8: NHC^{iPr}-Au-OTf catalyzed hydration of diphenylacetylene[a]

entry	Loading (mol%)[b]	T (°C)	Anion (X)	Conv.c (%)	Timed (h) (TOF[e])
1	0.1	65	OTf^-	82	8 (102)
2	0.05	80	OTf^-	42	8 (105)
3	0.05	120	OTf^-	94	4 (470)
4	0.025	120	OTf^-	85	8 (435)
5	0.01	120	OTf^-	27	5 (560)
6[f]	0.05	120	OTf^-	88	8 (220)
7	0.05	120	OTs^-	7	8 (17)

[a] Catalysis conditions: diphenylacetylene (1.75 mmol, 312 mg), 5% NBu_4OTf (0.087 mmol, 34.3 mg) and H_2O (1.92 mmol, 35 μL). [b] (moles of catalyst / moles of alkyne) x 100.c Determined by ^1H NMR; average value of three measurements. [d] Time necessary to reach the reported conversion. [e] TOF = (n product / n catalyst) / t(h) at the reported conversion. [f] with D_2O instead of H_2O.

Diphenylacetylene, 1.1 equiv of H_2O, and NHC^{iPr}-Au-OTf (from 0.01 to 0.1 mol% with respect to diphenylacetylene) were mixed with NBu_4OTf (5%) at the desired temperature. At 65°C with 0.1 mol% of catalyst, a high conversion of **13** into **13a** was obtained in 8h (**Table 8**, entry 1). The optimization of the reaction conditions was made by changing both temperature and catalyst loading (**Figure 18**). Almost full conversion (94%) of **13** was achieved by increasing the temperature to 120 °C and reducing the catalyst amount to 0.05 mol% (**Table 8**, entry 3). Unfortunately, decreasing the catalyst concentration (NHC^{iPr}-Au-OTf) down from 0.025 to 0.01 mol%, resulted in a progressive decay of the activity (**Table 8**, entries 4 and 5). The highest TOF (560 h^{-1}) was obtained at 120 °C with 0.01 mol% of catalyst loading (**Table 9**, entry 5), while the highest TON (3400) was obtained at 120°C with 0.025 mol% of NHC^{iPr}-Au-OTf. In these catalytic conditions, a very high EMY value (77) and an excellent E-factor value (0.03) were achieved.

The excellent results obtained by applying our protocol are highlighted in **Table 9**, where the results of the present catalytic condition are compared with the best ones reported in the literature. Tanaka and coworkers in 2002[18] studied the reaction using a phosphine gold complexes for the hydration of **2** by using strongly acidic conditions at 70 °C in methanol. A TON of 53 in 5 h was obtained, and the E-factor and EMY values were 6 and 10, respectively. Nolan and co-workers in 2009,[23] using a NHC gold(I) complexes, were able to reduce the catalyst loading down to 0.1%, using as solvent a 2:1 mixture of 1,4-dioxane/water, the temperature was increased to 120 °C and no acid was added, obtaining a maximum value of TON and TOF of 770 and 42 h^{-1}, respectively. Despite the increase of the TON, the EMY value obtained (13) was still low.

Moreover, TON of 400 and TOF of 67 h^{-1} were attained by the same group by using as the catalyst a dimeric $(NHC\text{-}Au)_2SO_4$ complex at 80 °C[104], however not improving the E-factor and EMY values. An appreciable maximum TOF of 283 h^{-1} was reached with a catalyst loading of 0.1 mol%. Although a marked improvement of E-factor (2.6) and EMY (28) values was reached, both are still very far from being acceptable in terms of effective green catalysis.

***Table 9**: Main parameters for hydration of diphenylacetylene in 1,2-diphenylethanone*

	Tanaka[18]	Nolan[23]	Nolan[104]	This work
Solvent	MeOH/H2O (2:1)	Dioxane/H2O (2:1)	MeOH/H2O (2:1)	-
TON	80	770	400	3400
TOF (h-1)	80	43	67	435
T (°C)	70	120	80	120
Ag+ additives	NO	YES	NO	NO
Other additives	YES (H2SO4)	NO	NO	YES (NBu4OTf)
E-factor	6	4.8	5	0.3
EMYa	10	13	10	77

a EMY= Effective mass yield

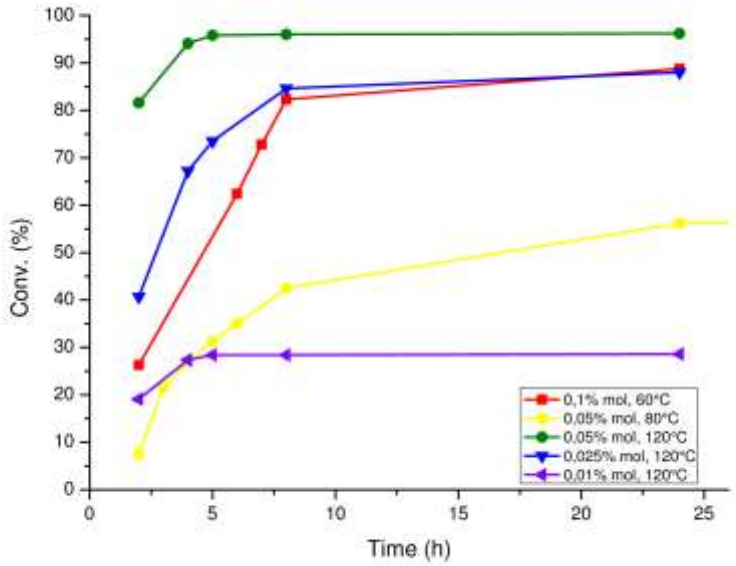

***Figure 19**: Hydration of diphenylacetylene with different loadings of NHC^{iPr}-Au-OTf, in the presence of 5% NBu$_4$OTf, at different temperatures.*

In order to shed some light on the reaction mechanism, we conducted some experiments using D_2O instead of H_2O to quantify the KIE value in these aprotic and apolar conditions at high temperature (**Table 8**, entry 6). Previously, we have found that the addition of 5% mol of NBut$_4$OTf resulted in a neat change of the KIE value from 3.8 to 2.5 in the solvent- and silver-free hydration of 3-hexyne as saw in previous chapter. These KIE values point out that the turnover-limiting step is the proton transfer. Using D_2O instead of H_2O, we observed a small reduction of TOF, which shifted from 470 to 433 h^{-1} (see Experimental part, **Table S6**, entries 3 and 6), and the calculated KIE was 1.2. Therefore, it is very plausible that in the hydration of diphenylacetylene the RDS can be the nucleophilic attack, because this substrate is much less reactive with respect to internal aliphatic alkynes.

Regarding the role of the counterion in the pre-equilibrium step, we have previously observed that when OTs^- is employed instead of OTf^-, the catalyst in the pre-equilibrium step is shifted towards the non-active inner sphere ion pair owing to the higher co-ordinating ability of OTs^- with respect to OTf^- towards cationic gold fragments. This difference is confirmed in the present work, as the conversion of 94% (4 h) shown by NHC^{iPr}-Au-OTf (**Table 8**, entry 3) drops to 7% (8 h) when NHC^{iPr}-Au-OTs is employed as the catalyst (**Table 8**, entry 7). We can conclude that, notwithstanding the temperature has been raised to 120 °C, the counterion effect is the same observed for the hydration of 3-hexyne. Thus, the equilibrium is strongly shifted towards the precatalyst when OTs^- is involved.

2.3. Hydration and alkoxylation of alkynes using NHC^{IPr}-Au-OTf in neoteric solvents

In the last two chapters, we investigated the activity of L-Au-X (L = NHC^{iPr}, BIAN, NHC^{CH2}, NAC, JPhos, $(RO)_3P$, PArF, PPh_3, and PCy_3; X^- = OAc^-, BAr^{F-}, BF_4^-, SbF_6^-, ClO_4^-, OTf^-, NTf_2^-, OTs^-, and TFA^-), as catalysts in the hydration of alkynes in neat conditions, without addition of acid and silver salts, at room/mild temperature and with suitable ionic additives.[105] The catalysis works with only two anions (OTf^- and NTf_2^-) owing to their intermediate co-ordinative and basic charateristic.[69]

On the other hand, for solid and/or viscous reagents these conditions are not suitable because of the immiscibility of the reagents. Moreover, it was observed that using a proper neutral (such as DMF and DMPU) or ionic (such as $NBut_4OTf$) additive could increase the reaction rate of the alkoxylation and hydration of alkynes. [70] According to the 12 principles of Green Chemistry[106], the use of green solvents with suitable functionalities seems to be a logical stop forward towards new, efficient and sustainable gold catalyzed reactions.

A key topic in organic synthesis is the replacement of VOS with green solvents[107], and bio-based solvents[108] are used in many transition metal catalyzed reactions. Thus, for example: water[109], γ-valerolactone[110], glycerol[111], lactic acid and its derivatives[112], D-limonene and *p*-cymene[113] are widely employed. Other examples of green solvents are biodiesel[114], $scCO_2$[115], perfluorinated hydrocarbons,[116] polyethylene glycol[117], Deep Eutectic Solvent[118] and ionic liquid[119].

Examples concerning the use of gold catalysts with neoteric solvents, instead of VOS, are missing in the literature. Recently, the group of García-Álvarez reported the use of DES in the tandem cycloisomerisation/Diels–Alder reaction using an iminophosphorane Au(I) complexes as catalyst.[120] The same catalyst, used in aqueous or eutectic-mixture solutions, was used in the cycloisomerization of alkynyl amides.[121] Another example of green chemistry in gold catalysis is the use of PPh_3-Au-Cl in PEG for the oxidation to amides, starting from aldehydes and amines.[122]

Here the results of the investigation on the activity of NHC^{iPr}-Au-OTf catalyst in the alkoxylation and hydration of alkynes in a wide set of neuteric solvents are reported. NHC^{iPr}-Au-OTf was synthesised according to the procedure developed by Nolan and co-workers[87], by addition of HOTf to the acetonyl complex NHC^{iPr}-Au-CH_2-(C=O)CH_3 (see Synthesis and characterization in the Experimental part) in order to completely avoid the use of any silver additive, even in the generation of the gold catalyst. NHC^{iPr}-Au-OTf has been used as catalyst in the methoxylation of **1** into **1a** (**Table 10**) and in the hydration of alkynes (**Table 11**, **Table S8** and **Table S9**) in different solvents.

***Table 10**: NHC^{iPr}-Au-OTf catalysed methoxylation of 3-hexyne[a]*

Entry	Solvent	Conv. (%) [b]	Time[c] (h)	TOF[d] (h^{-1})	ε_r[e]
		VOS			
1	chloroform	99	2	288	4.81
2	dichloromethane	96	6	220	8.93
3	acetone	98	4	280	21.0
4	3-nitrotoluene	98	6.5	180	22.2
5	nitromethane	63	24	80	37.3
5a	nitromethane[f]	27	24	14[g]	37.3
5b	nitromethane[h]	9	24	9[g]	37.3
		Green			
6	perfluoro-decalin[i]	99	1	495	1.94
7	*p*-cymene	99	1	495	2.24
8	d-limonene	96	4	205	2.4
9	propionic acid	77	2	350	3.35
10	ethyl palmitate[i]	99	2	340	3.07
11	anisole	96	2	315	4.3
12	isopropyl acetate	96	2	285	6.3
13	PEG-400	0	8	0	12.4
14	MIBK[j]	99	4	235	13.1
15	ethyl lactate	89	2	223[g]	15.4
16	cyclohexanone	94	4	290	16.1
17	propionitrile	9	2	20	29.7
18	γ-valerolactone	96	4	340	36.9
18a	γ-valerolactone[f]	69	6	84[g]	36.9
18b	γ-valerolactone[h]	52	8	36[g]	36.9
19	DMSO	51	24	5	47.2
20	glycerol	99	2	255	46.5

21	glycerol[k]	9	2	2	46.5
22	propylene carbonate	98	11	145	66.1
23	cit.ac.-DMU [l]	95	6.5	145	-
24	chOTf-DMU [m]	98	6	270	-

[a] Catalysis conditions: NHC^{iPr}-Au-OTf (0.0022 mmol, 1.5 mg) 3-hexyne (1.1 mmol, 125 µL), MeOH (2.2 mmol, 89 µL), solvent (200 µL). [b] Determined by ^{1}H NMR; average value of three measurements. [c]Time necessary to reach the reported conversion. [d] TOF = (mol $_{product}$ / mol $_{catalyst}$) / t calculated after 1 h of reaction. [e] ε_r = dielectric constant[123]. [f] Amount of solvent increased to 500 µL. [g] Calculated at 2h. [h] Amount of solvent increased to 1250 µL. [i] Two phases were observed.[124] [j] MIBK= methyl-isobutyl ketone. [k] Conducted without MeOH, TOF and conversion are related to the formation of acetal of glycerol. [l] Citric acid (2 equiv)/dimethyl urea (3 equiv). [m] Choline triflate (1 equiv)/ dimethyl urea (2 equiv).

A typical catalytic run was performed by mixing 3-hexyne, 2.0 equiv. of MeOH, the catalyst (0.2 mol% with respect to the substrate) and the proper solvent (0.2 mL) at 30 °C (**Table 10**). The progress of the reaction was checked by NMR spectroscopy, integrating the signal of the ketone formed by hydrolysis of the product 3,3-dimethoxyhexane (see the Experimental part).

The complex NHC^{iPr}-Au-OTf was inefficient in PEG-400 only, as no formation of the product was detected after 8h (**Table 10**, entry 13). On the contrary, high or full conversion (>99%) of **1** into **1a** was obtained in 1-24 h using green solvents instead of VOS (**Table 10**).

For the catalysis in VOS, full conversion (>96%) of **1** into **1a** was reached in 2 h in chloroform, 6 h in dichloromethane, 4 h in acetone and 6.5 h 3-nitrotoluene (**Table 10**, entries 1-4). Lower activity of the catalyst NHC^{iPr}-Au-OTf was found using nitromethane as solvent, with a yield of 63% after 24 h (**Table 10**, entry 5). As expected, an increase of volume of nitromethane, from 200 to 1250 µl, resulted in an increase of the reaction time (**Table 10**, entries 5a and 5b).

The use of neoteric solvents generally decreases the reaction time and gives higher conversions. Full conversion in 1 h was obtained using *p*-cymene and perfluorodecalin, while ethyl palmitate, anisole, isopropyl acetate, ethyl lactate, and glycerol, required a double time. With D-limonene, MIBK, cyclohexanone and γ-valerolactone, 4 h were necessary for obtaining full conversion and, finally, quantitative yield was obtained after 6 h, using DES solvents, which were formed by mixing 3 equiv. of dimethyl urea with 2 equiv. of citric acid (cit.ac.- DMU in **Table 10**, entry 23) or 2 equiv. of dimethyl urea with 1 equiv. of choline triflate (chOTf-DMU in **Table 10**, entry 24). With propylene carbonate (PC) and dimethyl sulfoxide (DMSO) the reaction proceeded very slowly. In fact, 11 h were necessary to reach 98% of conversion in PC, (**Table 10**, entry 22), while with DMSO only 51% of conversion in 24 h was obtained (**Table 10**, entry 19). As observed for nitromethane, if the volume of γ-valerolactone is increased up to 1250 µl a much longer reaction time was necessary (**Table 10**, entries 18, 18a, 18b) and full conversion was obtained in 24 h.

The analysis of the catalytic activity of NHC^{iPr}-Au-OTf in different solvents was made possible by comparing the values of turn over frequency (**Table 10**). The TOFs for the reaction run in VOS are between 288 (nitromethane) and 80 h^{-1} (chloroform) (**Table 10**, entries 1-5). A general trend was observed: increasing the polarity of the solvent, the TOF value decreases. This finding points out the specific role of the anion during the reaction, and therefore the importance of the equilibrium ion pair/free ions of NHC^{iPr}-Au-(3-hexyne)OTf (**Figure 20**).

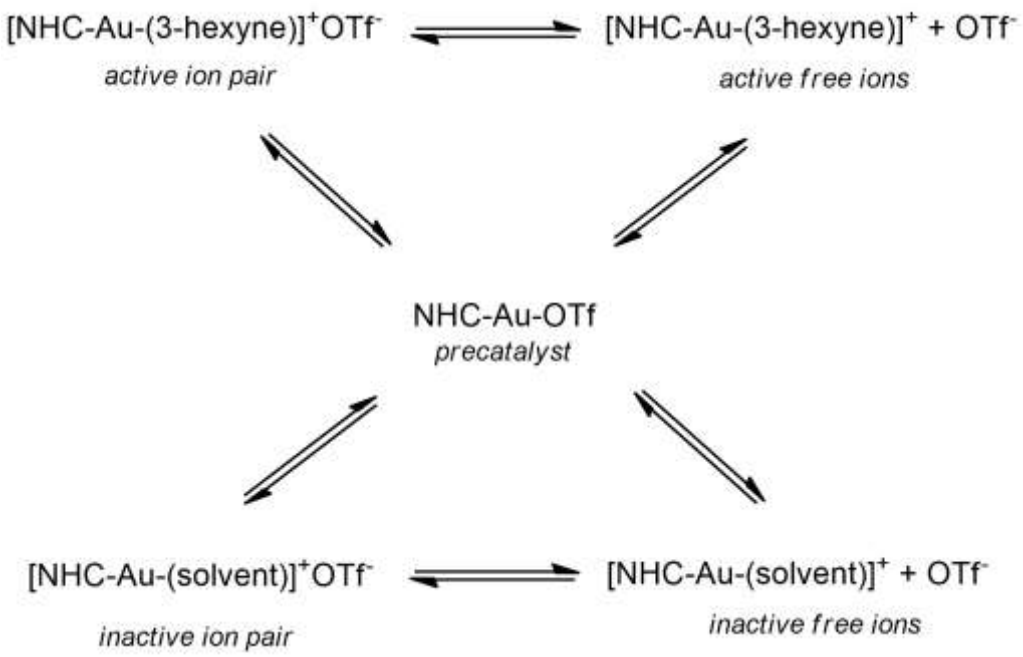

***Figure 20**: The equilibria of the precatalyst with alkyne and solvent and the free ions/ion pair.*

By means of PGSE (Pulsed field Gradient Spin Echo) NMR spectroscopy, were have already investigated the aggregation level, as a function of concentration and solvent, between the counterion and cationic linear gold complexes with different ligands, such as carbenes and phosphines.[125] Different scenarios were obtained: in chloroform (ε_r = 4.80) the ion pair is the predominant species, with highly polar solvents such as methanol (ε_r = 32.66) free ions is the main situation, while in medium polarity solvents such as methylene chloride (ε_r = 8.93) the presence of both free ions and ion pairs was detected.

As previously found, in the methoxylation of alkynes, experimental and theoretical observations demonstrate that the counterion can promote both nucleophilic attack[68b,69,32b] and proton shuttle.[31] So, during the nucleophilic attack the anion acts as a template through the formation of a hydrogen bond and during the protodeauration step it can help the displacement of the proton.

By decreasing the concentration of the catalyst and increasing the polarity of the solvent, the equilibrium of the precatalyst is moved to the free ions condition instead of ion pair (**Figure 20**), therefore the anion isn't involved during the nucleophilic attack and protodeauration steps. For this mechanism, a second molecule of methanol was supposed to participate in the reaction.[69] In this condition, the higher TOF value found using

acetone compared to that obtained using 3-nitrotoluene (very similar dielectric constant values, see **Table 10**, entry 3 vs. entry 4) can be attribute to the carbonyl functionality that has a role in the reaction mechanism.[70]

The catalytic activity of NHC^{iPr}-Au-OTf is directly correlated to the polarity of the green solvent. Moreover, peculiar functional groups present on the solvent could *i*) actively participate during the nucleophilic attack and/or protodeauration, *ii*) interact with the catalyst affecting its performances, due to the co-ordination of the solvent to the metal center with the formation of inactive NHC^{iPr}-Au(solvent)OTf species (**Figure 20**).

For solvents having low dielectric constant values (< 2.4) higher TOFs were obtained, this is the case of *p*-cymene and perfluorodecalin both with a TOF of 495 h^{-1} (**Table 10**, entries 6 and 7). Using propionic acid, ethyl palmitate, anisole, and isopropyl acetate as the solvent, whose dielectric constant values are distributed from 3.1 to 6.3, high TOF values were obtained in the range of 285-350 h^{-1} (**Table 10**, entries 9-12). An exception was found for D-limonene as a low TOF value of 205 h^{-1} was obtained notwithstanding its low dielectric constant (2.4) (**Table 10**, entry 8). This result should be ascribed to the greater affinity of the gold fragments to the double bond with respect to the triple bond.[98b] Complexes like L-Au-(alkyne/alkene)X have been synthesized and characterized and their behaviour in solution has been studied.[126] The active catalyst could be deactivated by the co-ordination of the D-limonene and consequently the TOF decreases (**Figure 20**).

For the propionic acid the TOF is in line with that found for the other solvents having similar dielectric constant, moreover the reaction does not speed up even in the presence of a Brönsted acid, in view of the fact that the rate determinate step is the nucleophilic attack.[68]

For the solvents having an intermediate dielectric constant value (from 12 to 20), the TOF value decreases when compared to those having low polarity. The TOFs span from 223 h^{-1} for ethyl lactate (**Table 10**, entry 15) to 290 h^{-1} for cyclohexanone (**Table 10**, entry 16). The higher value found for cyclohexanone could be ascribed to the presence of the carbonyl group, as for acetone (see above). Interesting, after 8 h no conversion was obtained using PEG-400. In a previous work, dealing with the alkoxylation of 3-hexyne using NHC^{iPr}-Au-X (X = OTs, BArF) as catalyst and triethylene glycol monomethyl ether as the solvent, it was noted that the decrease of the reaction rate is due the presence of the poly-ether functionality.[68b] Moreover, with both catalysts a complete conversion is obtained in similar reaction time because the O-H bond may be polarized by specific intramolecular interactions, suppressing the anion effect (note that when methanol is used as the nucleophile, the reaction promoted by NHC^{iPr}-Au-BArF is about five fold slower than that catalyzed by NHC^{iPr}-Au-OTs). Therefore, both the counterion and methanol can be inhibited by the solvation ability of PEG-400 during the reaction.

For the green solvents with dielectric constant higher than 27 (**Table 10**, entries 17-22) a contradictory behaviour has been found (TOF vs. ε). In particular, TOFs of 20 and 5 h^{-1} were obtained using propionitrile and DMSO, respectively (**Table 10** entries 17 and 19). This low catalytic activity of NHC^{iPr}-Au-OTf in these two solvents can be ascribed not only to their high dielectric constant, but also to their high co-ordination ability towards gold (**Figure 20**).[127] Nolan and coworkers,[128] who synthesized a stable NHC-Au-acetonitrile complex used as precatalyst, noticed that a strong excess of propionitrile inhibited the formation of the catalytic active gold-alkyne complex, reducing the TOF value (**Figure 20**). Also Zhdanko and Maier observed that 3-hexyne is less co-ordinating to gold than DMSO[32a] (**Figure 20**), consequently the use of DMSO will involve a reduction of catalytic activity.

Using glycerol as the solvent, notwithstanding its high dielectric constant of 46.5, a relative high TOF value of 255 h^{-1} has been obtained (**Table 10**, entry 20). It was already found, from experimental[70b] and theoretical[69] measurements, that the nucleophilic attack of MeOH can be promoted\assisted by a network of methanol molecules. Moreover, in glycerol, thanks to its high dielectric costant, the gold catalyst is prevalently present in solution as free ions, therefore during the nucleophilic attack the high catalytic activity could be ascribed also to the active role of glycerol in the reaction. Besides, methanol and glycerol should have similar coordination ability towards the gold center, but lower than that shown by 3-hexyne.[32a] It was observed (**Table 10**, entry 21) that using pure glycerol without MeOH, a negligible amount of the diacetal was formed. This finding rules out the possibility that glycerol can attack the alkyne thus diminishing the substrate amount during the nucleophilic attack of methanol.

Finally, a brief comment on the values of TOFs achieved using γ-valerolactone (340 h^{-1}) and propylene carbonate (145 h^{-1}) should be done (**Table 10**, entries 18 and 22). As previously suggested for high polarity solvents, the equilibrium is shifted to free ions instead of ion pairs (**Figure 20**). In each of these solvents a functional group that resembles those in DMPU and DMF is present, compounds known to increase the reaction rate in the alkoxylation of alkynes.[70] We are led to belief that these solvents have an active role during the reaction, in particular they *i*) allow the co-ordination of 3-hexyne not interacting with the NHC-Au^{+} fragment, *ii*) can interact with the methanol during the nucleophilic attack, and *iii*) can assist the protodeauration step.

For both DESs employed for this catalysis, the dielectric constant values are not reported in the literature,[129] however it is possible to justify their relatively high TOFs values (**Table 10**, entries 23 and 24). In the case of cit. ac.-DMU, the urea has the right functionality (as previously mentioned for γ-valerolactone and propylene carbonate) to promote the nucleophilic attack of MeOH to the substrate. Differently, the chOTf-DMU mixture increases the catalytic performance due to i) the urea functional group and ii) the huge amount of triflate ions that have an active role in the alkoxylation reaction.[69]

For all the solvents employed in this investigation, the TOF value has been plotted against the dielectric constant (**Figure 21**). It can be observed that the value of TOF is generally almost inversely correlated to the dielectric constant, with the exception of the solvents having particular functionalities able to help the reaction steps (like acetone, cyclohexanone, γ-valerolactone and propylene carbonate) or, on the opposite, to inhibit the reaction (D-limonene, propionitrile and DMSO). It appears clear from **Figure 21** that the major deviation is represented by γ-valerolactone.

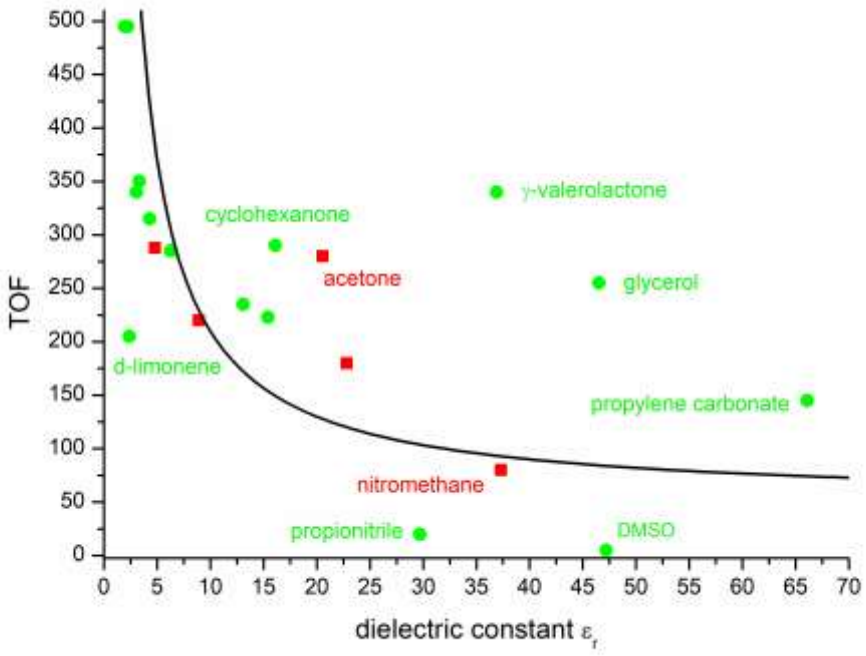

***Figure 21**: TOF vs dielectric constant for VOS (red, in the order from left to right: chloroform, dichloromethane, acetone, 3-nitrotoluene, and nitromethane) and green solvents (green, in the order form left to right: perfluoro-decalin, p-cymene, D-limonene, propionic acid, ethyl palmitate, anisole, isopropyl acetate, MIBK, ethyl lactate, cyclohexanone, propionitrile, γ-valerolactone, DMSO, glycerol, and propylene carbonate) employed in the methoxylation of 3-hexyne catalysed by NHCiPr-Au-OTf (selected values from Table 10).*

DFT calculations have been performed (see Experimental part), in order to deeply understand why γ-valerolactone gives an unexpected and good activity of NHC^{iPr}-Au-OTf in the methoxylation of 3-hexyne. We have focused on the more active catalysis in γ-valerolactone (GVL) with respect to the less active in nitromethane (NM), two solvents that have similar dielectric constant (ε_r = 36.9 for GVL, ε_r = 37.3 for NM, see **Table 10**). As mentioned above,[37,] it is known that the rate determining step (RDS) is the nucleophilic attack for the NHC gold(I)-catalyzed alkoxylation of alkynes where the anion, acting as a template, holds the alcohol in the right position for the outer-sphere attack, and moreover behaves as a hydrogen-bond acceptor, enhancing the nucleophilicity of the attacking alcohol. In the calculations, complex NHC'-Au-OTf (NHC' = 1,3 dimethylimidazol-2-ylidene) was considered as the catalyst and 2-butyne as the substrate. The influence of both solvents, NM and GVL, was analyzed in the addition of methanol to 2-butyne in the nucleophilic attack step, by adding an explicit solvent molecule. All the implicit solvent COSMO calculations have been performed using NM as the solvent (dielectric constant ε_r = 35.87 in ADF2014.05 program). The extreme

scenario would be γ-valerolactone replacing the anion role in the nucleophile activation of methanol, operating more efficiently and eventually the interaction solvent-anion, also increasing the solvent efficiency in this process, giving the superior performance of NHC^{iPr}-Au-OTf in GVL. To investigate this assumption, were studied the activation energy barriers for the nucleophilic attack step assisted by the solvent (both GVL and NM) and by the anion. These preliminary results are reported in the Experimental part (**Figure S12**-**Figure S17**) and show that the anion can activate the nucleophile much better than the solvent molecule. A higher activation energy barrier has been found for both NM and GVL-assisted nucleophilic attack, with respect to that obtained for the nucleophilic attack assisted by the counterion OTf^-. Thus, in this extreme scenario, it can be ruled out that the better performance of the catalyst for the activation of methanol in GVL could be ascribed to a replacement of OTf^- with a molecule of solvent. It seems that the interaction solvent-anion could influence the counterion role in the nucleophilic attack. Two different experimental conditions need to be studied: *i)* ion pairs as the major species, where the anion could have a different behavior in GVL and NM, and *ii)* free ions as the major species, where the solvent can activate the methanol in the absence of the anion.

First the condition *i)* has been analyzed, and it seemed helpful to analyze the nucleophilic attack step in the following conditions: i) using COSMO implicit solvent nitromethane (COSMO NM), ii) with COSMO NM plus one solvent molecule of NM, iii) with COSMO NM plus one solvent molecule of NM interacting with the anion, and iv) with COSMO NM plus one solvent molecule of GVL interacting with the anion. These four reaction profiles are shown in **Figure 22**.

The optimized geometrical structures of all the compounds shown in **Figure 22** are reported in the experimental part (Figures **Figure S12**, **Figure S15,**

Figure *S18*, Figure *S20*). Using only one implicit NM solvent molecule in the transition state structure, it has been found an activation barrier of 10.2 kcal/mol (TS COSMO NM, **Figure 22**) for the nucleophilic attack and the product formed is 2.8 kcal/mol lower in energy if compared to the reactant complex (Experimental part,

Figure S18). The OTf^- counterion is positioned far from the gold center close to the substrate, generating a hydrogen bond with the hydrogen of the methanol hydroxyl group. Using an explicit molecule of solvent (NM) the small interaction with the nucleophile decreases the activation energy barrier to 8.7 kcal/mol (TS_OTf(NM)', **Figure 22**). The hydrogen bond between NM and methanol can also stabilize the product with a lower 5.4 kcal/mol energy compared to the corresponding reactant complex (Experimental part, **Figure S19**). Introducing the explicit molecule of solvent (NM or GVL) and the anion, a different structure for the reactants complex should be taken into account because of different interactions.

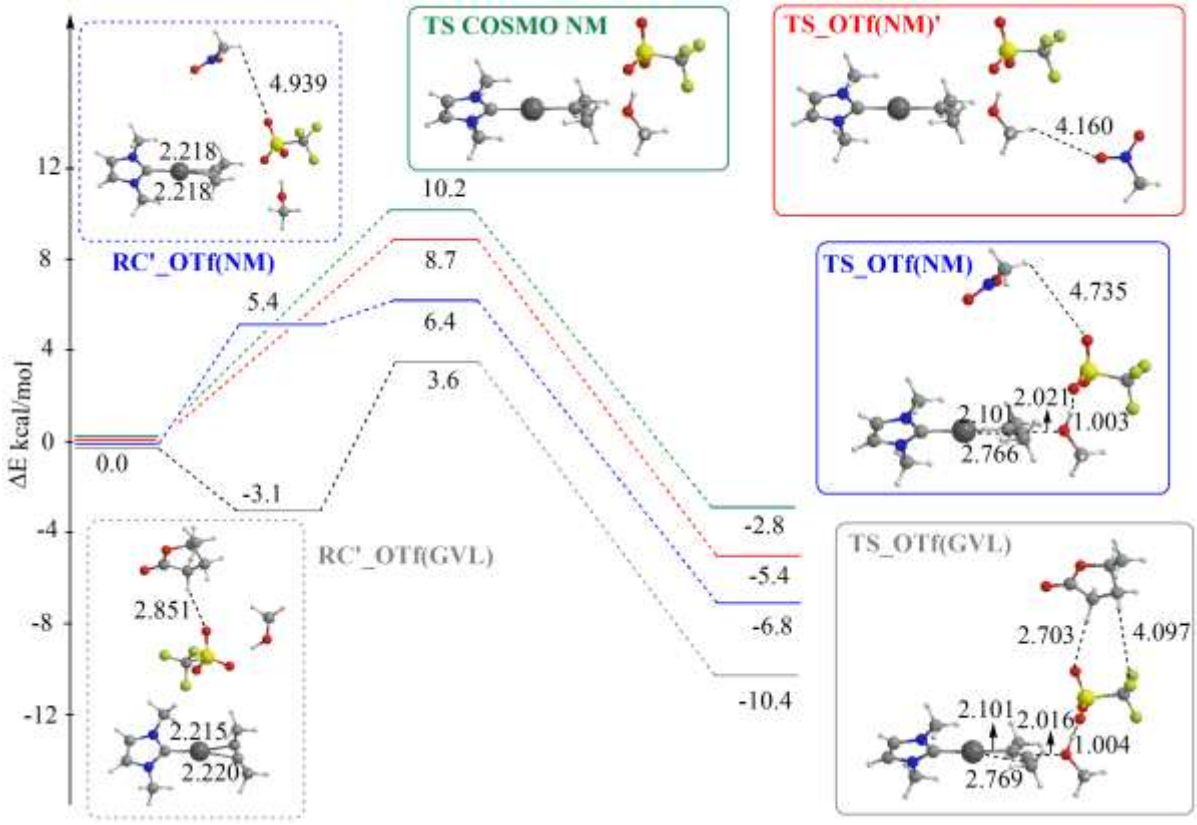

***Figure 22**: Energy profile for the nucleophilic attack step for the reaction between 2-butyne and methanol catalyzed by NHC'-Au-OTf. Energy profiles in different colors describe different process conditions. Green: implicit solvent COSMO NM; red: COSMO NM plus one explicit solvent NM molecule; blue: COSMO NM plus one explicit NM solvent molecule interacting with OTf^-; grey: COSMO NM plus one explicit GVL solvent molecule interacting with OTf^- . The structures of the most important involved species are also shown. Energy values (kcal/mol) refer to corresponding RC_X(Y) complex taken as zero.*

Two conformations are taken into account between the many possible structures arising from different positions of the anion with respect to gold, that where OTf^- is extracted from the metal center by interaction with a solvent molecule. We indicate them as complex RC'_OTf(GVL) and RC'_OTf(NM) for explicit GVL and NM molecule, respectively (**Figure 22** and **Figure S20** in the Experimental section). Comparing the corresponding RC_X(Y) structure where OTf^- is positioned above gold with a weak interaction (**Figure S12** and **Figure S15** in the Experimental part), there is a destabilization with NM-anion interaction of 5.4 kcal/mol, while the GVL-anion interaction stabilizes the structure of 3.1 kcal/mol (**Figure 22**). This outcome suggests that the interaction anion-solvent (ion-dipole) promotes the separation of ion pair $[NHC'\text{-Au-2-butyne}]^+/OTf^-$ in GVL due to the higher polarity in comparison with nitromethane (the dipole moment is 4.71 D for GVL and 3.46 D for NM), with a better stabilization for the RC'_OTf(GVL) complex compared to RC_OTf(GVL) structure. However, looking at the kinetics for the nucleophilic attack assisted by the anion interacting with the solvent molecule, the activation energy barrier is lower for nitromethane than for γ-valerolactone (1.0 kcal/mol for NM vs. 6.7 kcal/mol for GVL, **Figure 22**), notwithstanding the structure TS_OTf(NM) is less stable than TS_OTf(GVL). The global efficiency of the process, kinetic and thermodynamic, is regulated by the different

polarity of the solvents. Within this outline, to reach the transition state TS_OTf(NM) about all the energy barrier comes from the separation process of $[NHC'\text{-}Au]^+/OTf^-$, whereas to get the transition state TS_OTf(GVL), it appears to principally come from the GVL/OTf^- interaction (i.e., thanks to its high dipole moment, the affinity for the anion is higher for GLV), thus the anion doesn't participate during the nucleophilic attack. Moreover, the highest energy point for NM (blue) is about 6.4 kcal/mol and for GVL (grey) is 3.6 kcal/mol in the reaction profiles (**Figure 22**), in line with the experimental results. The consideration of the anion effect on the substrate activation, is required for the explanation of the larger stability of TS_OTf(GVL) with respect to TS_OTf(NM), which has been recognized by Zuccaccia et al.[37b,130] in the alkoxylation of alkynes promoted by L-Au-X catalysts**.** The ion pair separation of $[NHC'\text{-Au-2-butyne}]^+/OTf^-$ and the great affinity of GVL for OTf^-, should move more easily the 2-butyne from the symmetrical η^2 co-ordination to the cationic fragment $[NHC'\text{-Au}]^+$. In the transition state upon the butyne $\eta^2 \rightarrow \eta^1$ deformation, the substrate increases its electrophilicity making easier the charge transfer from the nucleophile to the carbon (C1) more far from gold. Moreover, the Au-C1 bond distance and the nucleophilic attack activation barrier can be correlated.[130] By simply comparing the Au-C1 distances, in TS_OTf(NM) is about 2.766 Å and in TS_OTf(GVL) is about 2.769 Å (**Figure 22**), the smaller deformation $\eta^2 \rightarrow \eta^1$ obtained whit OTf^-/NM in TS_OTf(NM) structure, compared with TS_OTf(GVL), indicates the decrease of the charge subtracted from the substrate and so the higher energy. By comparing their Au-C1 and Au-C2 bond distances in RC_OTf(GVL) and RC_OTf(NM) (Au-C1 = 2.220 Å, Au-C2 = 2.215 Å in RC_OTf(GVL); Au-C1 = Au-C2 = 2.218 Å in RC_OTf(NM)), this anion effect on the substrate activation is evident. The higher affinity of GVL to the $[NHC'\text{-Au}]^+$ fragment compared to OTf^-, leds the 2-butyne leaving the symmetrical η^2 coordination. Even if the deformation of the 2-butyne η^1 mode for TS_OTf(NM) and TS_OTf(GVL) complexes is very similar (the difference Δ(Au-C1) is 0.003 Å), the amount of electronic charge subtracted from the region where the nucleophilic attack occurs change significantly and, consequently, the activation energy barrier changes. To get an estimation, the difference of the η^1 deformation for 2-butyne in the transition states of [NHC-Au-2-butyne]OTs and $[P(^tBu)_3\text{-Au-2-butyne}]OTs$ for the nucleophilic attack of methanol is 0.008 Å, subtracting from the triple bond a difference in electronic charge of 0.016e, in agreement with the differences in the activation energy barriers on the order of few kcal/mol.[37b] For similar interactions, it makes sense to assume that the ΔC1 value we are facing, can directly regards the difference of stability calculated between TS_OTf(NM) and TS_OTf(GVL), on the order of few kcal/mol. Thus, the more efficient activation of the substrate by the fragment $[NHC'\text{-Au}]^+$ in different solvents (different polarity) gives a different grade of ion pair separation $[NHC'\text{-Au-2-butyne}]^+/OTf^-$, due to the different solvent/OTf^- affinity and, with the more polar solvent inducing, it affects the electrophilic character of the alkyne at the transition state.

Using experimental condition *ii)* with COSMO NM, plus one solvent molecule of NM (i.e. free ions), the solvent polarity effect on the nucleophilic attack step in the reaction between methanol and 2-butyne can be estimated by comparison between the energy profiles of chloroform (TCMA) (d = 1.01 D), nitromethane

(NM) (d = 3.46 D) and γ-valerolactone (GVL) (d = 4.71 D), in the absence of the OTf^- anion (free ions), in the increasing polarity order. Results are shown in **Figure 23** and optimized geometrical structures are reported in the Experimental part (

Figure ***S21*** and **Figure S23**). As expected, the solvents can stabilize the transition state structures in the order GVL (8.3 kcal/mol) > NM (10.3 kcal/mol) > TCMA (15.1 kcal/mol) following the polarity. Contrarily to TCMA and NM, the energy profile of GVL is appreciably different, in fact looking at the structures of transition state, it is possible to notice that the distance between the oxygen atom of methanol and the C1 carbon atom of 2-butyne decreases from 2.027 Å in $[TS\_GVL]^+$ to 1.978 Å in $[TS\_NM]^+$ and 1.884 Å in $[TS\_TCMA]^+$. At the same time, the slippage of 2-butyne from the symmetrical η^2 co-ordination become smaller in $[TS\_GVL]^+$ than in both $[TS\_TCMA]^+$ and $[TS\_NM]^+$, where the η^1 co-ordination of the substrate is due to the almost completely formed bond between the oxygen atom of methanol and the C1 of 2-butyne. In addition, thanks to the Voronoi Deformation Density (VDD)[131] analysis, the charge on the oxygen atom of the methanol is -0.146 for GVL, -0.126 for NM, and -0.098 for TCMA, thus suggesting that the electronic charge has been already transferred to C1 in $[TS\_TCMA]^+$ and $[TS\_NM]^+$, but not yet in $[TS\_GVL]^+$. At last, on the oxygen atom of the hydroxyl group of methanol the VDD charges in the structures TS_OTf(GVL) and TS_OTf(NM) (**Figure 23**) are both -0.141. These findings show the active participation of GVL on the polarization of the hydroxyl group of the methanol for the nucleophilic attack, thanks to its intrinsic polarity.

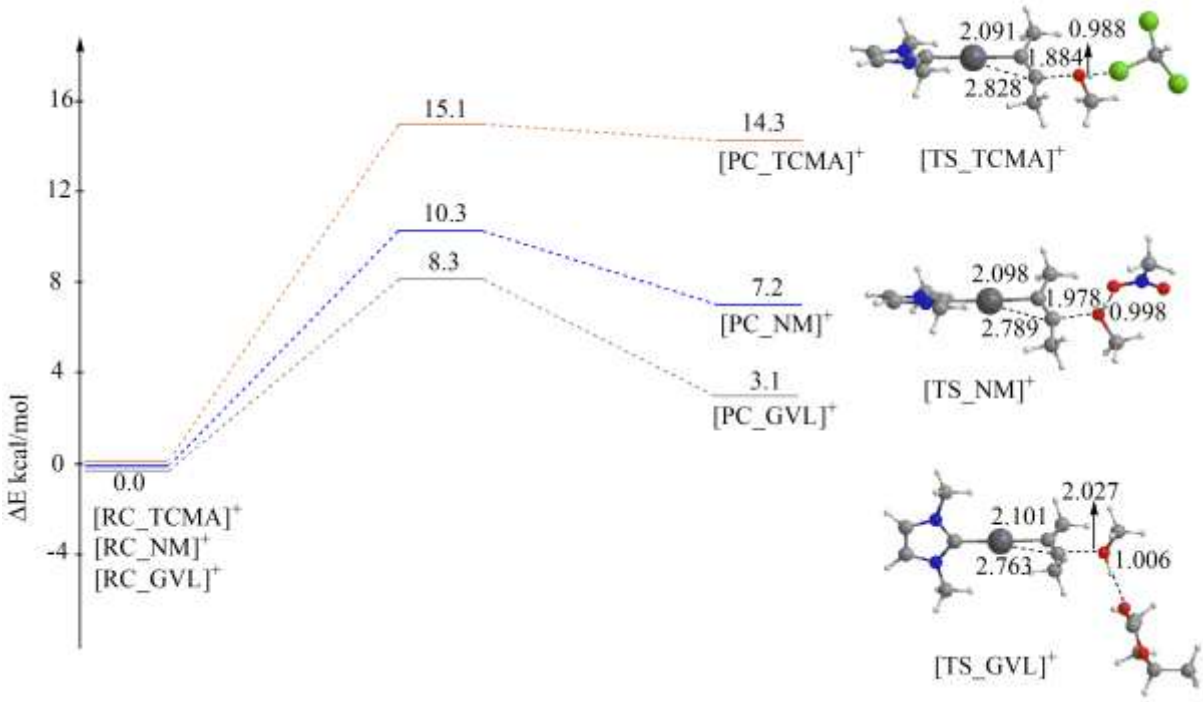

Figure 23*: Energy profile for the nucleophilic attack step for the reaction between 2-butyne and methanol catalyzed by [NHC'-Au]+. Energy profiles in different colours describe different solvents. Red: chloroform (TCMA); blue: nitromethane (NM); grey: γ-valerolactone (GVL). The structures of the transition states are also shown. Energy values (kcal/mol) refer to corresponding reactant complexes [RC_X]+ taken as zero.*

In conclusion, the catalytic activity of NHC^{iPr}-Au-OTf in the methoxylation of 3-hexyne is higher in γ-valerolactone than in nitromethane, and this can be attributed to the different polarity of the two solvents. This affects the participation of the counterion during the nucleophilic attack, if ion pairs are taken into account. For γ-valerolactone, the more polar solvent, the ion pair separation is higher than in nitromethane. The stability of the transition state is more enhanced by the lower anion affinity for the cationic fragment in the polar solvent which, on the other hand, increases the electrophilic character of the substrate. By the way, if free ions are taken into account, γ-valerolactone can both stabilize cationic transition states and increase the polarization of the hydroxyl group of methanol.

In the alkoxylation of alkynes, GVL has a beneficial role, therefore it was tested even in the reaction of hydration of diphenylacetylene (**13**), an inactivate solid alkyne, that cannot be hydrated in neat conditions at 30°C, as for liquid alkynes, above discussed.[105] GVL is suitable for this reaction because it possesses a good miscibility with water, has a high boiling point and might play a helpful role in the mechanism of hydration of alkynes. The main results are reported in **Table 11**.

The catalysis was run by mixing diphenylacetylene, 1.1 equiv. of H_2O and the gold catalyst (from 0.5 down to 0.05 mol% catalyst loading with respect to diphenylacetylene), and adding 240 μL of GVL at the suitable temperature (Table 2). The progress of the reaction was monitored by NMR spectroscopy (Experimental part). Almost full conversion of **13** into **13a** was obtained with 0.1 mol% of catalyst loading at 120°C (**Table 11**, entry 1) and with 0.25 mol% catalyst loading at 80° C (**Table 11**,entry 4). As expected, upon decreasing the temperature to 50 °C, it was necessary to increase the catalyst loading up to 0.5 mol% in order to have good conversion. On the other hand, with a catalytic loading below 0.05 mol% at 120° C the catalyst wasn't active or gave a poor conversion (**Table 11**, entries 2 and 3).

Similar results were obtained using ethyl lactate (**Table 11**, entry 7), while propylene carbonate gave worst results (**Table 11**, entry 8), in line with previous findings in the alkoxylation of 3-hexyne (**Table 10**, entry 22).

With a catalyst loading of 0.1 mol% at 120°C a high conversion (77 %) can be reached just in only 1 h (TOF of 770 h^{-1}) (**Table S8, Figure S5**), for comparison see **Table 11**, entry 1. With respect to the values found in the literature, such a value is one order of magnitude higher[23], confirming the beneficial effect of GVL for the hydration of diphenylacetylene with respect to VOS, as already discussed above for the alkoxylation of 3-hexyne.

***Table 11**: NHC^{iPr}-Au-OTf catalysed hydration of diphenylacetylene in GVL[a]*

Entry	Loading (mol%)[b]	T (°C)	Conv. (%)[c]	Time[d] (h)	TOF[e] (h^{-1})
1	0.1	120	99	3.5	283
2	0.05	120	15	6	50
3	0.02	120	-	30	-
4	0.25	80	86	7	49
5	0.5	50	90	9	20
6	0.25	50	70	9	31
7[f]	0.25	50	65	9	28
8[g]	0.25	50	34	24	6

[a] Catalysis conditions: diphenylacetylene (0.5 mmol, 89 mg), water (0.55 mmol, 9.9 μL) and GVL (240 μL). [b] (mol of catalyst / mol of alkyne) x 100. [c] Determined by ^{1}H NMR; average value of three measurements. [d] Time necessary to reach the reported conversion. [e] TOF = (mol $_{product}$ / mol $_{catalyst}$)/t(h) at the reported conversion. [f] ethyl lactate instead of GVL. [g] propylene carbonate instead of GVL.

Others alkynes were screened to verify the scope of this methodology (**Table S9**). Several internal and terminal alkynes were tested, bearing different alkyl and aromatic groups, using GVL as the solvent. The corresponding ketones were obtained in high yield, with values of TON and TOF comparable with those that reported in literature when VOS were used.

3

Conclusion and Perspectives

In conclusion, a highly sustainable and efficient protocol for the hydration of alkynes in solvent-, acid- and silver-free conditions, using as catalyst a NHC-gold (I) was developed, thanks to a complete rationalization of the role of the counterion. In particular, we investigated the activity of NHC^{iPr}-Au-X (X^- = BAr^{F-}, BF_4^-, SbF_6^-, OTf^-, NTf_2^-, ClO_4^-, OTs^-, and TFA^-) at room/mild temperature with suitable ionic additives in the first part of the thesis. The active/inactive catalytic behaviour of the gold complex is directly associate to the nature of the anion X^-, therefore full conversion of alkyne into ketone has been found only with two anions: OTf^- and NTf_2^-, both with intermediate co-ordinationing ability and basicity. For all other counterions no catalytic activity was observed, and this finding can be ascribed to the low co-ordination ability or basicity ($BArF^-$, BF_4^-, SbF_6^-, and ClO_4^-) or, to a too strong basic or co-ordinating nature (OTs^-, TFA^-).

The pivotal role played by the counterion was further highlighted in all the steps of the catalytic cycle: the pre-equilibrium, the nucleophilic attack and the proton transfers to the carbon atom (proton transfer and proton transfer', **Scheme 13**, page 34).

The KIE experiments performed in acidic conditions show the classical Lewis acid catalysis behavior: NHC-Au^+ fragment activates the alkyne and only with a proper counterion the nucleophilic attack occurs. Then, after the release of the product, the enol-ketone tautomerization does occur thanks to the Brönsted acid that easily performs proton transfer and proton transfer', giving a KIE equal to 1. Interestingly, a wrong choice of the counterion ($HClO_4$) stops the reaction, while normally the presence of a Brönsted acid has a positive effect in the hydration of alkynes.

However, the gold catalyst acts as Lewis acid in aprotic and neutral conditions during the nucleophilic attack with the assistance of the counterion, and helps in both proton transfers. The value of KIE in these conditions is much bigger than 1, indicating that the RDS is the proton transfer. This means that it is not conducted by traces of H^+ (otherwise the KIE value will be close to 1) but promoted by the metal centre.

The experimental kinetic findings are corroborated by DFT calculations. The role of the anion during the nuchleophilic attack has two different beneficial roles: i) it acts as a template, holding the reactive molecule of water in the right position for an anti-periplanar addition (**Scheme 1**); ii) it increases the nucleophilicity of the water molecule through the hydrogen bond HOH---OTf^-, polarizing the oxygen atom. In these calculations, the first anion-mediated proton transfer occurs in one step but the second proton transfer (**Scheme 13**, page 34) is much more difficult because of the decrease of basicity and hydrogen bond ability of OTf^- that are not enough strong to abstract the second proton from oxygen (intermediate OSIP'). The DFT calculations clearly suggest that the gold atom participates in this step in an anion/gold-mediated proton transfer to the unsaturated carbon atom. The formation of a peculiar square-planar gold intermediate was observed, where the counterion in trans position stabilizes the gold-proton interaction with H^+ acting as a Lewis acid and OTf^- as a σ-donor ligand. DFT calculations demonstrate that the second proton transfer step

takes place through a classical enol-ketone tautomerization mechanism in acidic condition, with a much lower energy barrier and that the RDS became the nucleophilic attack of the overall reaction mechanism, according to experimental KIE value.

The study was extended to other neutral ligands L as {NHC^{iPr}}, {PArF}, {BIAN}, {NHC^{CH2}}, {NAC}, {JPhos}, {PCy_3}, {PPh_3}, and {POR_3}. Decomposition of phosphane-based catalysts was observed by ^{31}P NMR spectroscopy during the catalysis with the exception of JPhos. On the other hand, NHC ligands showed superior performances due to their enhanced stability with respect to phosphanes in our conditions. We also observed that the use of silver salts in combination with L-Au-Cl complexes resulted in a decomposition of the in-situ formed catalyst even when NHC ligands were employed.

Starting from all the acquired theoretical and experimental knowledge, we tried to optimize the catalytic conditions and it was possible to work at room or mild temperature (60 °C), reducing the catalyst loading down to 0.01 mol% (with respect to the substrate) obtaining high values of TON and TOF (respectively 10^4 and 10^3 h^{-1}). This was also possible thanks to the use of ionic additives as ammonium, alkyl-ammonium salts and ionic liquid. The best result was obtained with the tetrabutylammonium triflate and it was observed that decreasing or increasing of the lipophilicity (alkylic chains) as compared to $^tBu_4NOTf$, does not affect the rate of reaction, viceversa rather it decreases.

The solvent-, acid- and silver-free conditions allowed us to obtain a very low value of E-factor (0.03-0.06) and high values of EMY (94-97). Finally, the absence of the solvent allows to easily separate, by distillation under reduced pressure, the volatile product from solid ionic additives and catalyst. Thanks to this new protocol it was possible to: i) recycle the catalytic system (up to four times) without observed loss of activity and ii) obtain a high-purity product without the presence of metal traces. The catalytic system is very versatile because preliminary results shown a good activity also for others substrates. In particular, a highly efficient and green methodology for the hydration of diphenylacetylene in solvent-, silver-, and acid-free conditions has been developed. It was possible to reduce, for the first time, the catalyst loading to 0.01 mol%, reaching the highest TON (3400), TOF (435 h^{-1}), and EMY (77) values as well as the lowest E-factor value (0.03). These results are remarkable and suggest that a sustainable production of 1,2-diphenylethanone with gold catalysts can be pursued if both the ligand and counterion effects are taken into account.

All these factors (low E-factor, high EMY and recyclability of the catalyst) are optimal in view of a bulk and sustainable production of chemicals with homogeneous gold (I) catalysts, a topic that is still considered a chimera in the literature.

For the solid or temperature-sensible substrates, a green methodology for the hydration and alkoxylation of alkynes was developed using cationic NHC gold catalysts in neoteric solvents, instead of traditional VOS. First of all, it was found that the reaction proceeds very well in most of the alternative solvents used (*p*-cymene,

propylene carbonate, ethyl lactate, glycerol, D-limonene and γ-valerolactone) with comparable or even better TOFs, in comparison with VOSs. On the other hand, when the reaction is performed in DMSO or propionitrile the TOFs are much lower (**Table 10**, page 46).

Secondarily, the activity of the catalyst (TOF) seems to be inversely correlated to the polarity of the solvent (dielectric constant) as shown in **Figure 21**. This behavior is in agreement with the role of the counterion in all the steps of the reaction (pre-equilibrium, nucleophilic attack, and protodeauration). A solvent with an enhanced dielectric constant will have the ion pair/free ions equilibrium (**Figure 20**) shifted toward the latter and so the beneficial effect of OTf^- during the nucleophilic attack (RDS) of methanol (water as well) is reduced. Moreover, the presence of suitable functional groups on the structure of the solvent that has proton acceptor/donor functionalities like in cyclohexanone, glycerol and DES (cit.ac.-DMU and chOTf-DMU) can increase the reaction rate, even for solvents that possess a medium-high dielectric constant. On the contrary, the solvent with a functional group that can co-ordinates to gold, like d-limonene (C=C), propionitrile (C≡N) and DMSO (S=O), slows down the reaction rate owing to the co-ordination of the solvent to the metal center. As a matter of fact, low polar non-co-ordinative neoteric solvent such as *p*-cymene and perfluorodecalin, showed to be the best solvents (TOF = 495 h^{-1}), and also the non co-ordinative polar aprotic GVL gave a good TOF value (340 h^{-1}). DFT calculations corroborate these particular experimental kinetic findings underling the importance of GVL in the stabilization of both product and intermediate of the reaction. The beneficial effect of this particular solvent was also found in the hydration of inactive diphenylacetylene, frequently used as a benchmark. As reported in chapter 1.3, comparable TON and one order of magnitude higher TOF were obtained with respect to that reported in the literature. For the first time, it was possible to obtain a sustainable production of chemicals with homogeneous gold catalysts in neoteric solvents.

In the very last years, the number of publications about homogeneous gold(III) catalysis has start increasing. In order to stabilize gold(III) complexes increasing the catalytic activity, the work on the design of bi- (P-C, C-C, C-N, N-N, N-O) or tri-dentate (C-N-C, N-C-N) ligands is still the main topic in this field. These particular ligands are used and studied for the reactions of isomerization, hydration, hydroamination, C-C coupling, and cycloisomerization.[132]

In spite of the recent findings for gold(I), the main works for gold(III) are focused only on the nature of the ligand, without a complete comprehension of the matching between ligand and counterion. Moreover, it is still not clear if has the same huge importance as for gold(I). Sustainable and green protocols for the reactions mentioned above are not still fully developed. In fact, silver additives, acids, solvents, high temperature and high catalyst loading are commonly used in homogeneous gold(III) catalysis.

With the results obtained in homogeneous gold(I) catalysis, it seems to be very stimulating to explore the use of gold(III) in the protocols developed in this PHD thesis, expanding the studies to others nucleophilic

addition reactions on substrates with unsaturated bonds (especially alkynes), in silver-, solvent-, and acid-free condition, using neoteric solvents or working in micellar catalysis, another still unexplored research field.

4

Experimental part

4.1. General procedures and materials

$NaAuCl_4*2H_2O$, tetrahydrothiophene (THT), tert-butylamine, tert-buthylisocyanide, acenaphthenequinone, paraformaldehyde, glyoxal 40%, chlorotrimethylsilane, 2,6-diisopropylphenylamine, acetic acid, methoxy(methyl)chloride, triphenylphosphine (PPh_3), tricyclohexylphosphine (PCy_3), (2-biphenyl)di-tert-butylphosphine (JPhos), tris(3,5-bis(trifluoromethyl)phenyl)phosphine (PArF), tris(2,4-di-tert-butyl)phosphite [$P(OR)_3$], silver trifluoromethansoulphonate (AgOTf), silver p-toluensulfonate (AgOTs), silver bis(trifluoromethanesulfonyl)imide ($AgNTf_2$), silver tetrafluoroborate ($AgBF_4$), silver hexafluoroantimonate (V) ($AgSbF_6$), sodium tetrakis[3,5-bis(trifluoromethyl)phenyl]borate (NaBArF), silver acetate (AgAc), silver trifluoroacetate (AgTFA), silver perchlorate ($AgClO_4$), 1-butyl-3-methylimidazolium trifluoromethansulfonate (BMIMOTf), trifluoromethanesulfonic acid (HOTf), perchloric acid ($HClO_4$), ammonium triflate (NH_4OTf), sodiumdodecyl sulphate (SDS), teatrabutylammonium p-toluensulfonate (NBu_4OTs), tetrabutylammonium trifluoromethanesulfonate (NBu_4OTf), Aliquat336, dibutylamine (Bu_2)NH, dimethylethyldodecyl ammonium chloride (Me_2)(Et)(Dod)NCl, alkynes (1-hexyne, 1-octyne, 3-phenyl-1-propyne, phenylacetylene, 1-phenyl-1-propyne, 4-octyne, 1,4-dimethoxy-2-butyne, methyl-2-hexynoate, 1-trimethylsilyl-1-hexyne, diethylacetylenedicarboxylate, 3-pentyl-1-ol, diphenylacetylene) and all the solvents were purchased from Ricci Chimica, Strem Chemicals and Sigma Aldrich and used without further purification.

All manipulations of moisture-sensitive materials were performed in flamed Schlenk glassware on a Schlenk line, interfaced to a high vacuum pump. All the new compounds were characterized in solution by ^{1}H, ^{13}C, ^{19}F, ^{31}P NMR spectroscopies. All the spectra were measured on Bruker AC-200 spectrometer. Referencing is relative to TMS (^{1}H and ^{13}C), CCl_3F(^{19}F) and 85% H_3PO_4 (^{31}P). The elemental analyses were carried out with a Carlo Erba 1106 elemental analyser.

4.2. Synthesis and characterization

Synthesis of Chloro(tetrahydrothiophene) gold (I).

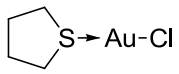

THT-Au-Cl, was prepared according to existing literature procedures.[133] To a stirred solution of $Na[AuCl_4]*2H_2O$ (1 g, 2.5 mmol) in H_2O/EtOH (20 mL, 1:1) was added tetrahydrothiophene (0.47 mL, 5.3 mmol) dropwise and the suspension stirred for 15 min. The precipitate was collected by filtration and washed with H_2O (2 x 10 mL) and dried under vacuum (yield 1,71 g, 95%).
^{1}H NMR (200 MHz, $CDCl_3$, 298 K): δ (ppm) 3.42 (bs, 4H), 2.17 (bs, 4H). ^{13}C {^{1}H}-NMR (200 MHz, $CDCl_3$, 298 K): δ (ppm) 40.5, 30.7. Anal. Calc. for C_4H_8AuClS (320.59): C, 14.99; H, 2.52; Au, 61.44; Cl, 11.06; S, 10.00. Found: C, 29.59; H, 0.88; S, 9.80.

General synthesis for phosphine gold(I) chloride complexes.

Starting from THT-Au-Cl (1 Eq) was dissolved in 5mL of CH_2Cl_2 subsequently, 1.1 eq of relative phosphine was added. The reaction mixture was stirred in the dark (using aluminium foil) for 1 hour or more if necessary. The reaction mixture was dried under reduced pressure and than re-dissolved with a minimum quantity of DCM and *n*-pentane (4mL) was added with the formation of a solid which was filtered off, washed with 3x2 mL of *n*-pentane and then dried under vacuum. The synthesis follows a modified procedure reported in literature.[134]

***Synthesis of tri-phenylphosphine gold(I) chloride*.**

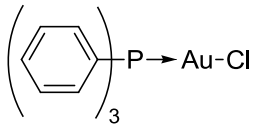

(Yield 87%) ^{1}H NMR (200 MHz, CD_2Cl_2, 298 K): δ (ppm) 7.56-7.24 (m, 15H). ^{13}C {^{1}H}-NMR (200 MHz, CD_2Cl_2, 298K): δ(ppm) 134.2, 132.2, 129.3, 128.5. ^{31}P {1H}-NMR (200 MHz, CD_2Cl_2, 298K): δ (ppm) 33.8. Anal. Calc. for $C_{18}H_{15}AuClP$ (494.71): C, 43.70; H, 3.06; Au, 39.81; Cl, 7.17; P, 6.26. Found: C, 43.61; H, 3.11.

***Synthesis of tri-cycloesilphosphine gold(I) chloride*.**

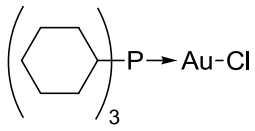

(Yield 90%) ^{1}H NMR (200 MHz, $CDCl_3$, 298 K): δ (ppm) 2.01-1.61 (m, 18H), 1.50-1.35 (m, 6H), 1.32-1.15 (m, 9H). ^{13}C {^{1}H}-NMR (200 MHz, $CDCl_3$, 298K): δ(ppm) 33.4, 33.1, 30.7, 27.4, 26.9, 25.8. ^{31}P {^{1}H}-NMR (200 MHz, $CDCl_3$, 298K): δ (ppm) 54.01. Anal. Calc. for $C_{18}H_{33}AuClP$ (515.85): C, 42.16; H, 6.49; Au, 38.41; Cl, 6.91; P, 6.04. Found: C, 42.20; H, 6.41.

Synthesis of (tris(2,4-di-tert-butylphenyl)phosphite)gold(I) chloride

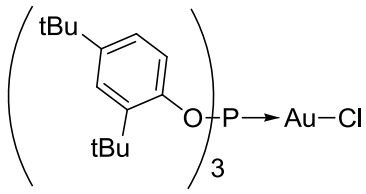

(Yield 75%) ^{1}H NMR (200 MHz, $CDCl_3$, 298 K): δ (ppm) 7.52-7.46 (m, 2H), 1.715 (d, J_{HH} = 8.5 Hz, 1H), 1.465 (s, 9H), 1.311 (s, 9H). ^{13}C {^{1}H}-NMR (200 MHz, $CDCl_3$, 298K): δ(ppm) 148.28, 147.38, 139.31, 125.51, 124.30, 119.37 (d, J = 8.6 Hz), 35.23, 34.80, 31.52, 30.69. ^{31}P {^{1}H}-NMR (200 MHz, $CDCl_3$, 298K): δ (ppm) 101.42. Anal. Calc. for $C_{42}H_{63}AuClO_3P$ (879.34): C, 57.37; H, 7.22; Au, 22.40; Cl, 4.03; O, 5.46; P, 3.52. Found: C, 57.42; H, 7.18.

Synthesis of tris(3,5-bis(trifluoromethyl)phenyl)phosphine)gold(I) chloride

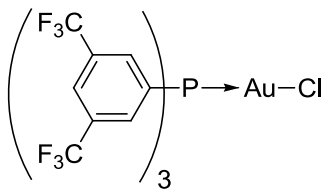

(Yield 92%) ^{1}H NMR (200 MHz, CD_2Cl_2, 298 K): δ (ppm) 8.18 (s, 3H), 7.94 (d, 6H, $^3J_{CP}$ = 13.5 Hz). ^{13}C {^{1}H}-NMR (200 MHz, CD_2Cl_2, 298 K): δ(ppm) 134.29 (dq, $^2J_{CP}$ = 15.3 Hz, $^3J_{CF}$ = 3.3 Hz), 133.34 (dq, $^2J_{CF}$ = 34.7 Hz, $^3J_{CP}$ = 12.8 Hz), 128.62, 128.41 (d, $^1J_{CP}$ = 67.6 Hz), 125.27 (q, $^1J_{CF}$ = 273 Hz), 122.3 (q, $^1J_{CP}$ = 273.7 Hz). ^{19}F NMR (200 MHz, CD_2Cl_2, 298 K): δ (ppm) -63.38. ^{31}P {^{1}H}-NMR (200 MHz, CD_2Cl_2, 298 K): δ (ppm) 35.77. Anal. Calc. for $C_{24\ h9}AuClF_{18}P$ (902.69): C, 31.93; H, 1.00; Au, 21.82; Cl, 3.93; F, 37.88; P, 3.43. Found: C, 32.05; H, 0.98.

Synthesis of 2-(di-tert-butylphosphino)-1,1'-biphenylgold(I) chloride

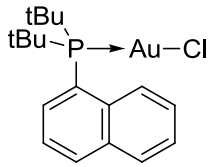

(Yield 91%) ^{1}H NMR (200 MHz, CD_2Cl_2, 298 K): δ (ppm) 7.89 (t, 1H, J_{HH} =7.2 Hz), 7.50 (m, 3H), 7.38 (t, 2H, J_{HH} = 7.5 Hz), 7.28 (m, 1H), 7.14 (d, 2H, J_{HH} =7.3 Hz), 1.40 (d, 18H, J=15.6). ^{13}C {^{1}H}-NMR (200 MHz, CD_2Cl_2, 298 K): δ(ppm) 149.6, 142.0, 133.3, 132.7, 132.6, 130.0, 128.8, 128.0, 127.4, 126.2, 37.4, 37.0, 30.2, 30.2. ^{31}P {1H}-NMR (200 MHz, CD_2Cl_2, 298 K): δ (ppm) 60.5. Anal. Calc. for $C_{18}H_{25}AuClP$ (504.78): C, 42.83; H, 4.99; Au, 39.02; Cl, 7.02; P, 6.14. Found: C, 42.91; H, 4.83.

***Synthesis of tert-Buthylisocyano gold(I) chloride*.**

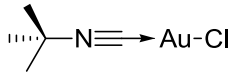

It was prepared according to a literature procedure.[135] In a Schlenk tube THT-Au-Cl (636 mg, 1.98 mmol) was dissolved in 10 mL of DCM and tert-buthylisocyanide (230 μL, 2mmol) was added at room temperature. The mixture was stirred for 15 minutes than purified by precipitation whit pentane obtaining a white solid (yield 566 mg, 90.4%)

^{1}H NMR (200 MHz, $CDCl_3$, 298 K): δ (ppm) 1.59 (t, 9H, J_{HH} = 1.9 Hz). ^{13}C {^{1}H}-NMR (200 MHz, $CDCl_3$, 298 K): δ (ppm) 122.2, 60.1, 29.7. Anal. Calc. for C_5H_9AuCln (315.55): C, 19.03; H, 2.87; Au, 62.42; Cl, 11.24; N, 4.44. Found: C, 42.91; H, 4.83, N, 4.50.

***Synthesis of [(tert-Buthylamino)$_2$methylidine]gold(I) Chloride*.**

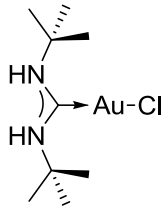

NAC was prepared according to a literature procedure.[136] Tert-butylamine (69.3 μL, 0.66 mmol) was added to a solution of tert-Buthylisocyano gold(I) chloride (173 mg, 0.55 mmol) in 4 mL of dichloromethane. The mixture was stirred at room temperature and protect from the light for 3 days. Dichloromethane was added to the mixture (that result milky) until it became limpid, then was filtered on a Silica pad, concentrated to minimum volume and precipitated with pentane. The white solid was filtered and dried under vacuum (yield 154 mg, 72.6%).

^{1}H NMR (200 MHz, CD_2Cl_2, 298 K): δ (ppm) rotamer A: 6.77 (bs, 2H), 1.59 (s, 18H), rotamer B: 6.37 (bs, 2H), 6.13 (bs, 2H), 1.60 (s, 9H), 1.40 (s, 9H). ^{13}C {^{1}H}-NMR (200 MHz, CD_2Cl_2, 298 K): δ (ppm) 189.31, 53.24, 31.48. Anal. Calc. for $C_9H_{20}AuClN_2$ (388.69): C, 27.81; H, 5.19; Au, 50.67; Cl, 9.12; N, 7.21. Found: C, 27.79; H, 5.22; N, 7.18.

Preparation of NHC^{iPr}-Cl 2 steps:

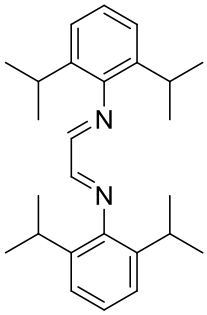

***i) Preparation of glyoxal-bis-(2,6-diidopropylphenyl)imine*.**

DAD^{iPr}, was prepared following the procedure reported in literature.[137] To a solution of 2,6-diisopropylphenylamine freshly distilled (49.25 g, 0.28 mol) in 200 mL of n-propanol at 23°C was added a mixture of: n-propanol (20 mL), water (50 mL) and a 40% aqueous solution of glyoxal (18.15 g, corresponding of 0.125 mol of glyoxal). After 1 h stirring at 70°C, 200 mL of water were added. The resulting white precipitate was collected by filtration and dried under vacuum (yield 95.1 g, 90.8%).

^{1}H NMR (200 MHz, $CDCl_3$, 298 K): δ (ppm) 8.11 (s, 2H), 7.25-7.1 (m, 12H), 2.94 (sept, 4H, J_{HH} = 6.9 Hz), 1.21 (d, 24 h, J_{HH} = 6.9 Hz). ^{13}C {^{1}H}-NMR (200, $CDCl_3$, 298 K): δ (ppm) 163, 148, 136.6, 125.1, 123.1, 28.1 22.4. Anal. Calc. for $C_{26}H_{36}N_2$ (376.58): C, 82.93; H, 9.64; N, 7.44. Found: C, 83.01; H, 9.59; N, 7.39.

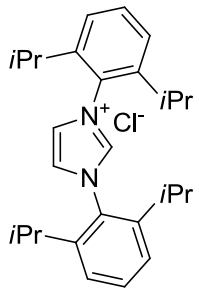

ii) ***Preparation of 1,3-bis-(2,6-diisopropylphenyl)imidazolium chloride*****.**

IPr*HCl, was prepared following the procedure reported in literature.[138] In a 500 mL round bottom flask containing DAD^{iPr} (1.0 g, 26.55 mmol), paraformaldehyde (0.797 g, 26.55 mmol) were added 240 mL of dry EtOAc and heated at 70°C with magnetic stirring. A solution of fresh-distilled chlorotrimethylsilane (3.37 ml, 26.55 mmol) in 5 mL of dry EtOAc was added in 45 minutes (IMPORTANT: faster addition gives low yield with a lot of purple impurities) over vigorous stirring and the resulting yellow suspension stirred for others 2 h at 70 °C. After cooling down to 10°C with a ice-bath, the suspention was filtered and washed with EtOAc and tBuOMe. The white solid was died under vacuum (yield 7.9 g, 79.5%).

^{1}H NMR (200 MHz, DMSO, 298 K): δ (ppm) 10.16 (s, 1H), 8.56 (s, 4H), 7.68 (t, 2H, J_{HH} = 7.7 Hz), 7.53 (d, 4H, J_{HH} = 7.8 Hz), 2.34 (sept, 4H, J_{HH} = 6.9 Hz), 1.25 (s, 12H, J_{HH} = 6.6 Hz) 1.15 (d, 12H, J_{HH} = 6.9 Hz). ^{13}C {^{1}H}-NMR (200 MHz, DMSO, 298 K): δ (ppm) 220.6, 146.2, 139.0, 129.0, 123.6, 121.5, 28.7, 24.8, 23.6. Anal. Calc. for $C_{27}H_{37}ClN_2$ (425.05): C, 76.29; H, 8.77; Cl, 8.34; N, 6.59. Found: C, 76.35; H, 8.65; N, 6.45.

Synthesis of 1,3-bis-(2,6-diisopropylphenyl)imidazolium gold(I) chloride**.**

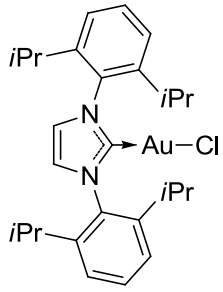

NHC^{iPr}-Au-Cl, was prepared according to existing literature procedures.[139] In Schlenk tube were added IPr*HCl (212.1 mg, 0.5 mmol), $KHCO_3$ (150 mg, 1.5 mmol) and THT-Au-Cl (160 mg, 0.5 mmol) with a solution of DCM:MeOH (5:1). The reaction mixture was stirred at room temperature for 3 days. The reaction mixture was filtered on celite pad, dried under vacuum, dissolved in a minimum quantity of DCM and re-precipitate with pentane. The resulting white powder was filtered and washed (3x2 mL) with pentane and then dried under vacuum (yield 280.1 mg, 91%).

^{1}H NMR (200 MHz, $CDCl_3$, 298 K): δ (ppm) 7.49 (m, 2H), 7.28 (d, 4H, J_{HH} = 8.2 Hz), 7.17 (s, 2H), 2.55 (sept, 4H, J_{HH} = 6.8 Hz), 1.34 (d, 12H, J_{HH} = 6.9 Hz), 1.21 (d,12H, J_{HH} = 6.9 Hz). ^{13}C {^{1}H}-NMR (200 MHz, $CDCl_3$, 298 K): δ (ppm) 175.3, 145.5, 133.9, 130.7, 124.2, 123.0, 28.8, 24.5, 24.0. Anal. Calc. for $C_{27}H_{36}AuClN_2$ (621.01): C, 76.29; H, 8.77; Cl, 8.34; N, 6.59. Found: C, 76.35; H, 8.65; N, 6.45.

Synthesis of (1,3-bis(2,6-diisopropylphenyl)-2,3-dihydro-1 H-imidazol-2-yl)(2-oxopropyl)gold.

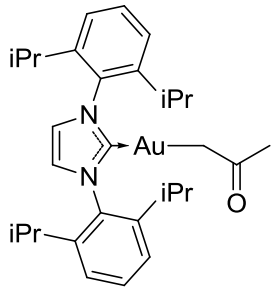

NHC^{iPr}-Au-CH_2COCH_3, was prepared according to existing literature procedures (Method A and Method B).[140]

Method A) In Schlenk tube were added IPr*HCl (132.58 mg, 0.31 mmol), K_2CO_3 (258.7 mg, 1.87 mmol) and THT-Au-Cl (100 mg, 0.31 mmol) in 5 mL of acetone. The reaction mixture was stirred at 60 °C for 72 hours. The reaction mixture was filtered on celite pad, dried under vacuum, dissolved in a minimum quantity of DCM and re-precipitate with pentane. The resulting white powder was filtered and washed (3x2 mL) with pentane and then dried under vacuum (yield 61.5 mg, 30.6%). Due to the low yield it was used the Method B.

Method B) In Schlenk tube were added NHC^{iPr}-Au-Cl (200.0 mg, 0.32 mmol) and K_2CO_3 (267.1 mg, 1.93 mmol) in 5 mL of acetone. The reaction mixture was stirred at 60 °C for 48 hours. The reaction mixture was filtered on celite pad, dried under vacuum, dissolved in a minimum quantity of DCM and re-precipitate with pentane. The resulting white powder was filtered and washed (3x2 mL) with pentane and then dried under vacuum (yield 165.5 mg, 79.9%)

^{1}H NMR (200 MHz, $CDCl_3$, 298 K): δ (ppm) 7.51 (m, 2H), 7.31 (m, 4H), 7.15 (s, 2H), 2.58 (sept, 4H, J_{HH} = 6.8 Hz), 2.08 (s, 2H), 1.56 (s, 3H), 1.35 (d, 12H, J_{HH} = 6.9 Hz), 1.24 (d, 12H, J_{HH} = 6.9 Hz). ^{13}C {^{1}H}-NMR (200 MHz, $CDCl_3$, 298 K): δ (ppm) 212.1, 193.1, 145.8, 134.4, 130.5, 124.2, 123.0, 40.7, 29.5, 28.8, 24.5, 24.0. Anal. Calc. for $C_{30}H_{41}AuN_2O$ (642.63): C, 56.07; H, 6.43; Au, 30.65; N, 4.36; O, 2.49. Found: C, 56.15; H, 6.38; N, 4.41.

Synthesis of NHC^{CH2}-Cl, 2 steps:

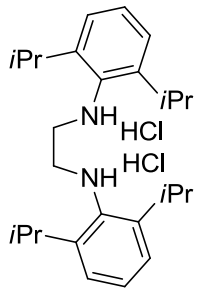

***i) Preparation of N,N'-bis(2,6-diisopropylphenylamino) ethane dihydrochloride*.**

It was prepared starting from DAD^{iPr} and following the procedure reported in literature.[137] In a 250 mL round bottom flask containing DAD^{iPr} (3.92 g, 0.01 mol) in a mixture of MeOH/THF (100 mL) was slowly added $NaBH_4$ (3.78 g, 0.1 mol) cooled with an ice bath. After 1.5 h the reaction (turning white from yellow) was quenched using a aqueous solution of NH_4Cl. The diamine was extracted using diethylether (3 x 50 mL) and the organic phase was washed with distilled water (3 x 50 mL). The organic phase was dried using $MgSO_4$ and the solvent evaporated by reduce pressure giving a white powder (3.6 g, 97%).

^{1}H NMR (200 MHz, $CDCl_3$, 298 K): δ (ppm) 7.40-7.25 (m, 6H), 3.72 (s, 4H), 3.58 (sept, 4H, J_{HH} = 6.6 Hz), 1.24 (d, 24 h, J_{HH} = 6.6 Hz). ^{13}C {^{1}H}-NMR (200 MHz, $CDCl_3$, 298 K): δ (ppm) 151.0, 142.7, 127.1, 124.8, 50.6, 27.2, 24.4. Anal. Calc. for $C_{26}H_{40}N_2$ (380.61): C, 82.05; H, 10.59; N, 7.36. Found: C, 82.72; H, 10.23; N, 7.88.

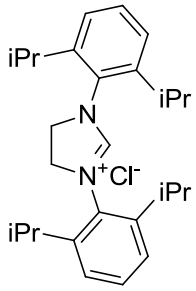

ii) ***Preparation of 1,3-bis[(2,6-diisopropyl)phenyl]imidazolidinium chloride*****.**

IPr*HCl, was prepared following the procedure reported in literature[137] In a Schlenk tube a mixture of N,N'-bis(2,6-diisopropylphenylamino) ethane dihydrochloride (8 g, 19.2 mmol), triethyl orthoformate (100 mL) and two drops of formic acid 96% was refluxed for 45 h. Once at room temperature it is observed the formation of a solid and it was collected by filtration. A recrystallization is needed in order to obtain a pure product (yield 4.82 g, 59%).^{1}H NMR (200 MHz, DMSO, 298 K): δ (ppm) 9.63 (s, 1H), 7.6-7.3 (m, 6H), 4.41 (s, 4H), 3.09 (sept, 4H, J_{HH} = 6.9 Hz), 1.36 (d, 12H, J_{HH} = 6.6 Hz), 1.25 (d, 12H, J_{HH} = 6.6 Hz). ^{13}C {^{1}H}-NMR (200 MHz, DMSO, 298 K): δ (ppm) 160.0 144.0, 131.0, 129.8, 124.7, 53.7, 28.3, 25.0, 23.3. Anal. Calc. for $C_{27}H_{39}ClN_2$ (427.06): C, 75.93; H, 9.20; Cl, 8.30; N, 6.56. Found: C, 76.05; H, 9.02; N, 6.68.

Synthesis of 1,3-Bis(2,6-di-(i-propyl)phenyl)-4,5-dihydroimidazolium gold(I) chloride.

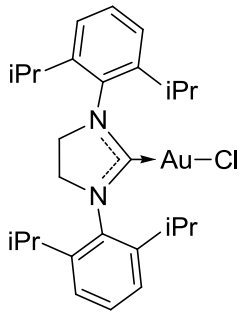

NHC^{CH2}-Au-Cl was prepared using a modified method present in literature.[142] In Schlenk tube with 30 mL of dichloromethane were added NHC^{CH2}*HCl (51 mg, 0.079 mmol) and THT-Au-Cl (25 mg, 0.078 mmol). The reaction mixture was stirred for 12 hours with an aluminium foil wrapped around the tube at room temperature. The solvent was removed under reduced pressure and the compound was dissolved in a minimum quantity of DCM and pentane was added with the formation of the solid. The yellow solid was filtered and washed with pentane (3 x 3 mL) and dried under vacuum (yield 51 mg, 86%).

^{1}H NMR (200 MHz, CD_2Cl_2, 298 K): δ (ppm) 7.53-7.35 (m, 2H), 7.25-7.22 (m, 4H), 4.05 (d, 4H, J_{HH} = 7.4 Hz), 3.08-3.02 (m, 4H), 1.41 (d, 12H, J_{HH} = 6.9 Hz), 1.33 (d, 12H, J_{HH} = 6.9 Hz). ^{13}C {^{1}H}-NMR (200 MHz, CD_2Cl_2, 298K): δ (ppm) 196.0, 146.5, 134.0, 130.0, 124.7, 53.8, 28.9, 25.4, 24.0. Anal. Calc. for $C_{27}H_{38}AuClN_2$ (623.02): C, 52.05; H, 6.15; Au, 31.61; Cl, 5.69; N, 4.50. Found: C, 52.21; H, 6.01; N, 4.78.

Preparation of BIAN-Cl, 2 steps:

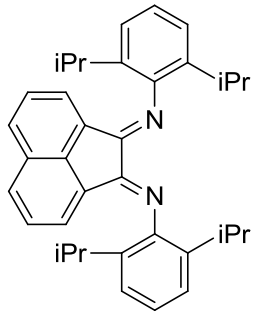

i) Synthesis of Bis[N,N'-(2,6-diisopropylphenyl)imino]acenaphthene.

The compound was prepared using a modified method present in literature.[141] Acenaphthenequinone (7.0 g, 38.4 mmol) was suspended in acetonitrile (150mL) and heated under reflux at 80 °C for 60 min. Acetic acid (65 mL) was then added, and heating was continued until the acenaphthenequinone had completely dissolved. To this hot solution was added freshly distilled 2,6-diisopropylphenylaniline (16.0 g, 89.9 mmol) in 30 min with the help of a dropping funnel, and the solution was heated under reflux for a further 5 h and then cooled to room temperature. The resulting orange-yellow solid was then filtered, washed with pentane (3 x 20 mL), and dried under vacuum (yield 18.1 g, 94%).

^{1}H NMR (200 MHz, CD_2Cl_2, 298 K): δ (ppm) 7.88 (d, 2H), 7.36-7.26 (m, 8H), 6.63 (d, 2H), 3.03 (sept, 4H J_{HH} = 7.1 Hz), 1.23 (d, 24 h, J_{HH} = 6.9 Hz). ^{13}C {^{1}H}-NMR (200 MHz, CD_2Cl_2, 298 K): δ (ppm) 161.1, 148.0, 141.2, 135.5, 131.6, 130.0, 129.2, 128.3, 124.6, 123.9, 123.5, 29.1, 23.2, 23.1. Anal. Calc. for $C_{36}H_{40}N_2$ (500.72): C, 86.35; H, 8.05; N, 5.59. Found: C, 86.71; H, 7.98; N, 5.72.

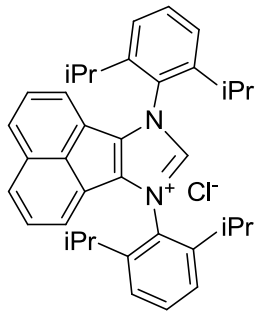

ii) Synthesis of 7,9-bis(2,6-diisopropylphenyl)-7H-acenaphtho[1,2-d]imidazol-9-ium chloride.

BIAN*HCl was prepared using a modified method present in literature.[142] In an argon-flushed Schlenk tube were added the Bis[N,N'-(2,6-diisopropylphenyl)imino]acenaphthene (484 mg, 0.97 mmol) with methoxy(methyl)chloride (1.5 mL, 19.4 mmol). The reaction mixture was stirred overnight at reflux (70°C). After cooling down the temperature was added 10 mL of diethylether with the formation of a yellow precipitate. The resulting solid was collected by filtration, washed with diethylether (3 x 3 mL) and with pentane (3 x 3 mL). The bright-yellow product was dried under vacuum (yield 493 mg, 92.5%).

^{1}H NMR (200 MHz, CD_2Cl_2, 298 K): δ (ppm) 12.11 (bs, 1H), 8.02 (d, J_{HH} = 8.3 Hz, 2H), 7.68 (t, J_{HH} = 8.3 Hz, 2H), 7.62 (t, J_{HH} = 8.3 Hz, 2H), 7.58 (d, J_{HH} = 7.7 Hz, 2H), 7.21 (d, J_{HH} = 7.1 Hz, 2H), 2.27 (sept, J_{HH} = 6.9 Hz, 4H), 1.40 (d, J_{HH} = 6.8 Hz, 12H), 1.16 (d, J_{HH} = 6.8 Hz, 12H). ^{13}C {^{1}H}-NMR (200 MHz, CD_2Cl_2, 298 K): δ (ppm) 145.4, 142.5, 138.1, 132.7, 130.8, 130.4, 129.4, 128.7, 125.4, 123.4, 123.4, 29.7, 24.8, 23.5. Anal. Calc. for $C_{37}H_{41}ClN_2$ (549.19) C, 80.92; H, 7.52; Cl, 6.46; N, 5.10. Found: C, 81.11; H, 7.21; N, 5.30.

***Synthesis of BIAN gold(I) chloride*.**

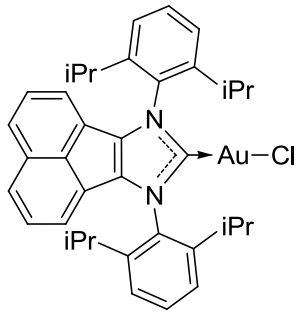

BIAN-Au-Cl was prepared using a modified method present in literature.[142] In Schlenk tube with 30 mL of dichloromethane were added BIAN-Cl (51 mg, 0.079 mmol) and THT-Au-Cl (25 mg, 0.078 mmol). The reaction mixture was stirred for 12 hours with an aluminium foil wrapped around the Schelnk tube at room temperature. The solvent was removed under reduced pressure and the compound was dissolved in a minimum quantity of DCM and re-precipitate with pentane. The yellow solid was filtered and washed with pentane (3 x 3 mL) and dried under vacuum (yield 51 mg, 86%).

^{1}H NMR (200 MHz, CD_2Cl_2, 298 K): δ (ppm) 7.84 (d, 2H, J_{HH} = 8.4 Hz), 7.68 (t, 2H, J_{HH} = 7.8 Hz), 7.46 (dd, 2H, J_{HH} = 8.4 Hz, J_{HH} = 7.0 Hz), 7.45 (d, 4H, J_{HH} = 7.9 Hz), 7.03 (d, 2H, J_{HH} = 7.1 Hz), 2.83 (*sept*, 4H, J_{HH} = 7.2 Hz), 1.38 (d, 12H, J_{HH} = 6.9 Hz), 1.21 (d, 12H, J_{HH} = 6.9 Hz). ^{13}C {^{1}H}-NMR (200 MHz, CD_2Cl_2, 297 K): δ (ppm) 175.6, 146.1, 138.4, 133.1, 131.3, 130.5, 129.0, 128.2, 125.6, 125.0, 121.7, 29.3, 24.59, 23.91. Anal. Calc. for $C_{37}H_{40}AuClN_2$ (745.15) C, 59.64; H, 5.41; Au, 26.43; Cl, 4.76; N, 3.76. Found: C, 59.7; H, 5.47; N, 3.72.

Synthesis of NHC^{iPr}-Au-OTf silver-free

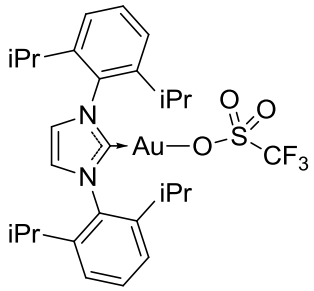

In a Schlenk flask were added 1 equiv. (319 mg, 0.50 mmol) of (NHC)-Au-(CH_2COCH_3) in 5 mL of chloroform and 1.1 equiv. (48.21 µL, 0.55 mmol) of trifluoromethanesulfonic acid. The reaction was stirred at ambient temperature for 3 hours. The solution was filtered through a paddle of Celite and the solvent was removed under vacuum. The residue was dissolved with a minimum quantity of CH_2Cl_2 and precipitated with n-pentane. The white microcrystalline product was collected by filtration, washed with n-pentane (2 x 2 mL) and dried under vacuum (yield 85.1%). ^{1}H NMR (200 MHz, CD_2Cl_2, 298 K): δ (ppm) 7.58 (t, 2H, J_{HH} = 7.8 Hz), 7.37 (d, 4H, J_{HH} = 7.7 Hz), 7.28 (s, 2H), 2.56 (sept, 4H, J_{HH} = 6.9 Hz), 1.35 (d, 12H, J_{HH} = 6.8 Hz), 1.24 (d, 12H, J_{HH} = 6.8 Hz). ^{13}C $\{^1$H$\}$-NMR (200 MHz, CD_2Cl_2, 298 K): δ (ppm) 166.0, 162.1, 146.4, 134.4, 131.2, 124.8, 124.3, 116.50, 29.4, 24. ^{19}F NMR (200 MHz, CD_2Cl_2, 298 K): δ (ppm) -73.89 (s, CF_3). Anal. Calc. for $C_{38}H_{26}AuF_3N_2O_3S$ (734.62) C, 45.78; H, 4.94; Au, 26.81; F, 7.76; N, 3.81; O, 6.53; S, 4.36. Found: C, 45.99; H, 4.81; N, 3.92; S, 4.21.

General synthesis for NHC-anion exchange using silver salts

A general NHC-Au-Cl catalyst (0.11 mmol) was dissolved in 5mL of CH_2Cl_2 subsequently, 1.1 eq (0.12 mmol) of AgX (X= ClO_4^-, Ac^-, OTf^-, OTs^-, TFA^-, NTf_2^-), was added, leading to the precipitation of AgCl. The reaction mixture was stirred in the dark (using aluminium foil) from 2 hour to overnight depending of the ligand. The reaction mixture was dried under reduced pressure and re-dissolved whit a minimum quantity of DCM, filtered on Celite® pad, concentred under vacuum and *n*-pentane (4mL) was added, resulting in the formation of precipitate. The resulting solid was filtered off, washed with 3x2 mL of *n*-pentane and then dried under vacuum.

Synthesis of NHC^{iPr}-Au-(3-hexyne)-Au-X (X= BF_4^-, SbF_6^-)

The NHC^{iPr}-Au-(3-hexyne)-X catalysts were prepared using a procedure already present in literature.[143] (NHC^{iPr})-Au-Cl (49.7 mg, 0.08 mmol) and 3-hexyne (14 µL, 0.12 mmol) were added in a Schlenk tube in 1 mL of CH_2Cl_2. Subsequently the proper AgX (0.12 mmol) was added. The reaction mixture was stirred at room temperature for 15 min observing the precipitation of AgCl. The reaction mixture was filtered on celite pad, washed with 3x1 mL of CH_2Cl_2, concentred under vacuum and re-precipitated with n-pentane. The white solid was collected by filtration and dried under reduced pressure.

Synthesis of NHC^{iPr}-Au-(3-hexyne)-SbF_6

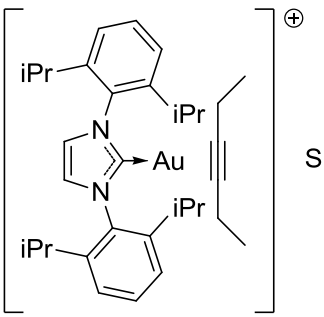

(Yield 85%) ^{1}H NMR (200 MHz, CD_2Cl_2, 298 K): δ (ppm) 7.62 (t, 2H, J_{HH} = 7.9 Hz), 7.55 (s, 2H), 7.41 (d, 4H, J_{HH} = 7.8 Hz), 2.56 (sept, 4H, J_{HH} = 7.0 Hz), 2.26 (m, 4H), 1.34 (d, 12H, J_{HH} = 7.0 Hz), 1.31 (d, 12H, J_{HH} = 7.5 Hz), 0.64 (t, 6H, J_{HH} = 7.5 Hz). ^{13}C-$\{^1$H$\}$ NMR (200 MHz, CD_2Cl_2, 298 K): δ (ppm) 178.0, 146.2, 133.4, 131.8, 125.3, 125.0, 87.7, 29.2, 24.8, 24.2, 15.1, 13.5. ^{19}F NMR (200 MHz, CD_2Cl_2, 298 K): δ (ppm) -120.1 m. Anal. Calc. for $C_{33}H_{46}AuBF_4N_2$ (754.50) C, 52.53; H, 6.15; Au, 26.11; B, 1.43; F, 10.07; N, 3.71. Found: C, 52.71; H, 6.03; N, 3.90.

Synthesis of NHC^{iPr}-Au-(3-hexyne)-BF$_4$

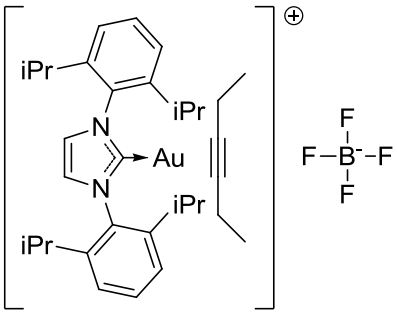

(Yield 89%)^{1}H NMR (200 MHz, CD_2Cl_2, 298 K): δ (ppm) 7.62 (t, 2H, J_{HH} = 7.9 Hz), 7.55 (s, 2H), 7.41 (d, 4H, J_{HH} = 7.8 Hz), 2.56 (sept, 4H, J_{HH} = 7.0 Hz), 2.26 (m, 4H), 1.34 (d, 12H, J_{HH} = 7.0 Hz), 1.31 (d, 12H, J_{HH} = 7.5 Hz), 0.64 (t, 6H, J_{HH} = 7.5 Hz). ^{13}C-{^{1}H} NMR (200 MHz, CD_2Cl_2, 298 K): δ (ppm) 178.0, 146.2, 133.4, 131.8, 125.3, 125.0, 87.7, 29.2, 24.8, 24.2, 15.1, 13.5. ^{19}F NMR (200 MHz, CD_2Cl_2, 298 K): δ (ppm) -153.56 (br, $^{11}BF_4$), -153.51 (br, $^{10}BF_4$). Anal. Calc. for $C_{33}H_{46}AuBF_4N_2$ (754.50) C, 52.53; H, 6.15; Au, 26.11; B, 1.43; F, 10.07; N, 3.71. Found: C, 52.71; H, 6.03; N, 3.90.

Synthesis of NHC^{iPr}-Au-(3-hexyne)-BArF

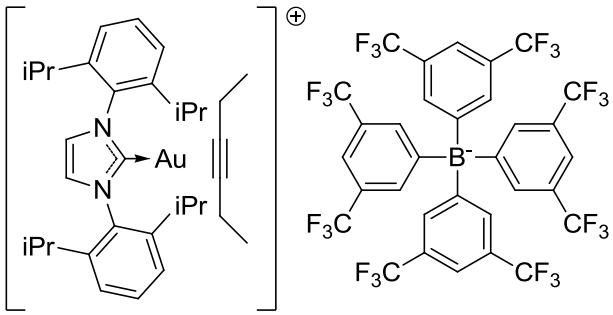

(Yield 75%) Starting from the compound NHC^{iPr}-Au-(3-hexyne)BF_4 then NaBArF (77.8 mg, 0.09 mmol) was added, resulting in the formation of a thin new precipitate. The reaction mixture was filtered again on Celite® pad, washed with 3x1 mL of CH_2Cl_2,concentered under vacuum and then n-pentane (4mL) was added, resulting in the formation of precipitate. The resulting solid was filtered off and washed with 3x2 mL of n-pentane. Then dried under vacuum to afford the product as a mild-yellow powder (yield 104.1 mg, 85%).^{1}H NMR (200 MHz, CD_2Cl_2, 298 K): δ (ppm) 7.72 (bs, 8H), 7.57 (t, 2H, J_3^{HH} = 7.8 Hz), 7.56 (bs, 4H), 7.43 (s, 2H), 7.37 (d, 4H, J_3^{HH} = 7.6Hz), 2.51 (sept, 4H, J_3^{HH} = 7.8 Hz), 2.3-2.07 (m, 4H, J_3^{HH} = 7.3 Hz), 1.29 (d, 12H, J_3^{HH} = 6.8 Hz), 1.26 (d, 12H, J_3^{HH} = 6.8 Hz), 0.61 (t, 6H, J_3^{HH} = 7.4 Hz). ^{13}C-{^{1}H} NMR (200 MHz, CD_2Cl_2, 298 K): δ (ppm) 178.6, 162.5 (m), 164.5, 135.5, 133.6, 132.2, 129.4 (m), 126.6, 125.3, 118.1, 87.9, 29.6, 25.0 (d), 24.3 (d), 15.3, 13.6. ^{19}F NMR (200 MHz, CD_2Cl_2, 298 K): δ (ppm) -62.84 (s, CF_3). Anal. Calc. for $C_{65}H_{58}AuBF_{24}N_{22}$ (1530.91): C, 51.00; H, 3.82; Au, 12.87; B, 0.71; F, 29.78; N, 1.83. Found: C, 51.02; H, 3.84; N, 1.82.

Synthesis of NHC-Au-X (NHC= NHC^{iPr}, NHC^{CH2}, BIAN; X= NTf$_2^-$, OTs$^-$, ClO$_4^-$, TFA$^-$, Ac$^-$)

NHC^{iPr}-Au-OTs

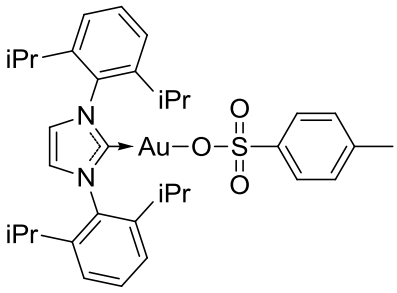

(Yield 90%) ^{1}H NMR (200 MHz, CD_2Cl_2, 298 K): δ (ppm) 7.55 (t, 2H, J_{HH} = 7.8 Hz), 7.39 (d, 4H, J_{HH} = 7.7 Hz), 7.31 (d, 2H, J_{HH} = 7.7 Hz), 7.21 (s, 2H), 6.98 (d, 2H, J_{HH} = 7.4 Hz), 2.47 (sept, 4H, J_{HH} = 6.8 Hz), 2.32 (s, 3H), 1.29 (d, 12H, J_{HH} = 6.8 Hz), 1.21 (d, 12H, J_{HH} = 6.8 Hz). ^{13}C {^{1}H}-NMR (200 MHz, CD_2Cl_2, 298 K): δ (ppm) 164.5, 145.7, 133.8, 131.1, 128.8, 126.4, 124.6, 123.6, 123.2, 29.05, 24.3, 21.6, 21.6. Anal. Calc. for $C_{34}H_{44}AuN_2O_3S$ (757.76): C, 53.89; H, 5.85; Au, 25.99; N, 3.70; O, 6.33; S. 4.23. Found: C, 53.91; H, 5.84; N, 3.6.

NHC^{iPr}-Au-TFA

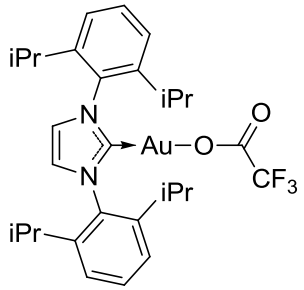

(Yield 91%) ^{1}H NMR (200 MHz, CD_2Cl_2, 298 K): δ (ppm) 7.58 (t, 2H, J_{HH} = 7.8 Hz), 7.37 (d, 4H, J_{HH} = 7.7 Hz), 7.28 (s, 2H), 2.56 (sept, 4H, J_{HH} = 6.9 Hz), 1.35 (d, 12H, J_{HH} = 6.8 Hz), 1.24 (d, 12H, J_{HH} = 6.8 Hz). ^{19}F NMR (200 MHz, CD_2Cl_2, 298 K): δ (ppm) -73.89; ^{13}C $\{^{1}H\}$-NMR (200 MHz, CD_2Cl_2, 298 K): δ (ppm) 166.0, 162.1, 146.4, 134.4, 131.2, 124.8, 124.4, 116.5, 29.5, 24.5. ^{19}F NMR (200 MHz, $CDCl_3$, 298 K): δ (ppm) -78.59. Anal. Calc. for $C_{29}H_{37}AuF_3N_2O_2$ (699.58): C, 49.79; H, 5.33; Au, 28.16; F, 8.15; N, 4.00; O, 4.57. Found: C, 49.82 ; H, 5.84; N, 3.86.

NHC^{iPr}-Au-ClO$_4$

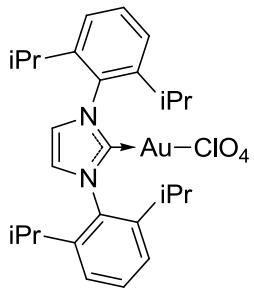

(Yield 80%) ^{1}H NMR (200 MHz, CD_2Cl_2, 298 K): δ (ppm) 7.59 (t, 2H, J_{HH} = 8.1 Hz), 7.38 (s, 2H), 7.33 (d, 3H, J_{HH} = 8.1 Hz), 2.50 (sept, 4H, J_{HH} = 7.0 Hz), 1.33 (d, 12H, J_{HH} = 6.9 Hz), 1.23 (d, 12H, J_{HH} = 6.8 Hz). ^{13}C $\{^{1}H\}$-NMR (200 MHz, CD_2Cl_2, 298 K): δ (ppm) 159.41, 1478, 133.49, 131.15, 124.50, 124.36, 28.91, 24.18, 23.84. Anal. Calc. for $C_{27}H_{36}AuClN_2O_4$ (684.28): C, 47.34; H, 5.30; Au, 28.75; Cl, 5.18; N, 4.09; O, 9.34. Found: C, 47.45 ; H, 5.70; N, 4.20.

NHC^{iPr}-Au-Ac

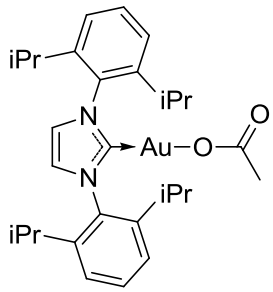

(Yield 78%) ^{1}H NMR (200 MHz, CD_2Cl_2, 298 K): δ (ppm) 7.59 (t, 2H, J_{HH} = 8.1 Hz), 7.38 (s, 2H), 7.33 (d, 3H, J_{HH} = 8.1 Hz), 2.52 (sept, 4H, J_{HH} = 7.0 Hz), 1.64 (s, 3H), 1.33 (d, 12H, J_{HH} = 6.9 Hz), 1.23 (d, 12H, J_{HH} = 6.8 Hz). ^{13}C $\{^{1}H\}$-NMR (200 MHz, CD_2Cl_2, 298 K): δ (ppm) 175.7, 168.7, 146.1, 134.5, 130.9, 124.5, 123.7, 29.2, 24.4, 24.1, 23.9. Anal. Calc. for $C_{29}H_{39}AuN_2O_2$ (644.60): C, 54.04; H, 6.10; Au, 30.56; N, 4.35; O, 4.96. Found: C, 53.85; H, 6.88; N, 4.12.

NHC^{iPr}-Au-NTf$_2$

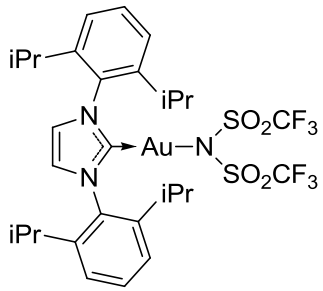

(Yield 95%) ^{1}H NMR (200 MHz, CD_2Cl_2, 298 K): δ (ppm) 7.57 (t, 2H, J_{HH} = 8.0 Hz), 7.35 (s, 2H), 7.32 (d, 3H, J_{HH} = 8.1 Hz), 2.50 (sept, 4H, J_{HH} = 7.0 Hz), 1.62 (s, 3H), 1.32 (d, 12H, J_{HH} = 6.9 Hz), 1.25 (d, 12H, J_{HH} = 6.8 Hz). ^{13}C $\{^{1}H\}$-NMR (200 MHz, CD_2Cl_2, 298 K): δ (ppm) 168.3, 146.0, 136.5, 133.2, 124.8, 124.1, 119.2 (m), 29.2, 24.4, 24.1, 23.9. Anal. Calc. for $C_{29}H_{36}AuF_6N_3O_4S_2$ (865.70): C, 40.23; H, 4.19; Au, 22.75; F, 13.17; N, 4.85; O, 7.39, S, 7.41. Found: C, 40.99; H, 4.01; N, 5.02; S, 7.11.

Synthesis of NHC^{CH2}-Au-X (X= OTs$^-$, OTf$^-$)

NHC^{CH2}-Au-OTs

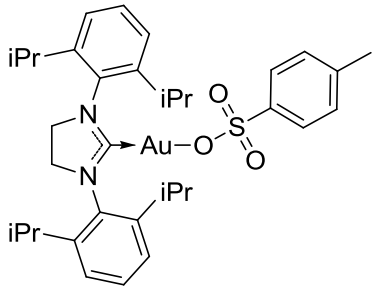

(Yield 94%) ^{1}H NMR (200 MHz, CD_2Cl_2, 298 K): δ (ppm) 7.88 (d, 2H, J_{HH} = 8.2Hz), 7.53-7.35 (m, 2H), 7.25-7.22 (m, 2H), 4.05 (d, 4H, J_{HH} = 7.4 Hz), 3.08-3.02 (m, 4H), 2.37 (s, 3H), 1.41 (d, 12H, J_{HH} = 6.9 Hz), 1.33 (d, 12H, J_{HH} = 6.9 Hz). ^{13}C {^{1}H}-NMR (200 MHz, CD_2Cl_2, 298K): δ (ppm) 196.0, 146.5, 141.7, 139.0, 134.0, 130.0, 128.9, 126.4, 124.7, 53.8, 28.9, 25.4, 24.0, 21.3. Anal. Calc. for $C_{34}H_{45}AuN_2O_3S$ (758.76): C, 53.82; H, 5.98; Au, 25.96; N, 3.69; O, 6.33; S. 4.23. Found: C, 54.03; H, 5.55; N, 3.82; S, 4.10.

NHC^{CH2}-Au-OTf

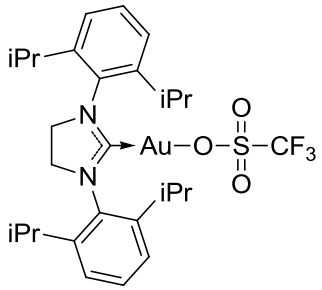

(Yield 95%) 7.53-7.35 (m, 2H), 7.25-7.22 (m, 4H), 4.05 (d, 4H, J_{HH} = 7.4 Hz), 3.08-3.02 (m, 4H), 1.41 (d, 12H, J_{HH} = 6.9 Hz), 1.33 (d, 12H, J_{HH} = 6.9 Hz). ^{13}C {^{1}H}-NMR (200 MHz, CD_2Cl_2, 298K): δ (ppm) 196.0, 146.5, 134.0, 130.0, 124.7, 53.8, 28.9, 25.4, 24.0. ^{19}F NMR (200 MHz, $CDCl_3$, 298 K): δ (ppm) -78.22. Anal. Calc. for $C_{28}H_{38}AuF_3N_2O_3S$ (736.64): C, 45.65; H, 5.20; Au, 26.74; F, 7.74; N, 3.80; O, 6.52; S. 4.35. Found: C, 49.47; H, 5.06; N, 3.92; S, 4.13.

Synthesis of BIAN-Au-X (X= OTs$^-$, OTf$^-$)

BIAN-Au-OTs

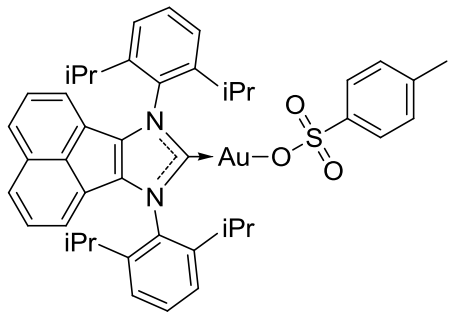

(Yield 96%) ^{1}H NMR (200 MHz, CD_2Cl_2, 298 K): δ (ppm) 7.84 (m, 4H), 7.68 (t, 2H, J_{HH} = 7.8 Hz, H7), 7.46 (dd, 2H, J_{HH} = 8.4 Hz, J_{HH} = 7.0 Hz, H9), 7.45 (d, 4H, J_{HH} = 7.9 Hz, H6), 7.21 (d, 2H, J_{HH} =8.0Hz), 7.03 (d, 2H, J_{HH} = 7.1 Hz, H8), 2.83 (*sept*, 4H, J_{HH} = 7.2 Hz, H4), 2.37 (s, 3H), 1.38 (d, 12H, J_{HH} = 6.9 Hz, H3), 1.21 (d, 12H, J_{HH} = 6.9 Hz, H5). ^{13}C {^{1}H}-NMR (200 MHz, CD_2Cl_2, 297 K): δ (ppm) 175.6, 146.1, 141.7, 139.0, 138.4, 133.1, 131.3, 130.5, 129.0, 128.9,128.2, 126.4, 125.6, 125.0, 121.7, 29.3, 24.59, 23.91, 21.3. Anal. Calc. for $C_{44}H_{47}AuN_2O_3S$ (880.89) C, 59.99; H, 5.38; Au, 22.36; N, 3.18; O, 5.45; S, 3.64. Found: C, 60.08; H, 5.24; N, 3.24; S, 3.43.

BIAN-Au-OTf

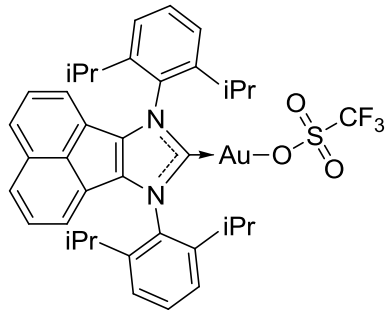

(Yield 91%) ^{1}H NMR (200 MHz, CD_2Cl_2, 298 K): δ (ppm) 7.84 (d, 2H, J_{HH} = 8.4 Hz, H10), 7.68 (t, 2H, J_{HH} = 7.8 Hz, H7), 7.46 (dd, 2H, J_{HH} = 8.4 Hz, J_{HH} = 7.0 Hz, H9), 7.45 (d, 4H, J_{HH} = 7.9 Hz, H6), 7.03 (d, 2H, J_{HH} = 7.1 Hz, H8), 2.83 (*sept*, 4H, J_{HH} = 7.2 Hz, H4), 1.38 (d, 12H, J_{HH} = 6.9 Hz, H3), 1.21 (d, 12H, J_{HH} = 6.9 Hz, H5). ^{13}C {^{1}H}-NMR (200 MHz, CD_2Cl_2, 297 K): δ (ppm) 175.6, 146.1, 165.8, 138.4, 133.1, 131.3, 130.5, 129.0, 128.2, 125.6, 125.0, 121.7, 29.3, 24.59, 23.91. Anal. Calc. for $C_{38}H_{40}AuF_3N_2O_3S$ (858.76) C, 53.15; H, 4.69; Au, 22.94; F, 6.64; N, 3.26; O, 5.59; S, 3.73. Found: C, 60.08; H, 5.24; N, 3.24; S, 3.43.

General synthesis of P-Au-OTs (P = PPh₃, JPhos, PCy₃, PArF, POR₃)

A general catalyst type P-AuCl (0.11 mmol) was dissolved in 5mL of CH_2Cl_2. Subsequently, 1.1 eq (0.12 mmol) of AgOTs was added, leading to the precipitation of AgCl. The reaction mixture was stirred overnight, and then dried. After the addition of 2 mL of fresh dichloromethane, the mixture was filtered on Celite® pad, washed with 3x1 mL of CH_2Cl_2, concentered under vacuum and then *n*-pentane (4mL) was added, resulting in the formation of precipitate. The resulting solid was filtered off and washed with 3x2 mL of *n*-pentane. Then dried under vacuum to afford the product as a white powder.

PPh₃-Au-OTs

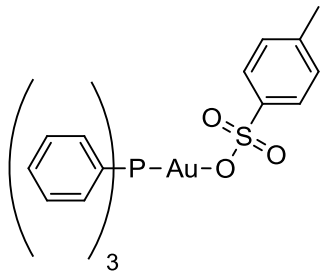

(Yield 78%) ^{1}H NMR (200 MHz, $CDCl_3$, 298 K): δ (ppm) 7.9-7.1 (m, 19H), 2.41 (s, 3H. ^{13}C {^{1}H}-NMR (200 MHz, $CDCl_3$, 298 K): δ (ppm) 141.7, 139.2, 134.1, 132.2, 129.4 129.0, 127.6, 126.5, 53.3. ^{31}P {1H}-NMR (81 MHz, $CDCl_3$, 298K): δ (ppm) 27.9. Anal. Calc. for $C_{25}H_{23}AuO_3PS$ (631.45): C, 47.55; H, 3.67; Au, 31.19; O, 7.60; P, 4.91; S, 5.08. Found: C, 47.19; H, 3.28; S, 4.99.

PPh₃-Au-OTs

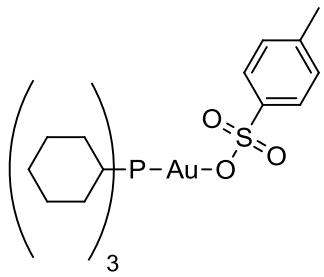

(Yield 75%) ^{1}H NMR (200 MHz, $CDCl_3$, 298 K): δ (ppm) 7.88 (d, 2H, J_{HH} =8.2Hz), 7.21 (d, 2H, J_{HH} =8.0Hz), 2.37 (s, 3H), 2.01-1.61 (m, 18H), 1.50-1.35 (m, 6H), 1.32-1.15 (m, 9H). ^{13}C {^{1}H}-NMR (200 MHz, $CDCl_3$, 298K): δ(ppm) 141.7, 139.0, 128.9, 126.4, 39.6, 33.1, 30.7, 27.4, 26.9, 25.8, 21.3. ^{31}P {^{1}H}-NMR (200 MHz, $CDCl_3$, 298K): δ (ppm) 54.01.. Anal. Calc. for $C_{25}H_{40}AuO_3PS$ (648.59): C, 46.30; H, 6.22; Au, 30.37; O, 7.40; P, 4.78; S, 4.94. Found: C, 46.76; H, 6.11; S, 4.63.

P(RO)$_3$-Au-OTs

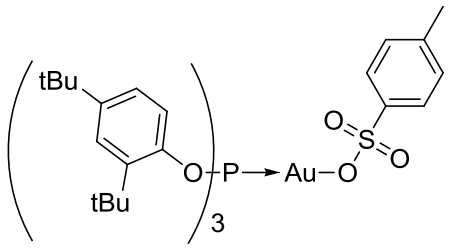

(Yield 63%) ^{1}H NMR (200 MHz, $CDCl_3$, 298 K): δ (ppm) 7.88 (d, 2H, J_{HH} =8.1Hz), 7.52-7.46 (m, 6H), 7.21 (d, 2H, J_{HH} =8.1Hz), 7.15 (m, J_{HH} = 8.5 Hz, 3H), 2.36 (s, 3H), 1.465 (s, 27H), 1.311 (s, 27H). ^{13}C {^{1}H}-NMR (200 MHz, $CDCl_3$, 298K): δ(ppm) 148.3, 147.3, 141.7, 139.3, 129.0, 126.3, 125.51, 124.30, 119.37 (d, J = 8.6 Hz), 35.23, 34.80, 31.52, 30.69, 21.3. ^{31}P {^{1}H}-NMR (200 MHz, $CDCl_3$, 298K): δ (ppm) 93.2. Anal. Calc. for $C_{49}H_{70}AuO_6PS$ (1015.08): C, 57.98; H, 6.95; Au, 19.40; O, 9.46; P, 3.05; S, 3.16. Found: C, 58.15 H, 6.72; S, 3.01.

PArF-Au-OTs

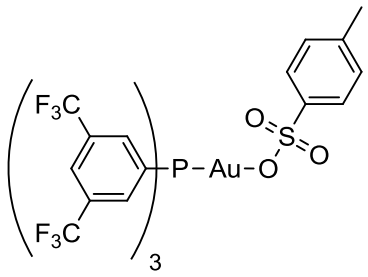

(Yield 72%) ^{1}H NMR (200 MHz, $CDCl_3$, 298 K): δ (ppm) 8.22 (s, 3H), 7.97 (d, 6H, J_{HP} = 13.5 Hz), 7.85 (d, 2H, J_{HH} = 7.3 Hz), 7.26 (d, 2H, J_{HH} = 7.4 Hz), 2.40 (s, 3H). ^{13}C {^{1}H}-NMR (50 MHz, $CDCl_3$, 298K): δ (ppm) 142.02, 139.26, 134.53 (m), 133.61 (m), 129.21, 128.86 (d, $^1J_{CP}$ = 64.8 Hz), 127.79 (m), 126.38,122.03 (m), 21.40. ^{19}F NMR (188 MHz, $CDCl_3$, 298K): δ (ppm) -63.88 (s, CF_3). ^{31}P {1H}-NMR (81 MHz, $CDCl_3$, 298K): δ (ppm) 32.45 (s, P). Anal. Calcd. for $C_{31}H_{16}AuF_{18}O_3PS$ (1038.43): C, 35.86; H, 1.55; Au, 18.97; F, 32.93; O, 4.62; P, 2.98; S, 3.09. Found: C, 35.90; H, 1.58.

JPhos-Au-OTs

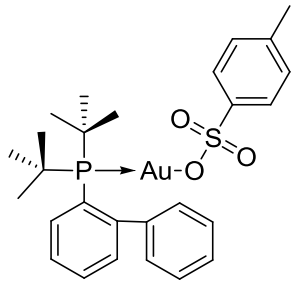

(Yield 75%) ^{1}H NMR (200 MHz, $CDCl_3$, 298 K): δ (ppm) 7.88 (d, 2H, J_{HH} = 8.2 Hz), 7.58 (t, 3H, J_{HH} = 7.3 Hz), 7.48-7.56 (m, 2H), 7.45 (t, 1H, J_{HH} = 7.7 Hz), 7.32 (t, 1H, J_{HH} = 5.4 Hz), 7.21 (d, 2H, J_{HH} = 8.0 Hz), 7.14 (d, 2H, J_{HH} = 7.4 Hz), 2.37 (s, 3H), 1.43 (d, 18H, J_{HH} = 15.5 Hz). ^{13}C {^{1}H}-NMR (200 MHz, $CDCl_3$, 298 K): δ (ppm) 133.6, 133.3, 130.7, 129.5, 128.8, 128.4, 126.9, 37.9, 21.0. ^{31}P {1H}-NMR (200 MHz, $CDCl_3$, 298 K): δ (ppm) 56.8. Anal. Calc. for $C_{25}H_{32}AuO_3PS$ (640.53): C, 46.88; H, 5.04; Au, 30.75; O, 7.49; P, 4.84; S, 5.01. Found: C, 47.01; H, 4.90; S, 4.17.

Dibutylammonium trifluoromethanesulfonate [(Bu)$_2$NH$_2$OTf]

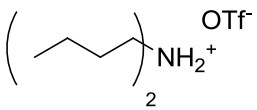

In a 10 mL flask, 1.1 equiv. of trifluoromethanesulfonic acid (576.3 mL, 6.53 mmol) was slowly added in a solution containing 1 equiv. of di-butylamine (1 mL, 5.93 mmol) in cyclohexane (5 mL) at 0°C. The mixture was then stirred overnight at room temperature. The solvent was removed under reduced pressure and the residue was washed several times with the minimum amount of cyclohexane and dried under vacuum. The reaction gave 1.18 g of white powder, 71% yield. ^{1}H NMR (200 MHz, $CDCl_3$, 298 K): δ (ppm) 7.37 (bs, 2H), 2.97 (bs, 4H), 1.71 (m, 4H), 1.38

(m, 4H), 0.93 (t, 6H, J_{HH} = 6.8 Hz); ^{13}C {^{1}H}-NMR (200 MHz, $CDCl_3$, 298 K): δ (ppm) 126.6, 48.37, 27.86, 19.75, 13.47; ^{19}F NMR (200 MHz, $CDCl_3$, 298 K): δ (ppm) -78.85; Found: N, 4.9; C, 39.9; H, 7.4; Calc. for $C_9H_{20}F_3NO_3S$: N, 5.01; C, 38.7; H, 7.22%.

Trioctylmethylammonium trifluoromethanesulfonate [Aliquat-OTf]

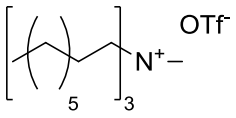

In a 50 mL flask, 1.1 equiv. of methyl trifluoromethanesulfonate (423.3 µL, 3.81 mmol) was slowly added to a solution containing 1 equiv. of Aliquat 336 (1.4 g, 3.46 mmol) in acetonitrile (30 mL) at 0°C. The reaction was then stirred overnight at room temperature. The solvent was removed under reduced pressure and the residue was dried under vacuum. The reaction gave 1.58 g of viscous orange oil, 96% yield. ^{1}H NMR (200 MHz, $CDCl_3$, 298 K): δ (ppm) 3.23 (m, 6H), 3.09 (s, 3H), 1.73-1.5 (bs, 6H), 1.44-1.17 (m, 30H), 0.87 (t, 9H, J_{HH} = 6.8 Hz); ^{13}C {^{1}H}-NMR (200 MHz, $CDCl_3$, 298 K): δ (ppm) 129.99, 123.61, 117.22, 110.93, 61.56, 48.46, 31.50, 29.23, 28.87, 26.07, 22.53, 22.45, 22.12, 13.95; ^{19}F NMR (200 MHz, CD_2Cl_3, 298 K): δ (ppm) -78.62; Found: N, 2.7; C, 60.9; H, 11.1; Calc. for C26H54F3NO3S: N, 2.71; C, 60.31; H, 10.51%.

Dodecylethyldimethylammonium trifluoromethanesulfonate [(Me)$_2$(Et)(Dod)NOTf]

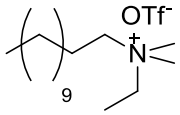

In a 50 mL flask, 1.1 equiv. of methyl trifluoromethanesulfonate (397.6 µL, 3.58 mmol) was slowly added to a solution containing 1 equiv. of dodecylethyldimethylammonium bromide (1.0 g, 3.25 mmol) in acetonitrile (30 mL) at 0°C. The reaction was then stirred overnight at room temperature. The solvent was removed under reduced pressure and the solid was dried under vacuum. The reaction gave 1.25 g of white powder, 98% yield. ^{1}H NMR (200 MHz, $CDCl_3$, 298 K): δ (ppm) 3.44 (q, 2H, J_{HH} = 6.6 Hz), 3.25 (m, 2H), 3.11 (s, 6H), 1.78-1.56 (bs, 2H), 1.45-1.18 (m, 21H), 0.87 (t, 3H, J_{HH} = 6.5 Hz); ^{13}C {^{1}H}-NMR (200 MHz, $CDCl_3$, 298 K): δ (ppm) 129.94, 123.72, 117.32, 111.4, 63.63, 59.40, 50.09, 31.74, 29.43, 29.29, 29.21, 29.16, 28.92, 25.99, 22.51, 22.40, 13.93, 8.00; ^{19}F NMR (200 MHz, $CDCl_3$, 298 K): δ (ppm) -78.59; Found: N, 3.2; C, 54.0; H, 9.4; Calc. for $C_{26}H_{54}F_3NO_3S$: N, 3.58; C, 52.15; H, 9.27%.

Choline trifluoromethan sulfonate

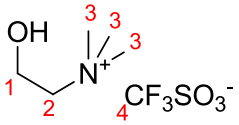

In a Schlenk flask under argon 1 equivalent of choline chloride (1 g, 7.16 mmol), previously dried at 80 °C in oven overnight, was dissolved in 5 mL of dry acetonitrile. The mixture was kept agitated with a magnetic stir bar at ambient temperature and 1.1 equivalents of methyl trifluoromethansulfonate (891.6 mL, 7.88 mmol) were slowly added. The reaction was stirred at ambient temperature for 2 hours, the solvent was removed under reduced pressure and the residue was kept under vacuum overnight. The reaction gave a white powder, 172.3 mg, yield 95%. ^{1}H NMR (200 MHz, D_2O, 298 K): δ (ppm) 4.08-3.96 (m, 1, 2H), 3.51-3.43 (m, 2, 2H), 3.16 (s, 3, 9H); ^{13}C {^{1}H}-NMR (200 MHz, D_2O, 298 K): δ (ppm) 131.69, 125.94, 125.39, 119.08, 70.03, 69.97, 69.91, 58.16, 56.49, 56.42, 56.34;

^{19}F NMR (200 MHz, $CDCl_3$, 298 K): δ (ppm) -73.74. Found: C, 28.3; H, 5.9; N, 25.8; S, 12.8. Calc. for $C_6H_{14}F_3NO_4S$: C, 28.5; H, 5.6; N, 25.3; S, 12.7%.

4.3. Catalysis

4.3.1. Hydration of alkynes chapter 2.1

Hydration of 3-hexyne (**Table 3**). In a 2 mL glass screw-top vial, NHC^{iPr}-Au-X (0.00175 mmol), distilled water (35 µL, 1.925 mmol,) and 3-hexyne (200 µL 1.75 mmol) were added. The vial was placed in a bath oil at 30°C with magnetic stirring. The reactions were checked by NMR.

Hydration of 3-hexyne (**Table 3** and**Table 4**). In a 2 mL glass screw-top vial, NHC^{iPr}-Au-OTf (0.00175 mmol, 1.3 mg), distilled water or deuterated water (35 µL, 1.925 mmol,) 3-hexyne (200 µL 1.75 mmol) and appropriate additives (0.00875-0.0875 mmol) were added. The vial was placed in a bath oil at indicated temperature with magnetic stirring. The reactions were check by NMR.

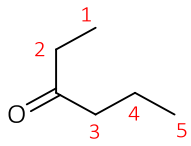

3-hexanone - ^{1}H NMR (200 MHz, $CDCl_3$, 298 K): δ (ppm) 2.36 – 2.39 (tq, $^{3}J_{HH}$ = 7.4 Hz, $^{3}J_{HH}$ = 7.3 Hz, 4H, H2 and H3), 1.58 (m, 2H, H4), 1.03 (t, $^{3}J_{HH}$ = 7.4 Hz, 3H, H1), 0.89 (t, $^{3}J_{HH}$ = 7.4 Hz, 3H, H5).

Table S1: *NHC^{iPr}-Au-OTf catalysed hydration of 3-hexyne[a]*

entry	Loading (mol%)[b]	T (°C)	Additives (mol%)[c]	Conv.[d] (%)	Time[e] (h) (TOF[f])
1	0.1	30	[BMIM]OTf (5)	<1	24
2	0.1	30	NH_4OTf (5)	2.3	2 (11)
				4.9	4 (12)
				11.2	6 (19)
				16.0	8 (20)
				78.3	14 (56)
				99.2	16 (62)
3	0.1	30	NBu_4OTf (5)	10.6	0.5 (212)
				42.9	1 (429)
				77.5	1.5 (516)
				99.0	2 (495)
4[g]	0.1	30	NBu_4OTf (5)	11.2	0.5 (224)
				41.5	1 (415)
				74.2	1.5 (495)
				98.6	2 (499)
5	0.1	30	NBu_4OTf (2.5)	7.24	0.5 (145)
				26.3	1 (263)
				48.9	1.5 (326)
				71.8	2 (359)
				97.2	2.5 (390)
6	0.1	30	NBu_4OTf (1)	6.8	0.5 (136)
				26.4	1 (264)

				43.6	1.5 (291)
				65.7	2 (328)
				88.6	2.5 (354)
				97.3	3 (324)
7	0.1	30	NBu_4OTf (0.5)	29.0	2 (145)
				55.2	4 (138)
				99.1	6 (165)
8	0.2	30	NBu_4OTf (5)	45.1	0.5
				98.0	2 (290)
9	0.05	40	NBu_4OTf (5)	21.5	1 (215)
				40.2	1.5 (603)
				93.0	3 (620)
10	0.05	50	NBu_4OTf (5)	15.4	0.5 (77)
				52.5	1 (525)
				95	1.5 (1267)
11	0.025	50	NBu_4OTf (5)	18.2	1 (728)
				42.9	2 (858)
				73.2	3 (976)
				>99	4 (1000)
12[h]	0.01	60	NBu_4OTf (5)	19.3	2 (965)
				42.9	4 (1072)
				>99	7 (1414)
13[h]	0.01	60	NBu_4OTf (10)	22.4	2 (1120)
				62.2	4 (1550)
				>99	6 (1668)
14[h]	0.005	70	NBu_4OTf (5)	<1	48
15	0.1	30	-	1.3	2 (6)
				4.6	4 (11)
				10.4	6 (17)
				15.3	8 (19)
				77.1	14 (55)
				98.15	16 (61)

[a] Catalysis conditions: 3-hexyne (1.75 mmol, 200 µL) and H_2O (1.92 mmol, 35 µL). [b] (moles of catalyst / mole of alkyne) x 100. [c] (moles of additive / moles of alkyne) x 100. [d] Determined by ^1H NMR; averaged value of three measurements. [e] Time necessary to reach the reported conversion. [f] TOF = ($n_{product}$ / $n_{catalyst}$) / t(h) at the reported conversion. [g] In the presence of 0.26 mmol of 3-hexanone. [h] 3-Hexyne (3.5 mmol, 400 µL) and H_2O (3.84 mmol, 70 µL).

Table S2: *NHC^{iPr}-Au-OTf catalysed hydration of 3-hexyne[a], acidic additives and KIE effect*

entry	Loading (mol%)[b]	Nucl.	Additives (mol%) [c]	Conv.[d] (%)	Time[e] (h) (TOF[f])
1	0.1	H_2O	NBu_4OTf (0)	1.3	2 (6)
				4.6	4 (11)
				10.4	6 (17)
				15.3	8 (19)
				77.1	14 (55)
				98.15	16 (61)
2	0.1	D_2O	NBu_4OTf (0)	0	2
				0	4
				0.3	6 (0.5)
				1.6	8 (2)
				17.9	14 (13)
				20.1	16 (13)
				28.3	20 (14)
				42.0	24 (17)
3	0.1	H_2O	NBu_4OTf (5)	10.6	0.5 (212)
				42.9	1 (429)
				77.5	1.5 (516)
				99.0	2 (495)
4	0.1	D_2O	NBu4OTf (5)	0	0.5
				2.5	1 (250)
				10.9	1.5 (163)
				23.5	2 (117)
				42.8	2.5 (171)
				53.7	3 (179)
				80.7	4 (201)
				97.3	5 (198)
5	0.1	H_2O	HOTf (5)	8.7	0.5 (43)
				38.5	1 (385)
				72.1	2 (360)
				90.6	3 (302)
				99.0	4 3 (330)
6	0.1	D_2O	HOTf (5)	22.3	0.5 (446)
				54.1	1 (541)
				77.23	2 (386)
				87.9	3 (293)
				94.9	4 3 (330)
7	0.1	H_2O	$HClO_4$ (5)	<1	24

[a] Catalysis conditions: 3-hexyne (1.75 mmol, 200 µL) and nucleophile (1.92 mmol, 35 µL). [b] (moles of catalyst / moles of alkyne) x 100. [c] (moles of additive / moles of alkyne) x 100.d Determined by 1H NMR; average value of three measurements. [e] Time necessary to reach the reported conversion. [f] TOF = ($n_{product}$ / $n_{catalyst}$) / t(h) at the reported conversion.[144]

Hydration of alkynes (**Table 6**). In a 2 mL glass screw-top vial, NHC^{iPr}-Au-OTf (0.00875 mmol, 6.43 mg), distilled water (35 µL, 1.925 mmol), tetrabutylammonium trifluoromethansulfonate (0.0875 mmol, 34 mg) and the relative alkyne (1.75 mmol) were added. The vial was placed in a bath oil at 50°C with magnetic stirring. The reactions were check by NMR.

The relative ketones are commercially available: 2-hexanone [**591-78-6**], 2-octanone [**111-13-7**], 1-phenylpropan-2-one [**103-79-7**], 1-phenylethanone [**98-86-2**], 1-phenylpropan-1-one [**93-55-0**], 4-octanone [**589-63-9**], 1,4-dimethoxybutan-2-one [**25680-86-8**], methyl-3-oxohexanoate [**30414-54-1**], diethyl oxalacetate [**108-56-5**], 5-hydroxy-2-pentanone [**1071-73-4**]. Their spectra are in agree with the standards.

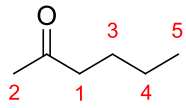	^{1}H NMR (200 MHz, $CDCl_3$, 298 K): δ (ppm) 2.39 (t, $^3J_{HH}$ =7.63, **1**), 2.13 (s, **2**), 1.56 (q, $^3J_{HH}$ =7.8, **3**), 1.30 (m, **4**), 0.9 (t, $^3J_{HH}$ =7.4 Hz, **5**)
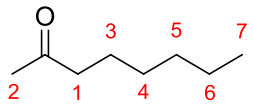	^{1}H NMR (200 MHz, $CDCl_3$, 298 K): δ (ppm) 2.41 (t, J=7.64 Hz, **1**), 2.13 (s, **2**), 1.70-1.41 (m, **3**), 1.30-1.20 (m, **4-5-6**), 0.88 (t, $^3J_{HH}$ =6.77 Hz, **7**)
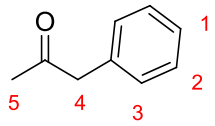	^{1}H NMR (200 MHz, $CDCl_3$, 298 K): δ (ppm) 7.97 (m, **1-2-3**), 3.70 (s, **4**), 2.15 (s, **5**)
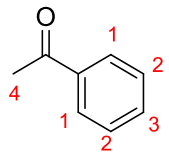	^{1}H NMR (200 MHz, $CDCl_3$, 298 K): δ (ppm) 8.02-7.92(m, **1**), 7.63-7.32 (m, **2** and **3**), 2.61 (s, **4**)
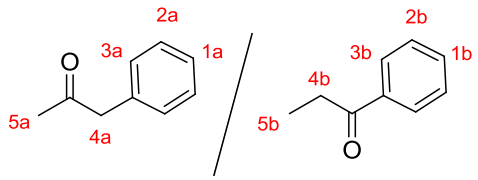	^{1}H NMR (200 MHz, $CDCl_3$, 298 K): δ (ppm) 8.01-7.93 (m, **3b**), 7.62-7.36 (m, **1b-2b**), 7.35-7.16 (m, **1a-2a-3a**), 3.70 (s, **4a**), 3.01 (q, $^3J_{HH}$ =7.21 Hz, **4b**), 2.15 (s, **5a**), 1.23 (t, $^3J_{HH}$ =7.25 Hz, **5b**)
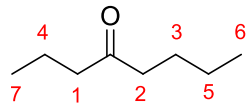	^{1}H NMR (200 MHz, $CDCl_3$, 298 K): δ (ppm) 2.39 (m, **1-2**), 1.57 (m, **3-4**), 1.30 (m, **5**), 0.91 (m, **6-7**)
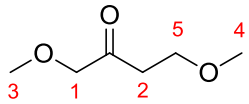	^{1}H NMR (200 MHz, $CDCl_3$, 298 K): δ (ppm) 4.05 (s, **1**), 3.66 (t, $^3J_{HH}$ =6.2 Hz, **5**), 3.43 (s, **4**), 3.32 (s, **3**), 2.67 (t, J=6.1 Hz, **2**)
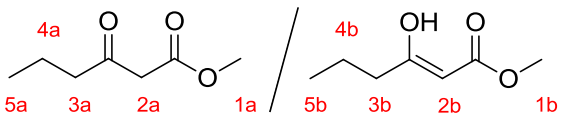	^{1}H NMR (200 MHz, $CDCl_3$, 298 K): δ (ppm) 12.01 (s, **OH**), 4.99 (s, **2b**), 3.73 (s, **1a**), 3.72 (s, **1b**), 3.44 (s, **2a**), 2.51 (t, $^3J_{HH}$ =7.3 Hz, **3a**), 2.4 (t, $^3J_{HH}$ =7.36 Hz, **3b**), 1.62 (m, **4a-4b**), 0.92 (t, $^3J_{HH}$ =7.37 Hz, **5a-5b**)

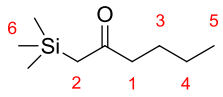	^{1}H NMR (200 MHz, $CDCl_3$, 298 K): δ (ppm) 2.42 (t, $^3J_{HH}$ =7.48, **1**), 2.14 (s, **2**), 1.65-1.2 (m, **3-4**), 0.9 (t, $^3J_{HH}$ =7.4, **5**), 0.06 (s, **6**)
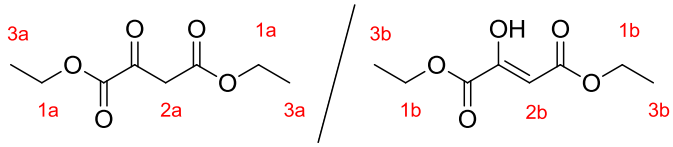	^{1}H NMR (200 MHz, $CDCl_3$, 298 K): δ (ppm) 11.67 (s, **OH**), 6.02 (s, **2b**), 4.43-4.08 (m, **1a-1b**), 3.81 (s, **2a**), 1.45-1.15 (m, **3a-3b**)
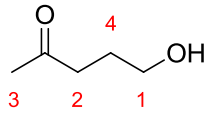	^{1}H NMR (200 MHz, $CDCl_3$, 298 K): δ (ppm) 3.63 (m, **1**), 2.59 (m, **2**), 2.17 (s, **3**), 1.79 (m, **4**)

Table S3: *NHC^{iPr}-Au-OTf catalyzed hydration of alkynes[a] and substrate scope*

entry	Loading (mol%)[b]	Substrate	Conv.[c] (%)	Timed (h) (TOF[e])
1	0.5	1-hexyne (**2**)	30.2	2 (30)
			52.4	4 (26)
			>99 (**2a**)	6 (34)
2	0.5	1-octyne (**3**)	21.5	2 (21)
			65.5	4 (33)
			>99 (**3a**)	6 (34)
3	0.5	3-phenyl-1-propyne (**4**)	22.0	2 (22)
			64.8	4 (32)
			>99 (**4a**)	6 (34)
4	0.5	Phenylacetylene (**5**)	10.2	2 (10)
			43.2	4 (21)
			63.5	6 (21)
			>99 (**5a**)	8 (25)
5	0.5	1-phenyl-1-propyne (**6**)	50.4 ((90 (**6a**), 10 (**6b**))	1 (100)
			>99 (90 (**6a**), 10 (**6b**))	2 (100)
6	0.1	4-octyne (**7**)	20.3	3 (68)
			80.2	6 (133)
7	0.5	1,4-dimethoxy-2-butyne (**8**)	45.8	1 (92)
			>99 (**8a**)	2 (100)
8	0.5	methyl-2-hexynoate (**9**)	28.2(90 (**9a**) , 10 (**9b**))	2 (28)
			67.8(90 (**9a**) , 10 (**9b**))	4 (34)
			>99 (90 (**9a**) , 10 (**9b**))	6 (34)
9	0.5	1-trimethylsilyl-1-hexyne (**10**)	10.1	2 (10)
			20.3	4 (10)
			54.0 (**10a**)	7 (15)

10	0.5	Diethylacetylenedicarboxylate (**11**)	33.2	1 (66)
			71 (47 (**11a**) , 53 (**11b**))	2 (71)
11	0.5	3-pentyl-1-ol (**12**)	48.3	1 (97)
			>99 (**12a**)	2 (100)

[a] Catalysis conditions: 50°C, alkyne (1.75 mmol) and water (1.92 mmol, 35 µL), 5% NBu4OTf (0,0875 mmol, 34 mg). [b] (moles of catalyst / moles of alkyne) x 100. [c] Determined by ^{1}H NMR; average value of three measurements; in brackets the products obtained (see below) with their molar ratio. [d] Time necessary to reach the reported conversion. [e] TOF = ($n_{product}$ / $n_{catalyst}$) / t(h) at the reported conversion.

Hydration of 3-hexyne (Recyclability test page 36). In a 2 mL glass screw-top vial, NHC^{iPr}-Au-OTf (0.00175 mmol, 1.3 mg), distilled water (32 µL, 1.75 mmol,) 3-hexyne (200 µL 1.75 mmol) and tetrabutylammonium trifluoromethansulfonate (0.0875 mmol, 34 mg) were added. The vial was placed in a bath oil at 30° with magnetic stirring. The reactions were check by NMR. After the complete conversion (two hours) the solution was distilled under vacuum and 3-hexanone was recovered in a Schlenk flask plunged in nitrogen liquid bath. Distilled water (32 µL, 1.75 mmol,) and 3-hexyne (200 µL 1.75 mmol) were added to the catalyst/additive solid mixture. The vial was placed in a bath oil at 30° with magnetic stirring. This procedure was repeated 4 times.

4.3.2. Hydration of alkynes chapter 2.2

Hydration of 3-hexyne with L-Au-Cl (Table S4).

L-Au-Cl (0.00175 mmol), AgOTf (0.45 mg, 0.00175 mmol), 3-hexyne (199 μL, 1.75 mmol), water (34.6 μL, 1.925 mmol) and NBu_4OTf (34.2 mg, 0.0875 mmol) were mixed in a 2 mL glass screw-top vial, which was then placed in a bath oil at 30 °C with magnetic stirring. The progress of the reaction was checked by ^1H NMR.

Hydration of 3-hexyne with L-Au-OTf or L-Au-OTs (Table S4 and Table S5).

L-Au-X (0.00175 mmol), 3-hexyne (199 μL, 1.75 mmol), water (34.6 μL, 1.925 mmol) and NR_4OTf (0.0875 mmol) were mixed in a 2 mL glass screw-top vial, which was then placed in a bath oil at 30 °C with magnetic stirring. The progress of the reaction was checked by ^1H NMR.

Hydration of diphenylacetylene (Table S6).

- With H_2O

NHC^{iPr}-Au-X (from 0.01 to 0.1 mmol), diphenylacetylene (312 mg, 1.75 mmol), water (34.6 μL, 1.925 mmol) and NBu_4OTf (34.3 mg, 0.0875 mmol) were mixed in a 2 mL glass screw-top vial, which was then placed in a bath oil at a fixed temperature (60, 80 or 120 °C) with magnetic stirring. The progress of the reaction was checked by ^1H NMR.

- With D_2O

NHC^{iPr}-Au-X (from 0.01 to 0.1 mmol), diphenylaceteylene (312 mg, 1.75 mmol), deuterium oxide (35 μL, 1.925 mmol) and NBu_4OTf (34.3 mg, 0.0875 mmol) were mixed in a 2 mL glass screw-top vial, which was then placed in a bath oil at 120°C with magnetic stirring. The progress of the reaction was checked by ^1H NMR.

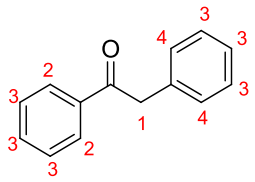

^1H NMR (200 MHz, $CDCl_3$, 298 K): δ (ppm) 8.01 (m, 2H, **2**), 7.62-7.39 (m, 6H, **3**), 7.31-7.27 (m, 2H, **4**), 4.28 (s, 1H, **1**).

Table S4: *L-Au-X (0.1 mol%) catalyzed hydration of 3-hexyne at 30 °C in the presence of NBu_4OTf [a,b]*

Entry	L [c]	X^-	AgOTf (mol%)	Conv. (%)[d]	Time[e] (h) (TOF[f])
1	NHC^{iPr}	OTf	-	10.6	0.5 (212)
				42.9	1 (429)
				77.5	1.5 (516)
				99.1	2 (495)
2	NHC^{iPr}	Cl^-	0.1	25.6	1 (256)
				66	1.5 (440)

				70	2 (350)
				70	2.5 (280)
3	BIAN	Cl^-	0.1	15.4	1 (154)
				67	1.5 (446)
				75.5	2 (380)
				75.5	2.5 (302)
4	NHC^{CH2}	Cl^-	0.1	16.1	1 (161)
				52.6	1.5 (350)
				75	2 (380)
				75	2.5 (300)
5	NAC	Cl^-	0.1	24	0
6	JPhos	Cl^-	0.1	18.3	1 (183)
				29.6	1.5 (197)
				46.9	2 (234)
				56.6	2.5 (226)
				66.9	3 (223)
				75.3	4 (188)
7	PCy_3	Cl^-	0.1	24	0
8	PArF	Cl^-	0.1	24	0
9	PPh_3	Cl^-	0.1	24	0
10	POR_3	Cl^-	0.1	24	0
11	NHC^{iPr}	OTs^-	-	14.1	1 (141)
				77.7	2 (388)
				99.9	3 (285)
12	BIAN	OTs^-	-	2	1 (20)
				2.6	1.5 (17)
				18.1	2 (90)
				63.5	2.5 (254)
				93.8	3 (312)
				97.8	4 (248)
13	NHC^{CH2}	OTs^-	-	0	1
				0	2
				2	4 (5)
				26.9	6 (45)
				63.3	6.5 (97)
				86.6	7 (123)
				98.5	8 (122)
14	NAC	OTs^-	-	3	1 (30)
				4.8	2 (24)
				8.7	3 (29)
				9.0	4 (22)
				9.1	24 (4)
15	JPhos	OTs^-	-	19.5	1(195)
				74.5	5 (148)
				85.3	24 (35)
16	PCy_3	OTs^-	-	0	1
				0	2
				2	6 (3)

				6	24 (3)
17	PArF	OTs^-	-	0	24
18	PPh_3	OTs^-	-	0	1
				0	2
				0	6
				3	24 (1)
19	POR_3	OTs^-	-	0	1
				1.1	5 (2)
				17	24 (7)
20	BIAN	OTf^-	-	24.7	1 (247)
				94.3	1.5 (629)
				>99	2 (495)
21	NHC^{CH2}	OTf^-	-	0	1
				25.1	2 (125)
				73.7	3 (245)
				>99	4 (248)

[a] Catalytic conditions: 3-hexyne (1.75 mmol, 200 µL), 5% NBu_4OTf (0.087 mmol, 34.3 mg), H_2O (1.92 mmol, 35 µL), L-Au-X (0.00175 mmol) and AgOTf (0.00175 mmol, 0,45 mg) when indicated. [b] mol% = (moles of catalyst / moles of alkyne) x 100. [c] see text. [d] Determined by ^1H NMR, averaged value of three measurements. [e] Time necessary to reach the reported conversion. [f] TOF = ($n_{product}$ / $n_{catalyst}$) / t(h) at the reported conversion. [g] from reference[144].

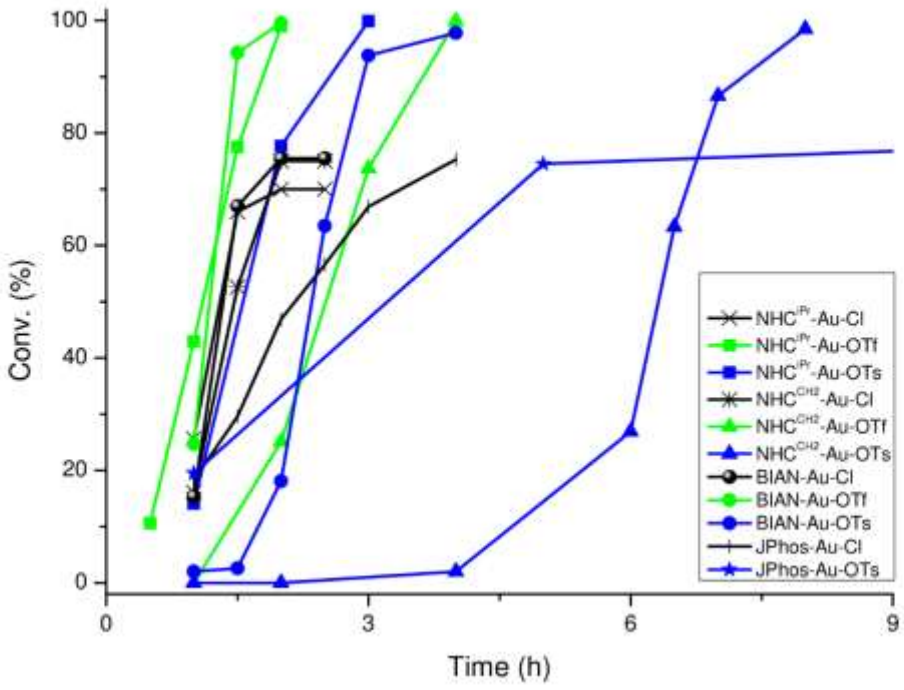

Figure S1: *Hydration of 3-hexyne with 0.1% cat. loading, at 30°C with 5% of NBu_4OTf*

Table S5: *NHC^{iPr}-Au-OTf catalyzed hydration of 3-hexyne*

entry	Loading (mol%)[b]	Additive	Conv.[c] (%)	Time[d] (h)
1	0.1	$(Bu)_2NH_2OTf$	0	2.5
			12.3	4 (31)
2		Aliquat-OTf	0	1
			2.4	2 (12)
			4.8	4 (12)
			41.9	6 (70)
			55.5	6.5 (85)
			68	7 (97)
			91.6	24 (38)
3		$(Me)_2(Et)(Dod)NOTf$	5.03	0.5 (100)
			44.1	1 (440)
			76.9	1.5 (512)
			92.9	2.5 (371)

[a] Catalysis conditions: 3-hexyne (1.75 mmol, 200 μL) and H_2O (1.92 mmol, 35 μL) at 30 °C. [b] (moles of catalyst / moles of alkyne) x 100.[c] Determined by ^1H NMR, average value of three measurements; in brackets the products obtained (see below) with their molar ratio. [d] Time necessary to reach the reported conversion.

Table S6: *NHC^{iPr}-Au-X catalyzed hydration of diphenylacetylene*

entry	Catalyst loading (mol%)[b]	T (°C)	X^-	Conv.[c] (%)	Time[d] (h) (TOF[e])
1	0.1	60	OTf^-	26.3	2 (131)
				62.4	6 (104)
				72.8	7 (104)
				82.3	8 (102)
				88.9	24 (37)
2	0.05	80	OTf^-	7.5	2 (75)
				21.5	3 (143)
				27.1	4 (135)
				31.3	5 (125)
				35.0	6 (116)
				42,5	8 (105)
				56.2	24 (47)
				60.1	72 (17)
3	0.05	120	OTf^-	81.6	2 (816)
				94.1	4 (470)
				95.8	5 (383)
				96.0	8 (240)
				96.2	24 (8)
4	0.025	120	OTf^-	40.7	2 (814)
				67.2	4 (672)
				73.5	5 (588)
				84.6	8 (435)
				88.0	24 (13)

5	0.01	120	OTf^-	19.1	2 (955)
				27.4	4 (685)
				28.4	5 (560)
				28.4	8 (355)
				28.6	24 (119)
6[f]	0.05	120	OTf^-	47.0	2 (470)
				64.9	3 (433)
				75.7	4 (378)
				83.6	5 (334)
				86.0	6 (287)
				87.7	8 (220)
				89.7	24 (75)
7	0.05	120	OTs^-	1.4	2 (14)
				3.4	3 (23)
				4.1	4 (20)
				4.6	5 (18)
				6.9	6 (23)
				7.4	8 (17)

[a] Catalysis conditions: diphenylacetylene (1.75 mmol, 312 mg), 5% NBu_4OTf (0.087 mmol, 34.3 mg) and H_2O (1.92 mmol, 35 µL). [b] (moles of catalyst / moles of alkyne) x 100. [c] Determined by ^1H NMR; average value of three measurements; [d] Time necessary to reach the reported conversion. [e] TOF = ($n_{product}$ / $n_{catalyst}$) / t(h) at the reported conversion. [f] Using D_2O instead of H_2O.

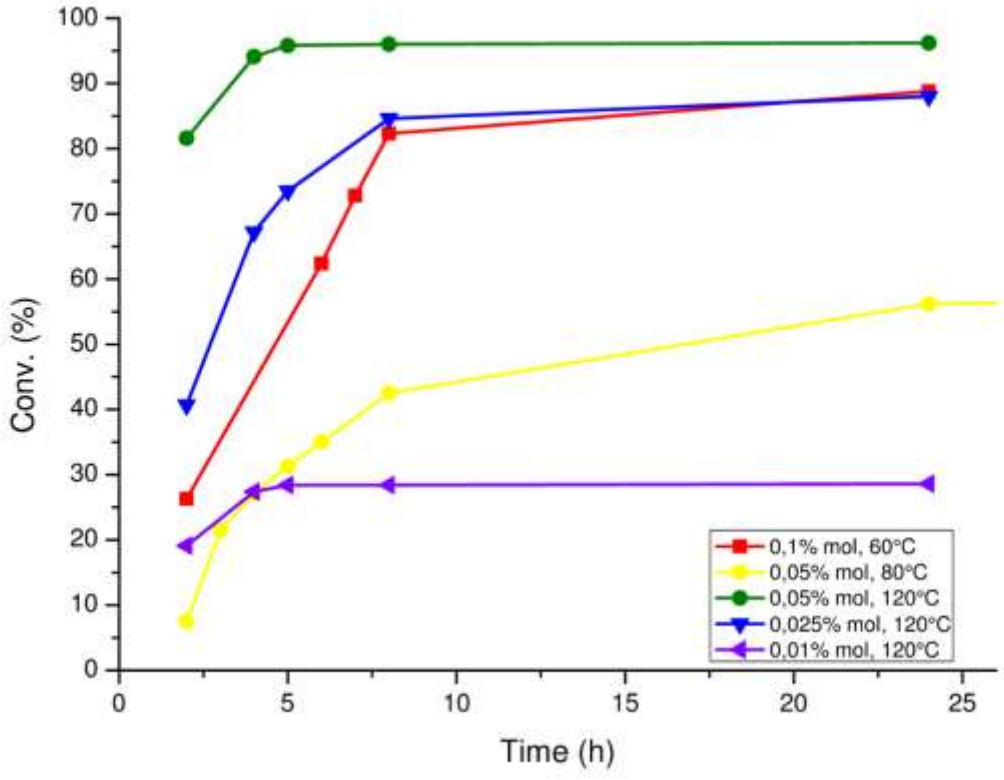

Figure S2: *Hydration of diphenylacetylene at different temperatures and catalyst loadings.*

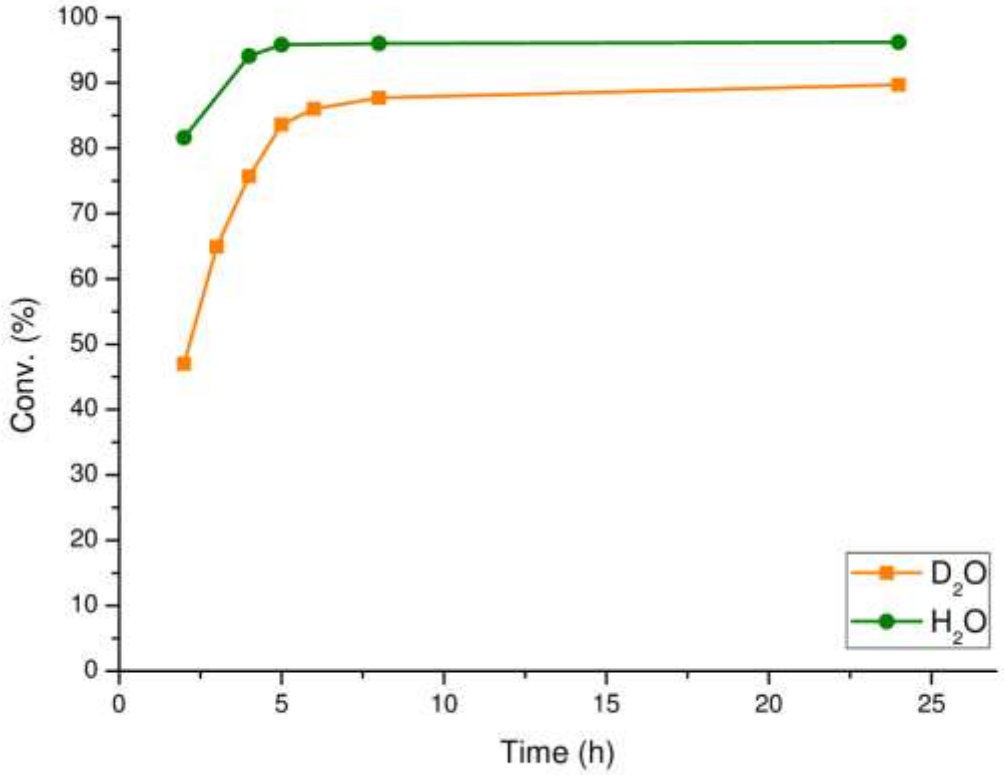

Figure S3: *Hydration of 3-hexyne with H_2O and D_2O at 120°C using a 0.05 mol% catalyst loading. (**Table S6**)*

In order to better understand which catalytic species are present at the end of the hydration of 3-hexyne, we recorded the ^{31}P-NMR spectra for PPh_3-Au-OTs and JPhos-Au-OTs after 20 hours from the beginning of the catalysis. The reaction mixture where put in a NMR tube containing a capillary filled with D_2O. In **Table S7** chemical shift of the main gold species that can be present are reported.[145,146]

Table S7: NMR chemical shift for ^{31}P

Ligand	Free	Oxide	Au-Cl	Au-OTf	Au-OTs	Au-η^2-hexyne	$[AuP_2]^+$
PPh_3	-5.4	31.6	33.8	29.4	27.9	37	45
JPhos	18.9	-	60.5	57.4	56.8	64.6	-

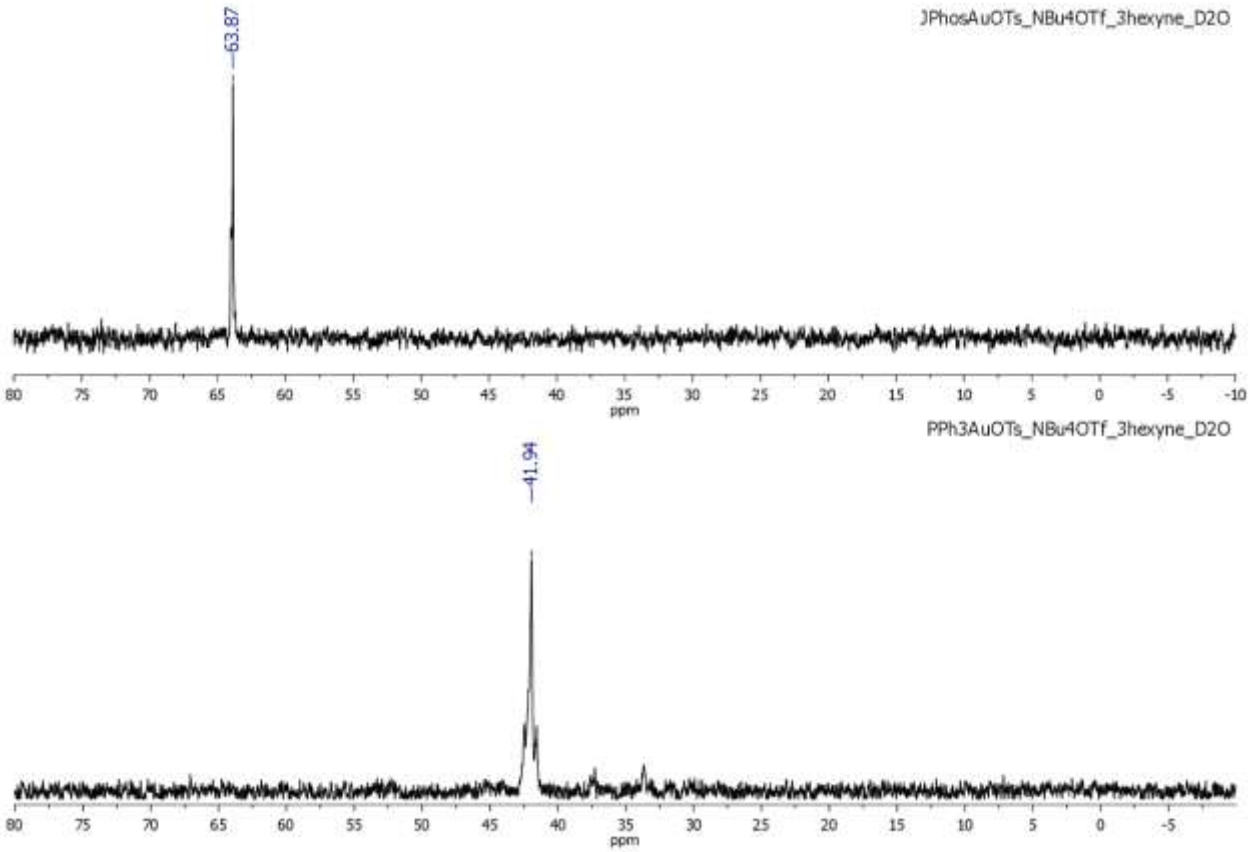

Figure S4: *^{31}P NMR spectra of PPh_3-Au-OTs (down) and JPhos-Au-OTs (up) in hydration of 3-hexyne.*

4.3.3. Hydration and alkoxylation of alkynes chapter 2.3

Methoxylation of 3-hexyne (Table 10, page 46).

NHC^{iPr}-Au-OTf (1.62 mg, 0.0022 mmol), anhydrous methanol (89 µL, 2.2 mmol), 3-hexyne (125 µL, 1.1 mmol) and 200 µL of the solvent were added into a 2 mL glass screw-top vial. Using DES as solvent: cholinetriflate\dimethylurea (0.47\0.95 mmol, 120\84 mg) or citric acid\dimethylurea (0.64\0.96 mmol, 122.6\84.3 mg). The vial was placed in a bath oil at 30°C with magnetic stirring. The reactions were checked by NMR: 10 µL of the reaction mixture was added to a 500 mL of non-anhydrous $CDCl_3$. The progress of the reaction was monitored integrating the signal of 3-hexanone formed by hydrolysis of the product 3,3-dimethoxyhexane (due to adventitious water present in $CDCl_3$) and 3-hexyne.

Hydration of diphenylacetylene (Table S8).

NHC^{iPr}-Au-OTf (from 0.000025 to 0.0025 mmol), diphenylaceteylene (89 mg, 0.5 mmol), water (9.9 µL, 0.55 mmol) and 240.1 µL of γ-valerolactone were added into a 2 mL glass screw-top vial,. The vial was placed in a bath oil at 120-80-50 °C with magnetic stirring. The reactions were checked by NMR: 10 µL of the reactions mixture was added to a 500 mL of non-anhydrous $CDCl_3$. The progress of the reaction was monitored integrating the signal of 1,2-diphenylethanone and diphenylaceteylene.

Hydration of 3-hexyne (Table S9).

NHC^{iPr}-Au-OTf (1.29 mg, 0.00175 mmol), 3-hexyne (199 µL, 1.75 mmol), water (34.65 µL, 1.925 mmol) and 200 µL of γ-valerolactone were added into a 2 mL glass screw-top vial. The vial was placed in a bath oil at 30 °C with magnetic stirring. The reactions were checked by NMR: 10 µL of the reactions mixture was added to a 500 mL of non-anhydrous $CDCl_3$. The progress of the reaction was monitored integrating the signal of 3-hexanone and 3-hexyne.

Hydration of phenylacetylene (Table S9).

NHC^{iPr}-Au-OTf (from 0.0005 to 0.0025 mmol), phenylaceteylene (55 µL, 0.5 mmol), water (9.9 µL, 0.55 mmol) and 185.1 µL of γ-valerolactone were added into a 2 mL glass screw-top vial. The vial was placed in a bath oil at 120, 80 or 50 °C with magnetic stirring. The reactions were checked by NMR.

Hydration of 3-phenyl-1-propyne (Table S9).

NHC^{iPr}-Au-OTf (0.73 mg, 0.001 mmol), 3-phenyl-1-propyne (124 µL, 1 mmol), water (19.8 µL, 1.1 mmol) and 106.2 µL of γ-valerolactone were added into a 2 mL glass screw-top vial. The vial was placed in a bath oil at 120 °C with magnetic stirring. The reactions were checked by NMR.

Hydration of 1-phenyl-1-propyne (Table S9).

NHC^{iPr}-Au-OTf (0.73 mg, 0.001 mmol), 1-phenyl-1-propyne (125 µL, 1 mmol), water (19.8 µL, 1.1 mmol) and 105.2 µL of γ-valerolactone were added into a 2 mL glass screw-top vial. The vial was placed in a bath oil at 120 °C with magnetic stirring. The reactions were checked by NMR.

Table S8: *NHC^{iPr}-Au-OTf catalyzed hydration of diphenylacetylene in γ-valerolactone.*[a]

entry	Loading (mol%)[b]	Temp (°C)	Conv.[c] (%)	Time[d] (h)	TOF[e] (h^{-1})
1	0.1	120	76	1	760
			95	2	475
			97	3	323
			99	3.5	283
2	0.05	120	14.8	2	148
			15	6	50
			18.2	24	15
			21.9	30	15
3	0.02	120	0	2	0
			0	9	0
			0	30	0
			0	72	0
4	0.25	80	30.1	1	120
			63.5	3	85
			82.8	5.5	60
			85.8	7	49
			88.4	24	15
5	0.5	50	26.8	1	54
			40.5	2	41
			77.8	5	31
			85.9	6	25
			90.3	9	20
6	0.25	50	10.5	1	42
			22.5	2	45
			48.3	5	39
			59.9	7	34
			70.2	9	31
			89.4	24	15
7[f]	0.25	50	65	9	28
8[g]	0.25	50	1.4	1	5.6
			2.2	4	2.2
			8.0	9	3.5
			33.6	24	5.6

[a] Catalysis conditions: diphenylacetylene (0.5 mmol, 89 mg), water (0.55 mmol, 9.9 μL) and γ-valerolactone (240 μL).[b] (mol of catalyst / mol of alkyne) x 100. [c] Determined by ^{1}H NMR; average value of three measurements. [d] Time necessary to reach the reported conversion. [e] TOF = (mol product / mol catalyst)/t(h) at the reported conversion. [f] ethyl lactate instead of GVL. [g] propylene carbonate instead of GVL.

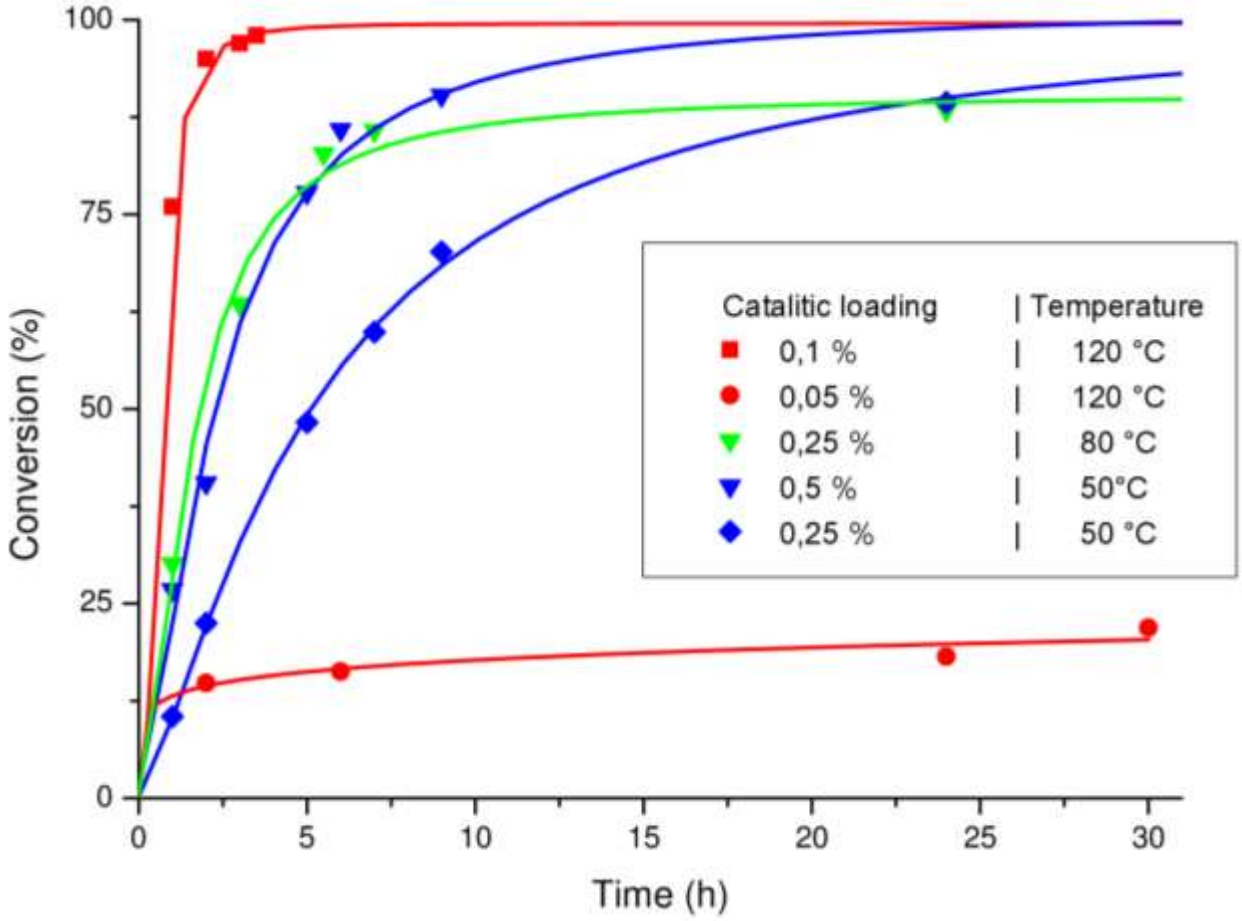

Figure S5: *NHC^{iPr}-Au-OTf catalyzed hydration of diphenylacetylene in γ-valerolactone (**Table S8**)*

Table S9: *Hydration of alkynes in γ-valerolactone.*[a]

Entry	Substrate	Temp (°C)	Loading (mol %)[b]	Conv (%)[c]	Time (h)[d]	TOF[e] (h^{-1})	I.R. ($\%_a$:$\%_b$)[f]
1	3-phen-1-propyne	120	0.1	96	0.5	1920	-
				>99	1	990	-
2	1-phenyl-1-propyne	120	0.1	50	0.5	1000	96:4
				55	1	550	84:16
				57	1.5	380	83:17
				64[a]	2.5	256	84:17
3	3-hexyne	30	0.1	24	2	120	-
				84	5	168	-
				92	8	115	-
4	Phenylacetylene	120	0.1	90.1	0.5	1802	-
				94.9	1	949	-
				99.5	1.5	663	-
5	"	120	0.05	46.5	16	58	-
				65.9	42	31	-
				79.3	89	18	-
6	"	120	0.01	0	89	0	-
7	"	120	0.005	0	89	0	-
8	"	80	0.2	80.8	1	404	-
				97.5	2	244	-
				98.9	5	99	-
				99.3	7	71	-
9	"	80	0.1	10.8	1	108	-
				17.1	2	86	-
				26.3	5	53	-
				23.8	7	34	-
10	"	80	0.1	6.1	1	61	-
				10.2	3	34	-
				10.9	5.5	20	-
				13.9	7	20	-
				16.6	24	7	-
11	"	50	0.5	45.4	1	91	-
				92.7	2	93	-
				99.9	5	40	-
12	"	50	0.25	13.8	1	55	-
				25.7	2	51	-
				60.7	5	49	-
				69.5	7	40	-
				86.6	9	38	-

[a] Catalysis conditions: see above. [b] (mol of catalyst / mol of alkyne) x 100. [c] Determined by ^{1}H NMR; average value of three measurements. [d] Time necessary to reach the reported conversion. [e] TOF = (mol product / mol catalyst)/t(h) at the reported conversion. [f]Isomeric ratio

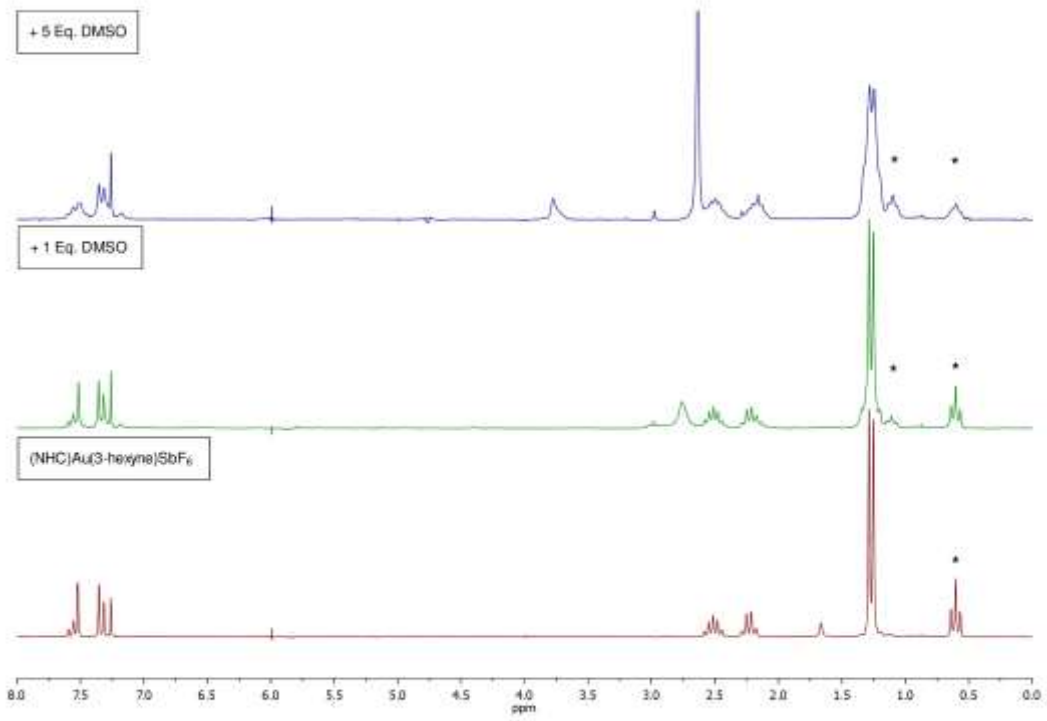

Figure S6: *^{1}H NMR spectra of NHC^{iPr}-Au-(3-hexyne)SbF_6 ($CDCl_3$) in presence of different equivalents of DMSO. (* denotes signal CH_3 of 3-hexyne)*

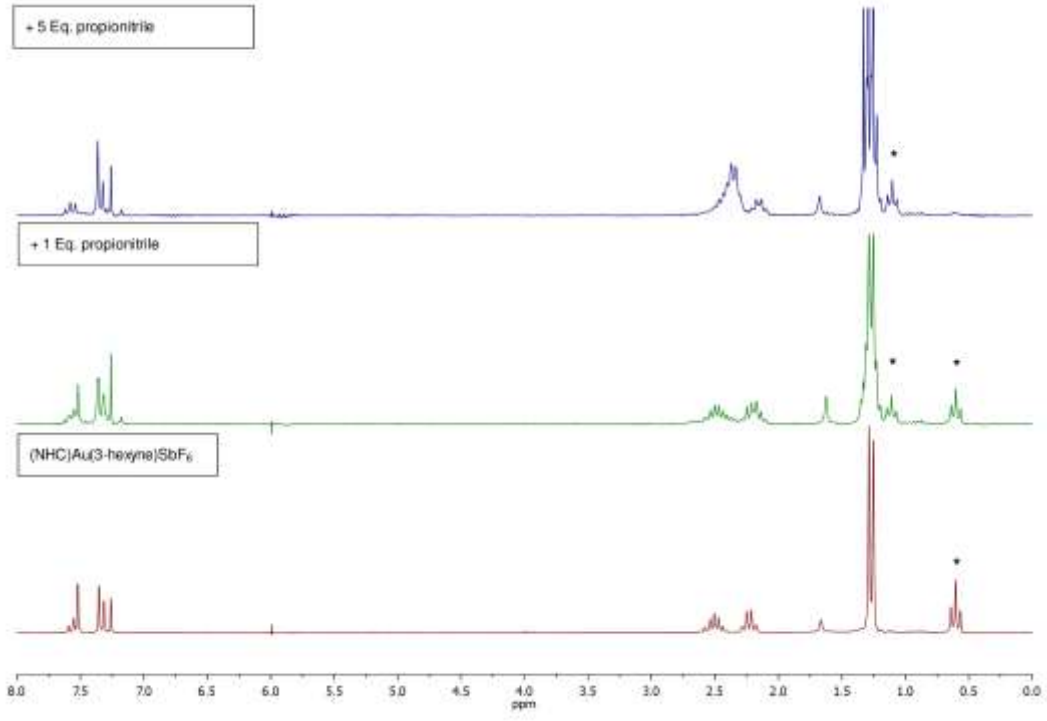

Figure S7: *^{1}H NMR spectra of NHC^{iPr}-Au-(3-hexyne)SbF_6 ($CDCl_3$) in presence of different equivalents of propionitrile. (* denotes signal CH_3 of 3-hexyne)*

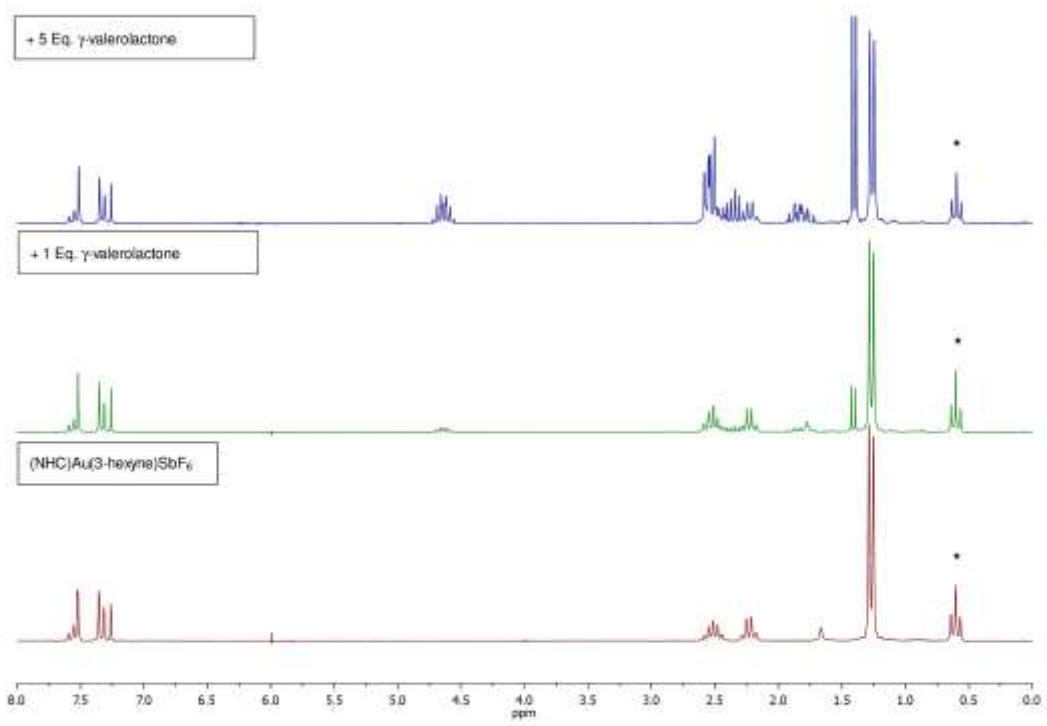

Figure S8: *^{1}H NMR spectra of NHC^{iPr}-Au-(3-hexyne)SbF_6 ($CDCl_3$) in presence of different equivalents of γ-valerolactone. (* denotes signal CH_3 of 3-hexyne)*

4.4. Computational

Complex [NHC'-Au-OTf] (NHC' = 1,3-dimethylimidazol-2-ylidene ; OTf^- = trifluoromethanesulfonate or triflate anion) was chosen as a model for the catalytically active species. For the calculation, water and 2-butyne were selected as nucleophile and substrate respectively. A complete computational study was performed with ADF2014.05 [147] program to identify the structures of the intermediates and transition states of the catalytic process for the carbene-gold(I) catalyzed addition of water or methanol to alkyne reaction, in other cases with a molecule of γ-valerolactone (GVL), nitromethane (NM) or chloroform (TCMA). For geometry optimizations, calculations were carried out at the DFT level of theory using the GGA functional BP86. [148] All atoms were described with a Slater-type TZ2P triple-ς quality basis set, using the frozen core approximation (1s for C, N, O, and F; 2p for S and 4d for Au). Frequency calculations at the same BP86 level of theory have been also performed to identify all stationary points as minima (zero imaginary frequencies) or transition states (one imaginary frequency). Relativistic effects were treated with the scalar zero-order regular approximation, ZORA model. [149] Solvation effects have been taken into account by the Conductor like Screening Model COSMO[150] using nitromethane as solvent. Final energies have been computed with ORCA package[151] by single point double-hybrid B2PLYP functional[152] calculations on the optimized BP86 gas phase structures with a Def2-TZVP basis set for all atoms and ECP for gold to account for relativistic effects. This combined BP86 geometry optimization and B2PLYP energy calculation approach has been shown to give an high accuracy to describe gold species along reaction paths in benchmark studies.[153] Unless otherwise specified, the B2PLYP functional is used for energy calculations. Due to the fact that the investigated reaction involves four to five molecules ($[NHC\text{-}Au]^+$, 2-butyne, water/methanol, the counterion OTf^- and one molecule of solvent when taken into account), the reference energy has been set to the most stable adduct involving the four molecules for activation barriers evaluation, in order to minimize entropy problems. Indeed, as reported in the Supporting Information of previous communications of Zuccaccia et al.,[37] where the energy profile for a similar reaction involving four molecules, ($[NHC\text{-}Au]^+$, 2-butyne, methanol and the anion X^-), was calculated, the entropic contribution was found to be small. For this reason, computational mechanistic analysis is presented in enthalpy energies in this work. All calculations were performed for the closed shell singlet state.

Pre-equilibrium step: $X^- = OTs^-, OTf^-$

In **Figure S9** are shown the optimized geometries of the water gold co-ordinated (denoted as ICH_2OX) and anion co-ordinated (denoted as ICX) adducts involved in the pre-equilibrium step for $X^- = OTf^-$ and OTs^-. In the presence of nucleophile and anion, calculations show that gold-water bond adducts ICH_2OX are more stable than gold-anion bond adducts ICX for both counterions (1.4 kcal/mol for OTf^-, and 0.9 kcal/mol for OTs^-). Since previous calculations on methoxylation[36,69] pointed out that the pre-equilibrium step is driven by the *net* balance between the anion co-ordinating and proton acceptor abilities which in turn depends on the *presence of the nucleophile (methanol)*, these findings suggest that the pre-equilibrium in the presence of water for OTs^- is mostly driven by its stronger proton acceptor ability rather than by its stronger co-ordinating power with respect to OTf^-. Notable, for OTf^- both water and anion substitution by the substrate is an exothermic process (-4.2 kcal/mol water/substrate substitution and -5.6 kcal/mol OTf^-/substrate substitution, respectively), whereas for OTs^- both water and anion substitution by substrate is an endothermic process (+1.7 kcal/mol water/substrate substitution, +0.8 kcal/mol OTs^-/substrate substitution, respectively).

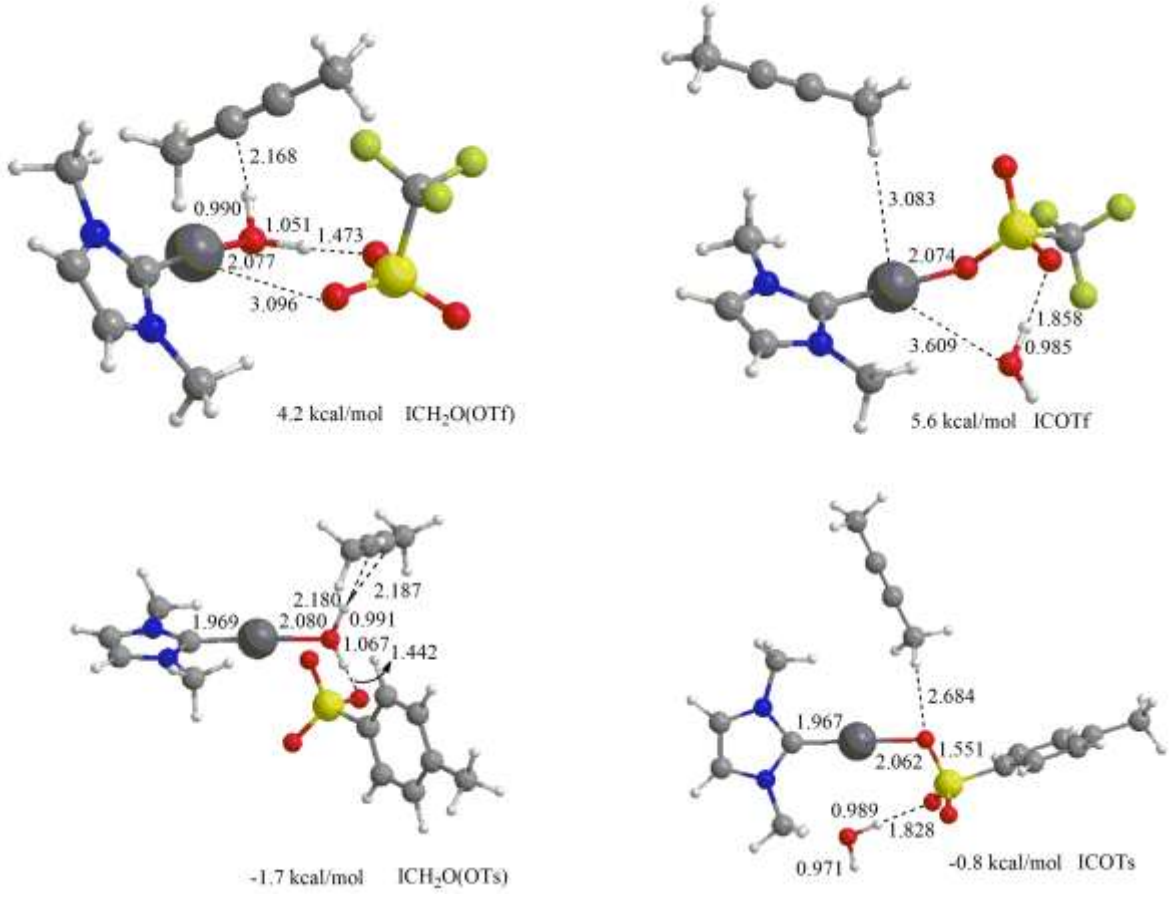

Figure S9: *Optimized geometries of the water co-ordinated $ICH_2O(X)$ (left) and anion co-ordinated ICX (right) species involved in the pre-equilibrium step: top) $X^- = OTf^-$; bottom) OTs^-. Energies with respect to ICsub (for OTf^- top) and OTs^- bottom), respectively, with corresponding ICsub structures shown in Figure 2 in the text and Figure S7 below) in kcal/mol and distances in Å.*

In **Figure S10** the energy profiles for the OTs^- / H_2O substitution in [NHCAu($OTsH_2O$)] complex by 2-butyne are shown. For OTs^-, the initial H_2O co-ordinated species, $ICH_2O(OTs)$, has been calculated to be 0.9 kcal/mol more stable than the initial X co-ordinated species, ICOTs, and it is taken as zero point energy.

The OTs^- substitution in ICOTs is feasible, even if the relatively high activation barrier of 10.5 kcal/mol, with a slightly endothermic process (0.8 kcal/mol). The reverse process would require a lower energy barrier of 9.7 kcal/mol (**Figure S10** bottom).

The activation barrier for the H_2O substitution by the alkyne is significantly higher (14.4 kcal/mol) and the ICsub is less stable than $ICH_2O(OTs)$ by 1.7 kcal/mol, consequently rises the energy barrier for the reverse process to 12.7 kcal/mol (**Figure S10** top).

The unpredicted stability of $ICH_2O(OTs)$ can be attributed to: i) the formation of a relatively strong hydrogen bond between H_2O and OTs^- and ii) to the high proton acceptor ability of OTs^-, reason for the lack of reactivity in the hydration of alkynes (**Figure S9**)

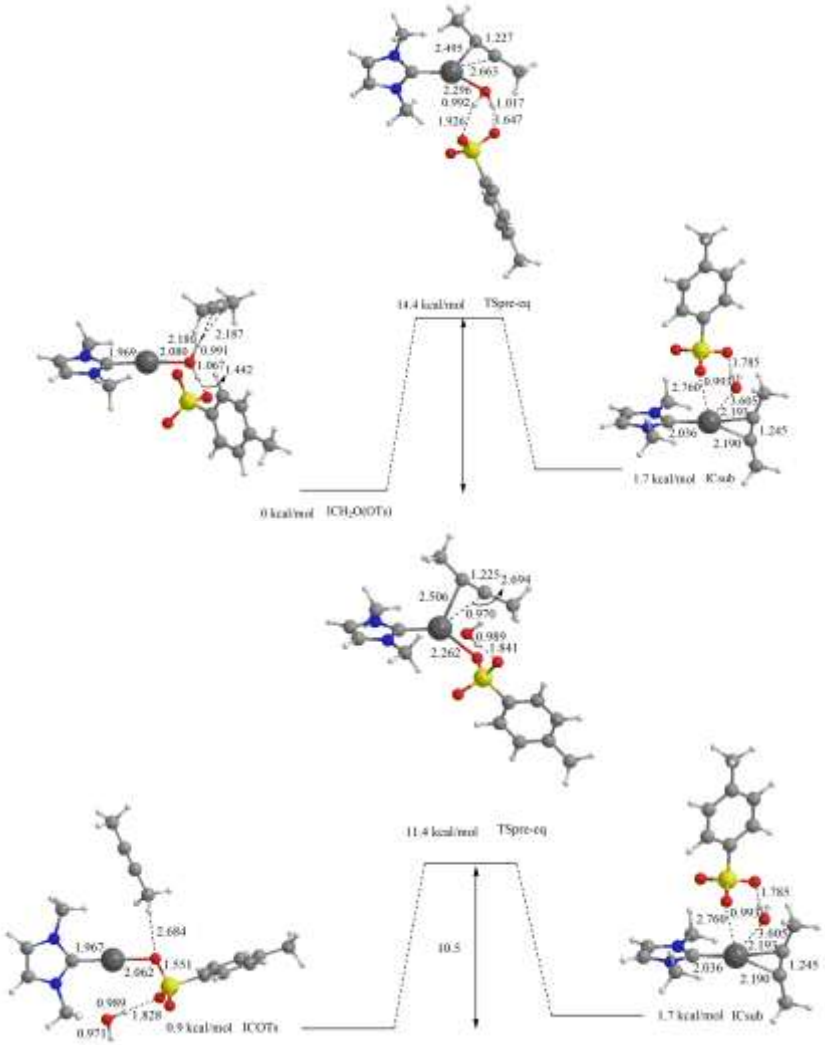

Figure S10: *Energy profiles and corresponding geometries of the species involved in the pre-equilibrium step: X^- = OTs^- ; top) H_2O substitution by substrate; bottom) OTs^- substitution by substrate. Energies with respect to $ICH_2O(OTs)$ in kcal/mol and distances in Å.*

Formation of α-auro ketone as in-cycle or off-cycle intermediate

An alternative path to proton transfer (step II) has been considered, in order to analyze the role of α-auro ketone as in-cycle or off-cycle intermediate.

After the formation of HOTf subsequently to the nucleophilic attack step, intermediate I could give rise to α-auro ketone instead of enol complex II. In these calculations HOTf wasn't take into account and a full geometry optimization of intermediate I has been performed (see **Figure 15**). Conformation denoted I' in **Figure S11** has been revealed to be more stable than I by 3.5 kcal/mol (two different conformations in the OH orientation, towards gold in I' and in an outside position in I). In **Figure S11** the energy profile for the hydrogen transfer from OH to Cα bonded to gold in intermediate I' is shown. A very high energy barrier of 45.9 kcal/mol has been found. Interestingly, the transition state TS α-auro ketone structure shown a gold-mediated hydrogen migration. The high activation barrier do not include any role of α-auro ketone intermediate as in-cycle or off-cycle.

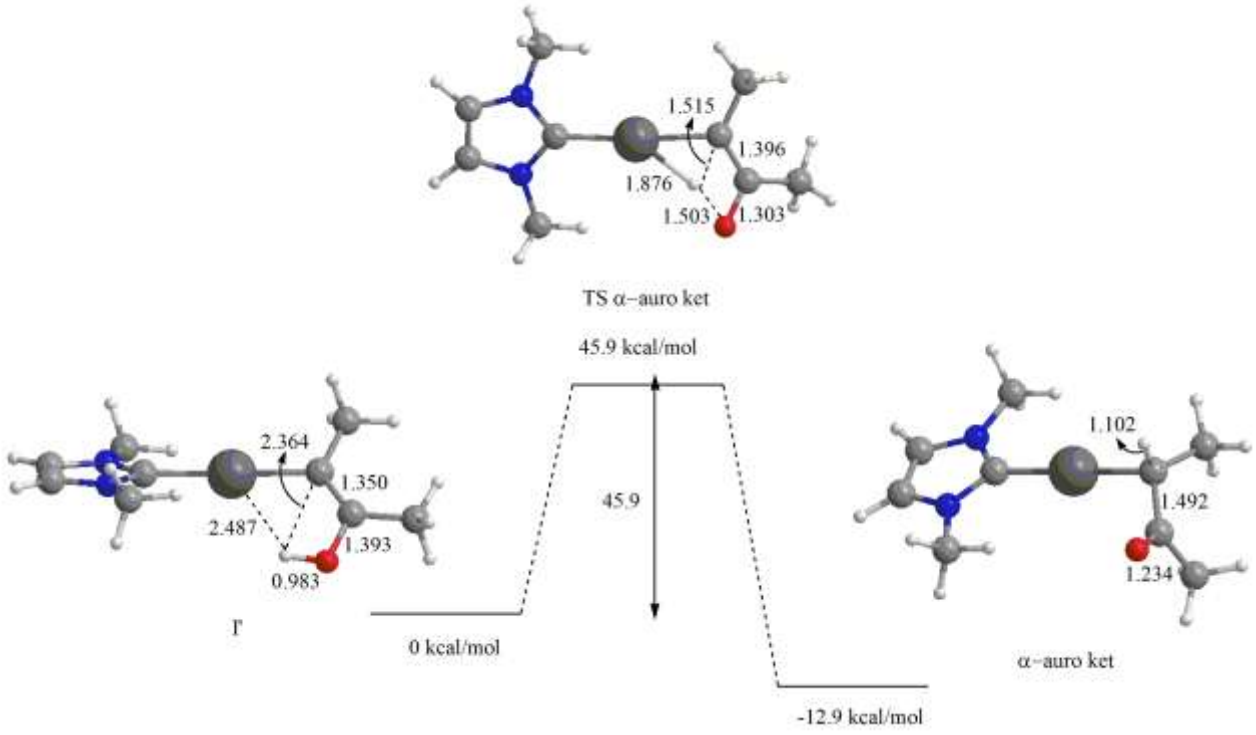

Figure S11: *Energy profile and corresponding geometries of the species involved in the OH hydrogen transfer to Cα bonded to gold in intermediate I'. Energies (with respect to I' taken as zero point energy) in kcal/mol and distances in Å.*

Solvent (GVL, NM)-assisted nucleophilic attack step for the addition of methanol to 2-butyne

The reactant complex RC_X(Y) (where the anion (RC_OTf(GVL)) or the γ-valerolactone solvent (RC_GVL(OTf)), acts as a hydrogen-bond acceptor increasing the nucleophilicity of the attacking methanol) are the starting complex for the calculations (**Figure S12** and **Figure S13**).

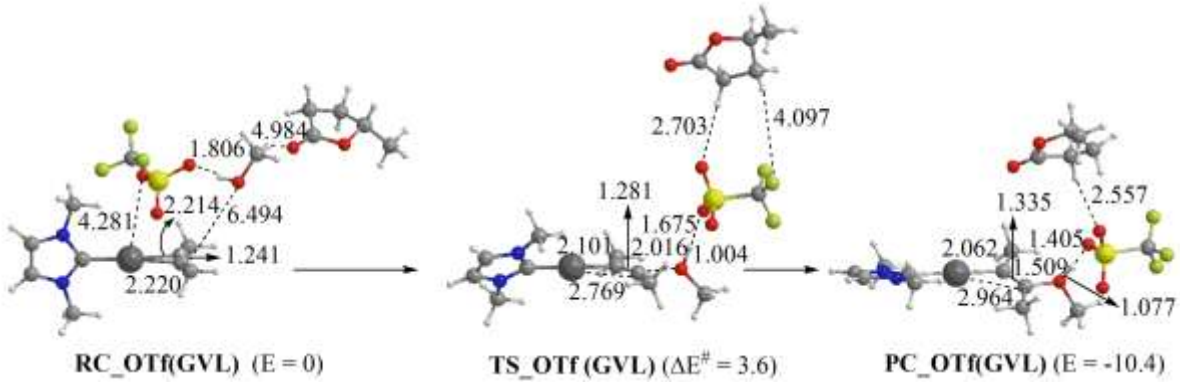

Figure S12: *Reactant complex RC_OTf(GVL), transition state TS_OTf(GVL) and product complex PC_OTf(GVL) in the methanol nucleophilic attack for the addition of methanol to 2-butyne reaction assisted by OTf⁻ anion. Energies values (kcal/mol) refer to RC_OTf(GVL) taken as zero. Bond lengths are in angstrom.*

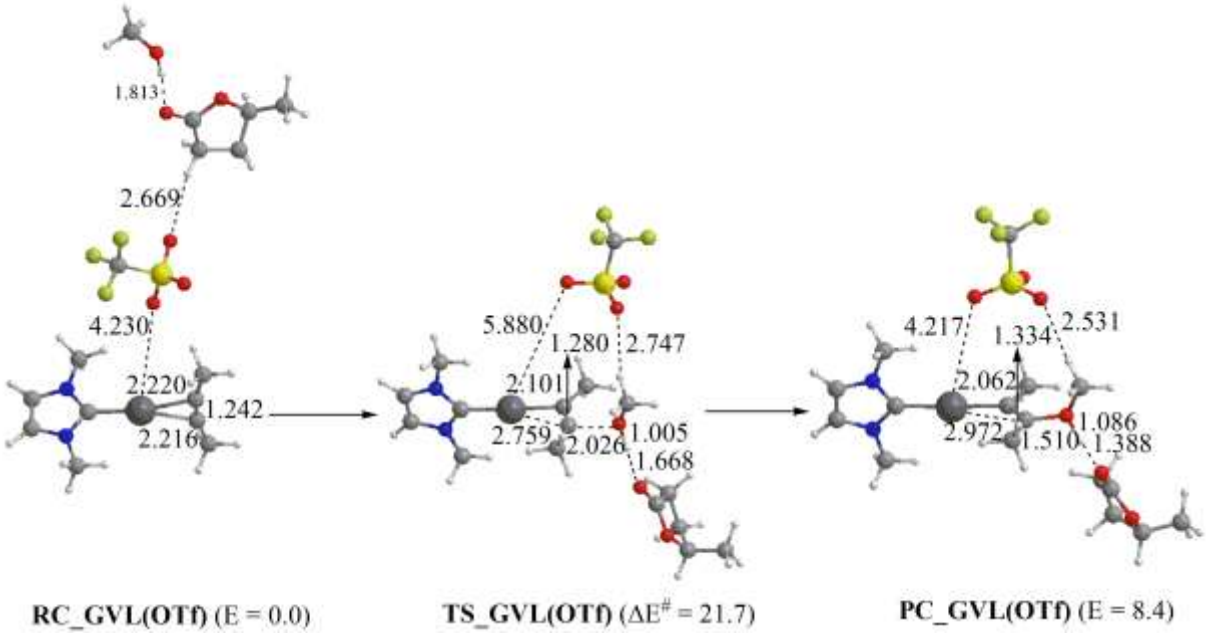

Figure S13: *Reactant complex RC_GVL(OTf), transition state TS_GVL(OTf) and product complex PC_GVL(OTf) in the methanol nucleophilic attack for the addition of methanol to 2-butyne reaction assisted by solvent GVL molecule. Energies values (kcal/mol) refer to RC_GVL(OTf) taken as zero. Bond lengths are in angstrom.*

Note that for the methanol attack to the butyne co-ordinated species, [NHC'-Au-(2-butyne)]$^+$, any interaction between the anion and the solvent molecule is switched off both in RC_OTf(GVL) and RC_GVL(OTf). Interestingly, in the structure of the transition state TS_OTf(GVL) an anion-solvent interaction arises which moves the anion towards an outer position at the substrate side. On the contrary, the classic template structure of RC_X(Y) with the anion between Au and methanol, weakly interacting with Au, is maintained in TS_GVL(OTf). An activation barrier of 3.6 kcal/mol was found for the transition state structure anion-mediated and an activation barrier of 21.7 kcal/mol was calculated for the solvent-mediated nucleophilic attack to the substrate. The transition state TS_X(Y) evolves with the formation of the product complex of this step PC_X(Y), which is more stable than RC_X(Y) by 10.4 for the anion-assisted (PC_OTf(GVL)) and less stable than RC_X(Y) by 8.4 kcal/mol for the solvent-assisted (PC_GVL(OTf)) process. This result suggests that the nucleophile is more activated by the anion than the solvent molecule thus excluding the hypothesis that the better performance of the catalyst in GVL could be ascribed to GVL replacing the counterion in the activation of methanol. Starting from RC_GVL(OTf) was calculated the TS_GVL(OTf)' intermediate in order to verify if the solvent-anion interaction enhance the efficiency of the solvent in the nucleophile activation (**Figure S14**).

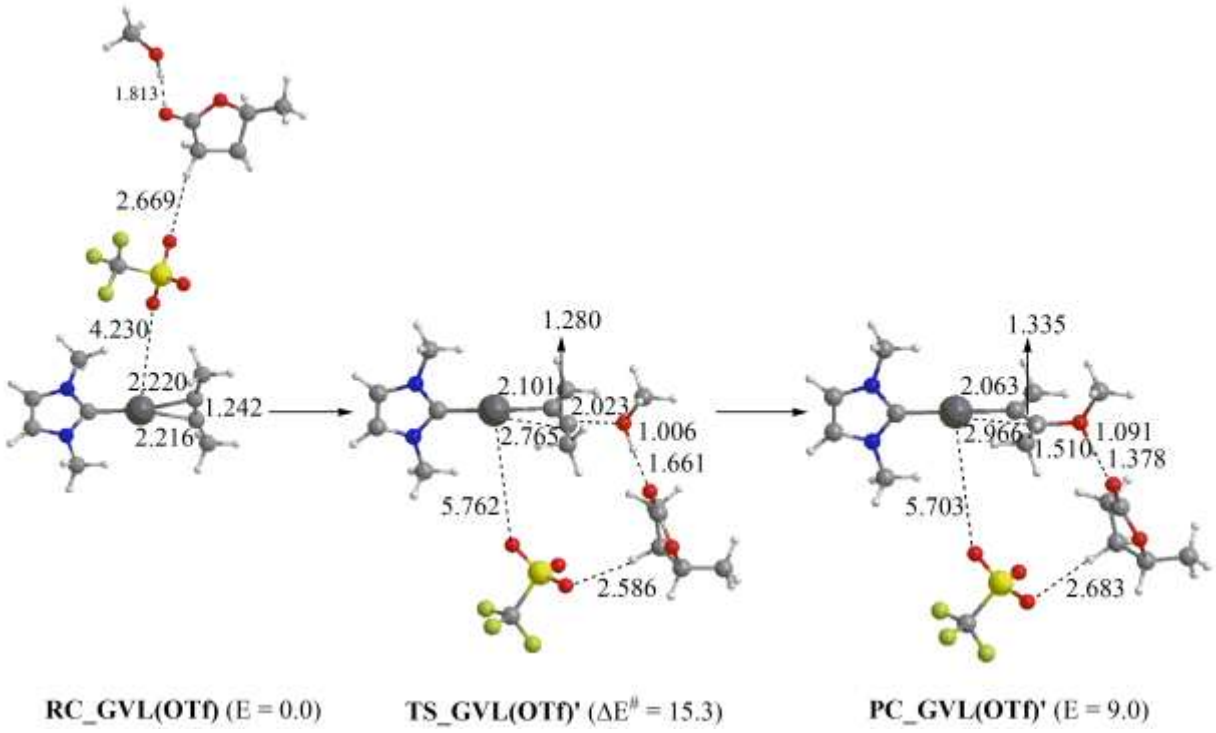

Figure S14: *Reactant complex RC_GVL(OTf), transition state TS_GVL(OTf)' and product complex PC_GVL(OTf)' in the methanol nucleophilic attack for the addition of methanol to 2-butyne reaction assisted by a solvent GVL molecule interacting with OTf$^-$ anion. Energies values (kcal/mol) refer to RC_GVL(OTf) taken as zero. Bond lengths are in angstrom.*

The activation energy barrier is lower with respect to that calculated with TS_GVL(OTf) (15.3 vs. 21.7 kcal/mol, respectively) but it is still higher than that calculated with TS_OTf(GVL) (3.6 kcal/mol), the result confirms that the OTf^- anion is necessary in the nucleophilic activation of methanol using γ-valerolactone as solvent.

Corresponding calculations have been performed by replacing with nitromethane the γ-valerolactone molecule. Similar results are obtained which show that OTf^- rather than the solvent is involved in the nucleophilic activation of methanol in nitromethane as well. The activation barrier amounts to 33.9 kcal/mol for the solvent-mediated (**Figure S16**) and to 6.4 kcal/mol for the anion-mediated (**Figure S15**) nucleophilic attack to the substrate. Similarly, the interaction solvent-anion enhances the efficiency of the solvent in the nucleophile activation (the calculated activation energy barrier is 18.8 kcal/mol, **Figure S17**). Note that the activation energy barrier for the anion-assisted nucleophilic attack is larger in nitromethane (6.4 kcal/mol) than in γ-valerolactone (3.6 kcal/mol), in line with experiment.

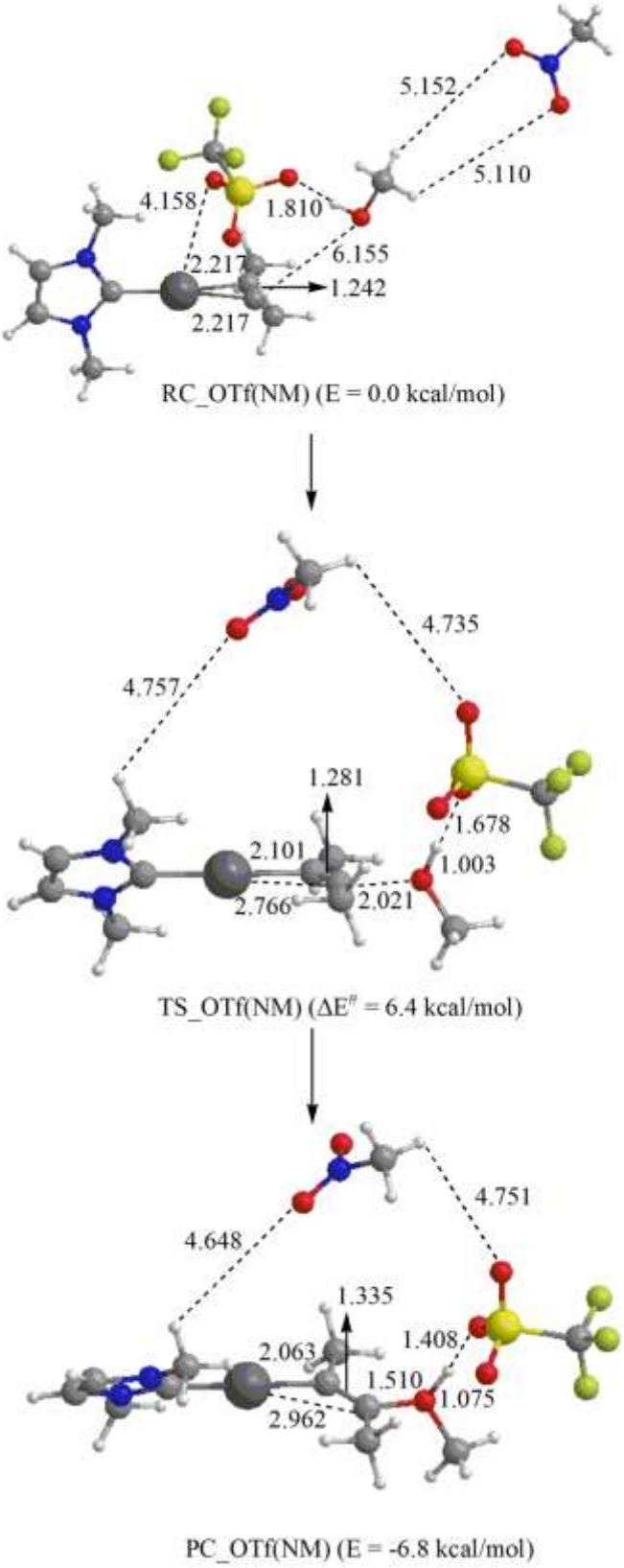

Figure S15: *Reactant complex RC_OTf(NM), transition state TS_OTf(NM) and product complex PC_OTf(NM) in the methanol nucleophilic attack (RDS) for the addition of methanol to 2-butyne reaction assisted by OTf⁻ anion. Energies values (kcal/mol) refer to RC_OTf(NM) taken as zero. Bond lengths are in angstrom.*

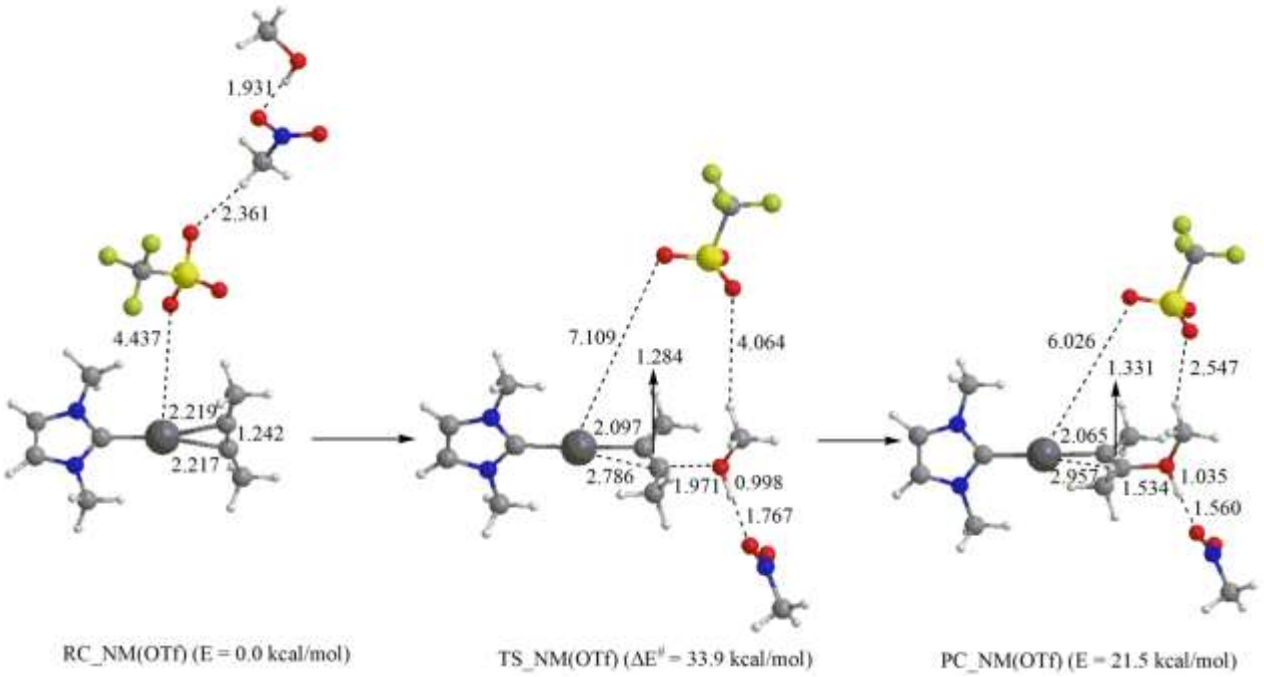

Figure S16: *Reactant complex RC_NM(OTf), transition state TS_NM(OTf) and product complex PC_NM(OTf) in the methanol nucleophilic attack (RDS) for the addition of methanol to 2-butyne reaction assisted by a solvent NM molecule. Energies values (kcal/mol) refer to RC_NM(OTf) taken as zero. Bond lengths are in angstrom.*

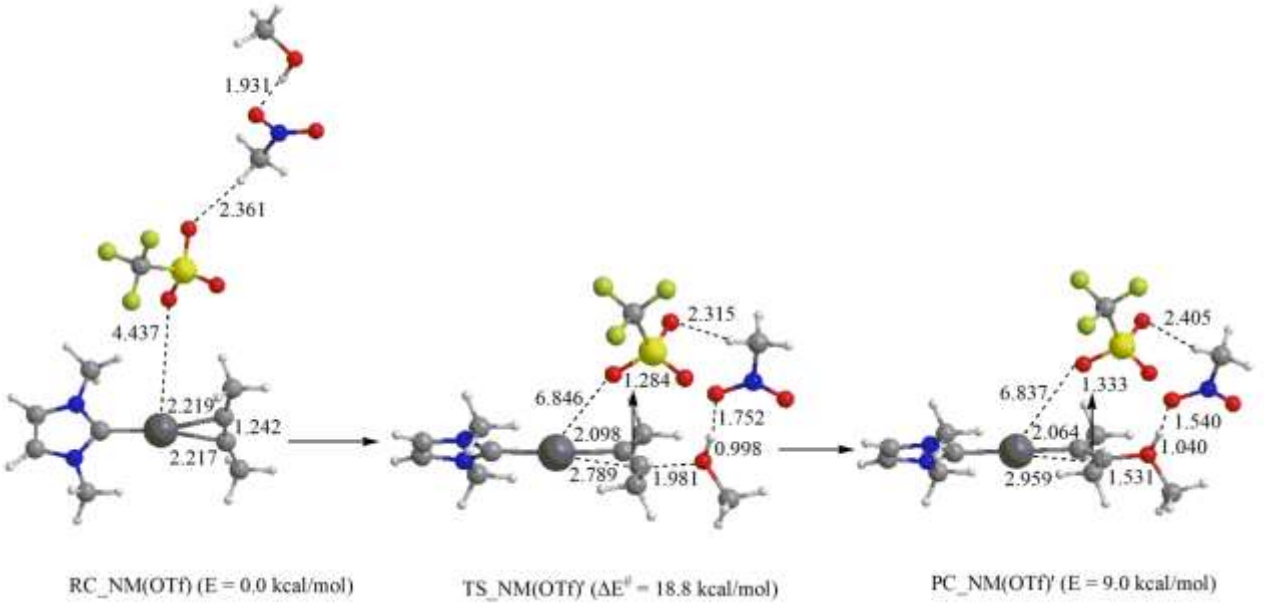

Figure S17: *Reactant complex RC_NM(OTf), transition state TS_NM(OTf)' and product complex PC_NM(OTf)' in the methanol nucleophilic attack (RDS) for the addition of methanol to 2-butyne reaction assisted by a solvent NM molecule interacting with OTf^- anion. Energies values (kcal/mol) refer to RC_NM(OTf) taken as zero. Bond lengths are in angstrom.*

Solvent-anion interaction in the nucleophilic attack step for the addition of methanol to 2-butyne: ion pairs

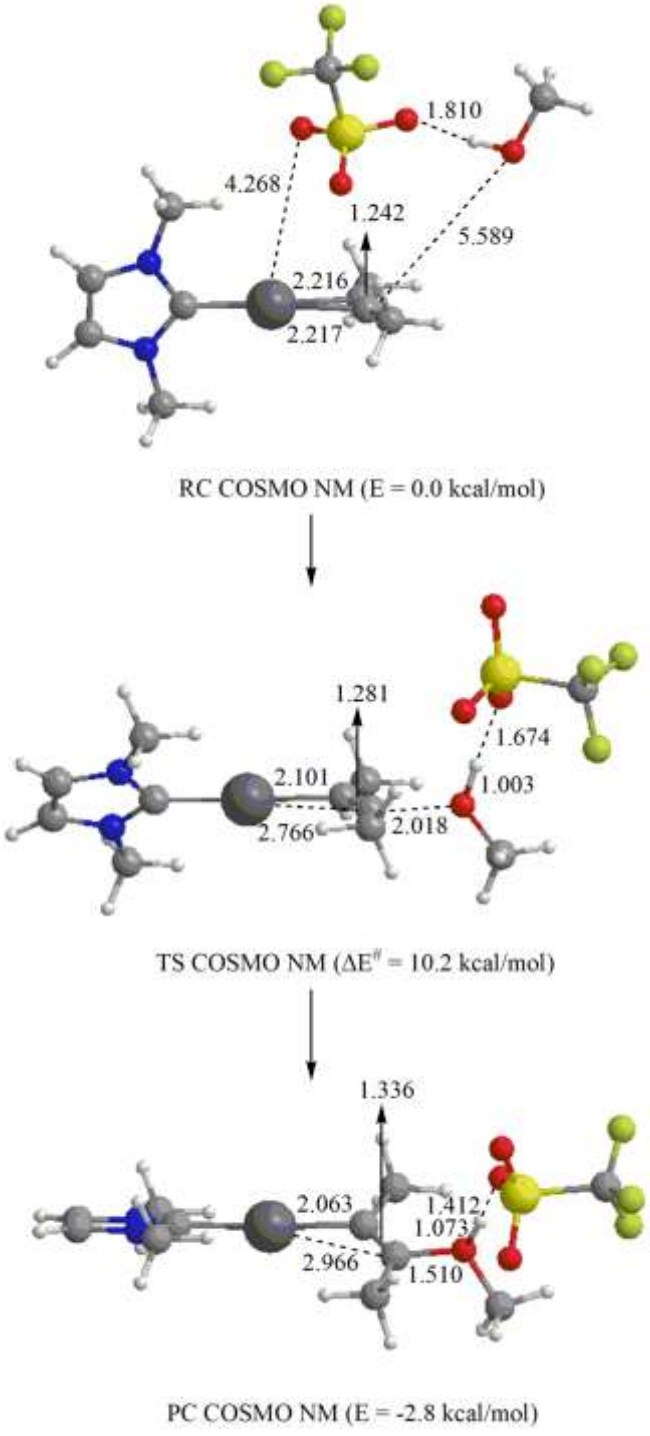

Figure S18: Reactant complex RC COSMO NM, transition state TS COSMO NM and product complex PC COSMO NM in the methanol nucleophilic attack (RDS) for the addition of methanol to 2-butyne reaction assisted by OTf^- anion including only implicit COSMO solvent NM. Energies values (kcal/mol) refer to RC COSMO NM taken as zero. Bond lengths are in angstrom.

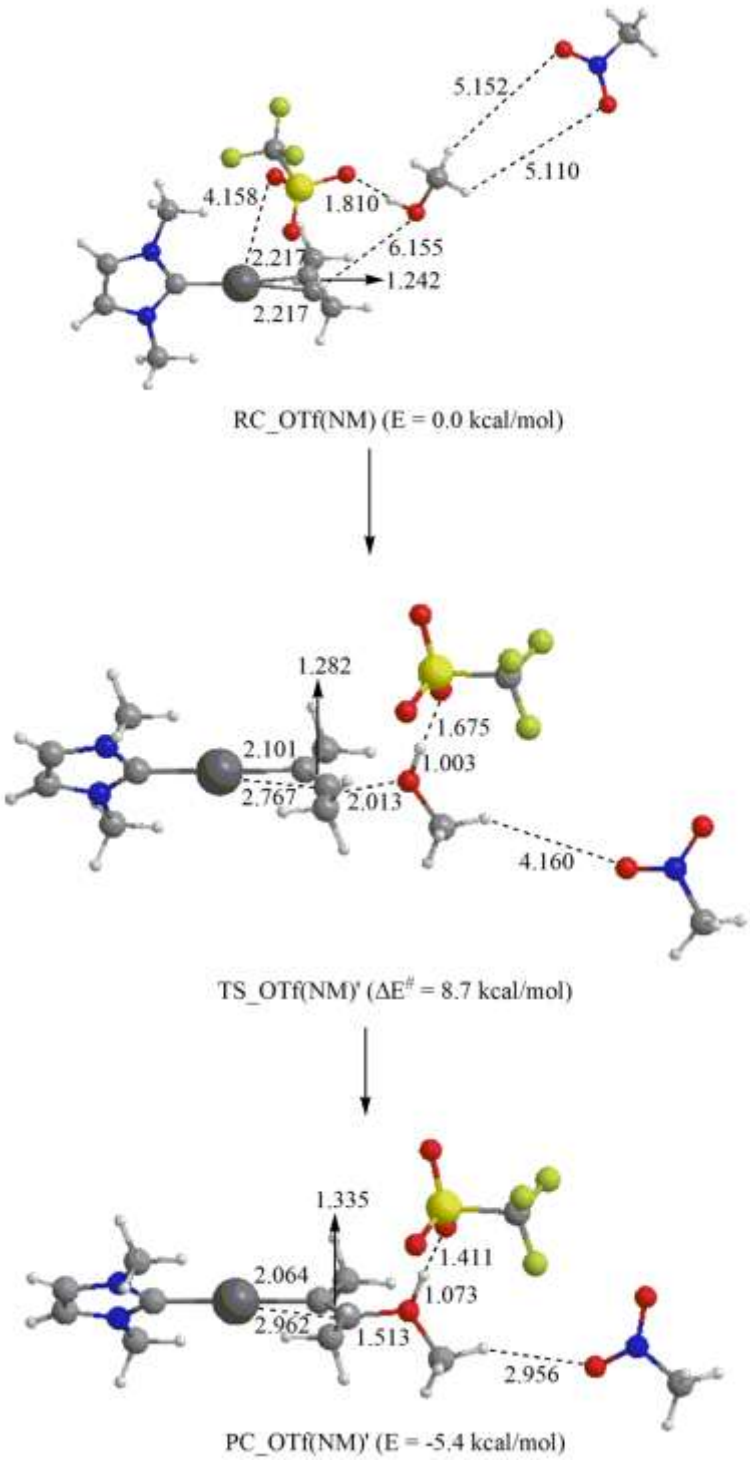

Figure S19: *Reactant complex RC_OTf(NM), transition state TS_OTf(NM)' and product complex PC_OTf(NM)' in the methanol nucleophilic attack (RDS) for the addition of methanol to 2-butyne reaction assisted by OTf^- anion in the presence of an explicit NM solvent molecule interacting with methanol. Energies values (kcal/mol) refer to RC_OTf(NM) taken as zero. Bond lengths are in angstrom.*

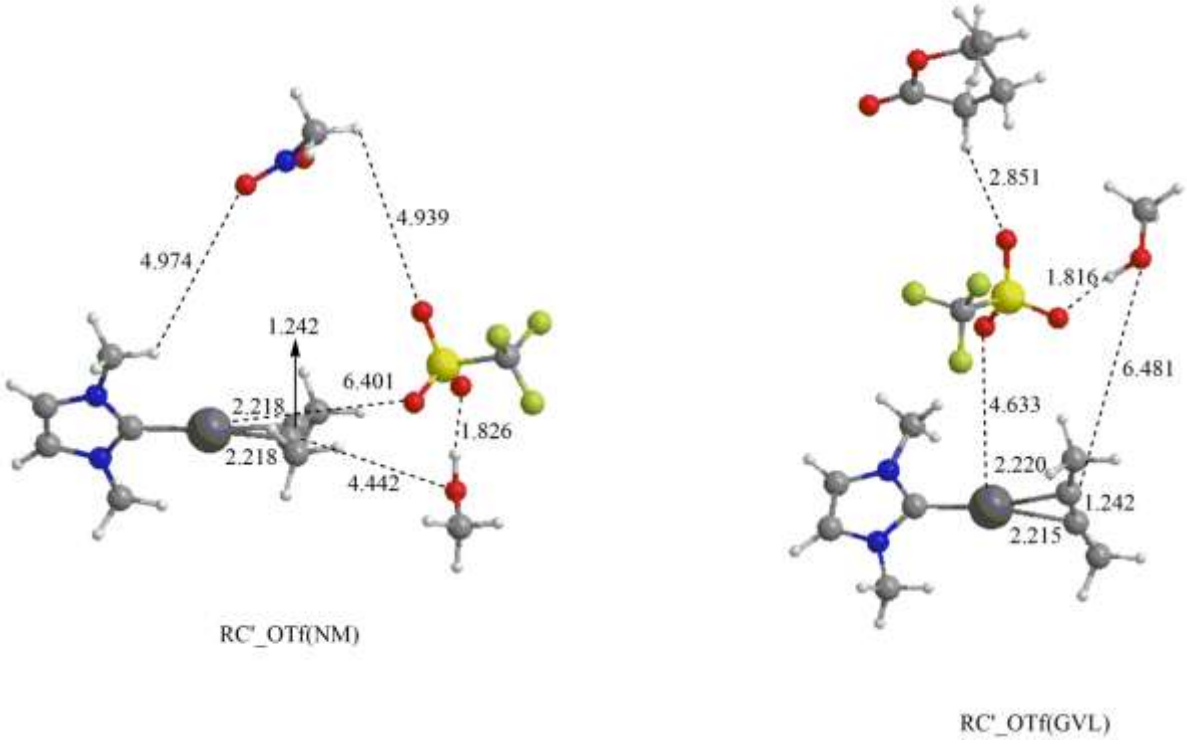

Figure S20: *Reactant complexes RC'_OTf(NM) and RC'_OTf(GVL) optimized geometrical structures. Bond lengths are in angstrom.*

Solvent-nucleophile interaction in the nucleophilic attack step for the addition of methanol to 2-butyne: free ions

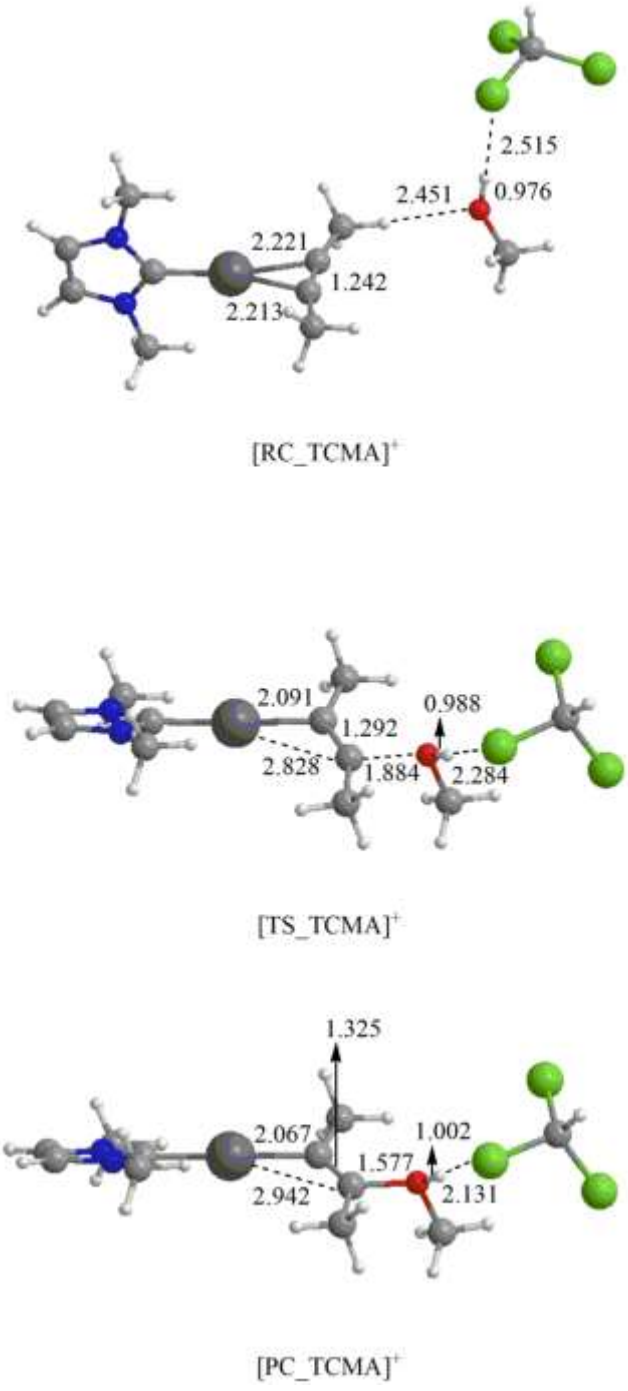

Figure S21: *Reactant complex [RC_TCMA]⁺, transition state [TS_TCMA]+ and product complex [PC_TCMA]+ in the methanol nucleophilic attack (RDS) for the addition of methanol to 2-butyne reaction assisted by an explicit TCMA solvent molecule interacting with methanol in the absence of the anion. Bond lengths are in angstrom.*

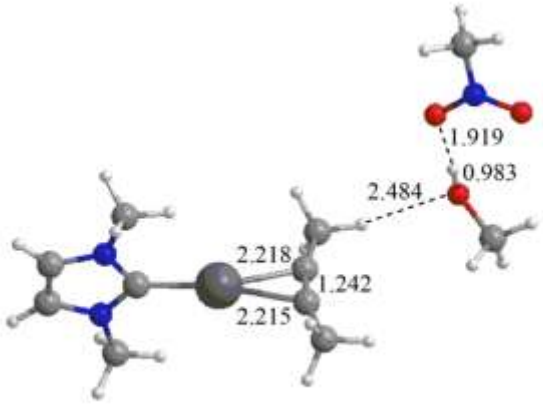

[RC_NM]$^+$

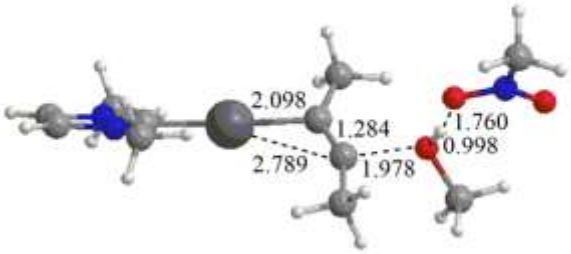

[TS_NM]$^+$

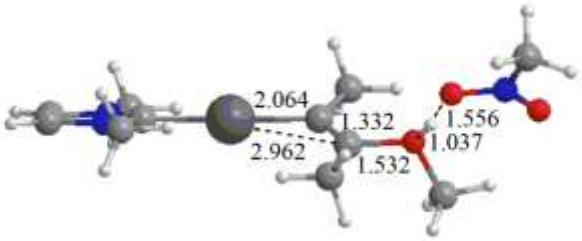

[PC_NM]$^+$

Figure S22: *Reactant complex [RC_NM]$^+$, transition state [TS_NM]$^+$ and product complex [PC_NM]$^+$ in the methanol nucleophilic attack (RDS) for the addition of methanol to 2-butyne reaction assisted by an explicit NM solvent molecule interacting with methanol in the absence of the anion. Bond lengths are in angstrom.*

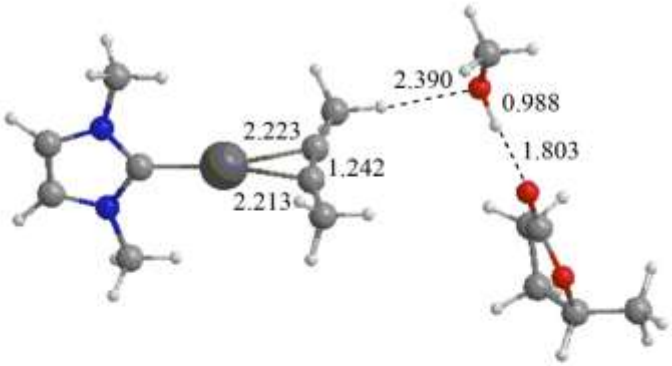

$[RC\_GVL]^+$

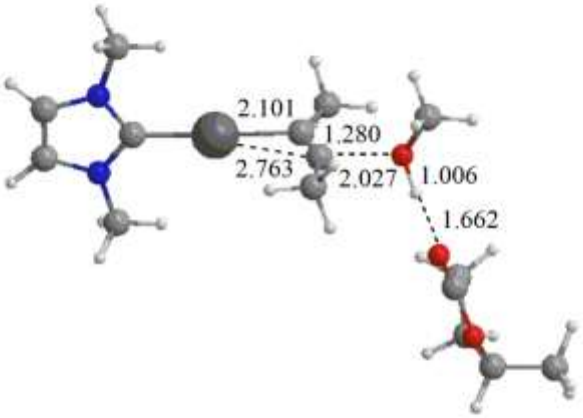

$[TS\_GVL]^+$

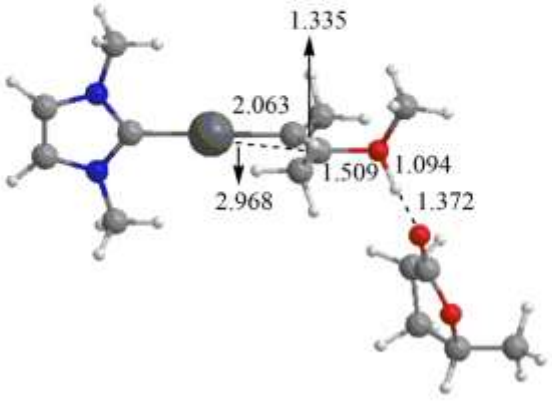

$[PC\_GVL]^+$

Figure S23: *Reactant complex $[RC\_GVL]^+$, transition state $[TS\_GVL]^+$ and product complex $[PC\_GVL]^+$ in the methanol nucleophilic attack (RDS) for the addition of methanol to 2-butyne reaction assisted by an explicit GVL solvent molecule interacting with methanol in the absence of the anion. Bond lengths are in angstrom.*

[1] *La Niece, Susan (senior metallurgist in the British Museum Department of Conservation and Scientific Research) (15 December 2009). Gold. Harvard University Press. p. 10. ISBN 0-674-03590-9. Retrieved 10 April 2012.*

[2] D. A. Daniel, *Anthropological Quarterly*, **1992**, *65*, 187-194.

[3] https://www.gold.org/about-gold/gold-supply. *Retrieved 26 December 2016.*

[4] W.F. Kean and I.R.L. Kean, *Inflammopharmacology*, **2008**, *16*, 112-125.

[5] P.S. Fricker, *Gold Bulletin*, **1996**, *2*, 53-60.

[6] W. A. Herrmann and B. Cornils, *Angew. Chem.*, **1997**, *109*, 1074; W. A. Herrmann, B. Cornils, *Angew. Chem., Int. Ed.*, **1997**, *36*, 1048.

[7] http://www.infomine.com/investment/metal-prices/.

[8] G.C. Bond and P.A. Sermon, *Gold Bull.*, **1973**, *6*, 102.

[9] G.C. Bond and P.A. Sermon, *Chem. Comm.*, **1973**, 444.

[10] G. J. Hutchings, *Chem. Commun.*, **2008**, 1148-1164; K. German, *Chemik.*, **2006**, *59*, 242.

[11] a) M. J. S. Dewar, *Bull. Soc. Chim. Fr.*, **1951**, *18*, C71-C79; b) J. Chatt, L. A. Duncanson, *J. Chem. Soc.*, **1953**, 2939–2947.

[12] A. S. K. Hashmi and F. D. Toste, *Modern Gold Catalyzed Synthesis*, **2012**, WILEY-VCH Verlag GmbH & Co. KGaA, Weinheim, Germany.

[13] R. G. Pearson, *J. Am. Chem. Soc.*,**1963**, *22*, 3533.

[14] R. D. Crabtree, *The Organometallic Chemistry of the Transition Metals, 6th Edition*, **2014**, Whiley, Weinheim, Germany.

[15] F. Scherbaum, A. Grohmann, B. Huber, C. Krüger and H. Schmidbaur, *Angew. Chem. Int. Ed. Engl.*, **1988**, *27*, 1544-1546.

[16] A.S.K. Hashmi, *Chem. Rev.*, **2007**, *107*, 3180.

[17] A.Y. Fukuda and K. Utimoto, *J. Org. Chem.*, **1991**, *56*, 3729–3731;

[18] J.H. Teles, S. Brode and M. Chabanas, *Angew. Chem., Int. Ed.*, **1998**, *37*, 1415.

[19] E. Mizushima, K. Sato, T. Hayashi and M. Tanaka, *Angew. Chem., Int. Ed.*, **2002**, *41*, 4563.

[20] P. Roembke, H. Schmidbaur, S. Cronje and H.J. Raubenheimer, *Mol. Catal. A: Chem.*, **2004**, *212*, 35.

[21] W. Wang, G.B. Hammond and B. Xu, *J. Am. Chem. Soc.*, **2012**, *134*, 5697−5705.

[22] S.K. Schneider, W.A. Herrmann and E.Z. Herdtweck, *Anorg. Allg. Chem.*, **2003**, *629*, 2363.

[23] N. Marion, R.S. Ramon and S.P. Nolan, *J. Am. Chem. Soc.*, **2009**, *131*, 448–449.

[24] H. C. Shen, *Tetrahedron*, **2008**, *64*, 3885-3903.

[25] Y. Fukuda, K. Utimoto and H. Nozaki, *Heterocycles*. **1987**, *25*, 297-300.

[26] E. Mizushima, T. Hayashi and M. Tanaka, *Org. Lett.*, **2003**, *5*, 3349.

[27] V. Lavallo, G.D. Frey, S. Kousar, B. Donnadieu, M. Soleilhavoup and G. Bertrand, *Angew. Chem., Int. Ed.*, **2008**, *47*, 5224–5228.

[28] For some selected examples, see: a) C. Nevado and A.M. Echavarren, *Chem. Eur. J.*, **2005**, *11*, 3155−3164; b) D. Weber and M.R. Gagné, *Org. Lett.*, **2009**, *11*, 4962−4965.

[29] D. Wang, R. Cai, S. Sharma, J. Jirak, S.K. Thummanapelli, N.G. Akhmedov, H. Zhang, X. Liu, J.L. Petersen and X. Shi, *J. Am. Chem. Soc.*, **2012**, *21*, 9012-9019.

[30] C. Brouwer and C. He, *Angew. Chem., Int. Ed.*, **2006**, *45*, 1744−1747.

[31] G. Kovács, G. Ujaque and A. Lledós, *J. Am. Chem. Soc.*, **2008**, *130*, 853−864.

[32] (a) A. Zhdanko, M. Strçbele and M.E. Maier, *Chem. Eur. J.*, **2012**, *18*, 14732−14474; (b) A. Zhdanko and M.E. Maier, *ACS Catal.*, **2014**, *4*, 2770−2775.

[33] A. Homs, I. Escofet and A.M. Echavarren, *Org. Lett.*, **2013**, *15*, 5782−5785.

[34] R.L. LaLonde, B.D. Sherry, E.J. Kang, and F.D. Toste, *J. Am. Chem. Soc.*, **2007**, *129*, 2452.

[35] Y. Xia, A.S. Dudnik, V. Gevorgyan and Y. Li, *J. Am. Chem. Soc.*, **2008**, *130*, 6940**–**6941.

[36] L. Biasiolo, M. Trinchillo, P. Belanzoni, L. Belpassi, V. Busico, G. Ciancaleoni, A. D'Amora, A. Macchioni, F. Tarantelli and D. Zuccaccia, *Chem. Eur. J.*, **2014**, *20*, 14594−14598.

[37] a) L. Biasiolo, A. Del Zotto and D. Zuccaccia, *Organometallics*, **2015**, *34*, 1759. b) L. D'Amore, G. Ciancaleoni, L. Belpassi, F. Tarantelli, D. Zuccaccia and P. Belanzoni, *Organometallics*, **2017**, *36*, 2364.

[38] M. Jia and M. Bandini, *ACS Catal.*, **2015**, *5*, 1638−1652 and reference cited therein.

[39] J. Schieβl, J. Schulmeister, A. Doppiu, E. Wörner, M. Rudolph, R. Karch and A.S.K. Hashmi, *Adv. Synth. Catal.* , **2018**, *360*, 2493-2502.

[40] B.M. Trost, *Science*, **254**, 1471-1477.

[41] a) R.A. Sheldon, I. Arends and U. Hanefeld, *Green chemistry and catalysis*, **2007**, Wiley-VCH Verlag GmbH, Weinheim, 1-47; b) P.T. Anastas and M.M. Kirchoff, *Account of Chemical Research*, **2002**, *35*, 686-694.

[42] P.T. Anastas and J.C. Warner, *Green Chemistry: Theory and Practice*, Oxford University Press: New York, **1998**, 30.

[43] a) D.J.C. Constable, A.D. Curzons and V.L. Cunningham, *Green Chem.*, **2002**, *4*, 521−527; b) M.S. Singh and S. Chowdhury, *RSC Adv.*, **2012**, *2*, 4547−4592; c) M.B. Gawande, V.D. Bonifacio, R. Luque, P.S. Branco and R.S. Varma, *ChemSusChem*, **2013**, *7*, 24−44.

[44] R.A. Sheldon, *Chemistry and industry*, **1992**, London (*23*), 903-906

[45] T. Hhudlicky, D.A. Frey, L. Koroniak, C.D. Claeboe and L.E. Brammer, *Green Chemistry*, **1999**, *1*, 57-59.

[46] J.O. Metzger, *Angew. Chem. Int. Ed.*, **1998**, *37*, 2975**–**2978.

[47] P.T. Anastas, *Handbook of Green Chemistry*; WILEY-VCH Verlag GmbH & Co. KGaA, Weinheim, Germany, **2010**. Vol. *5*.

[48] Acetaldehyde. In *Ullmann's Encyclopedia of Industrial Chemistry*, 7th ed.; Wiley-VCH: Weinheim, **2006**.

[49] T. W. Clarkson and L. Magos*, Crit. Rev. Toxicol.*, **2006**, *36*, 609-662.

[50] a) *Report of the Social Scientific Study Group on Minamata Disease, In the Hope of Avoiding Repetition of a Tragedy of Minamata Disease*, National Institute for Minamata Disease; b) *Minamata Disease The History and Measure*s - Chapter 2, Ministry of the Environment Government of Japan.

[51] a) D. Garayalde and C. Nevado, *ACS Catal.*, **2012**, *2*, 1462−1479; b) C. Obradors and A.M. Echavarren, *Chem. Commun.*, **2014**, *50*, 16−28; c) Y.M. Wang, A.D. Lackner and F.D. Toste, *Acc. Chem. Res.*, **2014**, *47*, 889−901; d) A. S. K. Hashmi, *Acc. Chem. Res.*, **2014**, *47*, 864; e) H.S. Yeom and S. Shin, *Acc. Chem. Res.*, **2014**, *47*, 966; f) L. Zhang, *Acc. Chem. Res.*, **2014**, *47*, 877; g) D. Qian, Zhang, *J. Chem. Soc. Rev.*, **2015**, *44*, 677−698; h) R. Dorel and A.M. Echavarren, *Chem. Rev.*, **2015**, *115*, 9028−9072; i) D. Pflästerer, A.S.K. Hashmi, *Chem. Soc. Rev.*, **2016**, *45*, 1331-1367.

[52] a) Y. Xi, D. Wang, X. Ye, N.G. Akhmedov, J.L. Petersen and X. Shi, *Org. Lett.*, **2013**, *16*, 306−309; b) M. Blanco Jaimes, C.R.N. Böhling, J.M. Serrano-Becerra and A.S.K. Hashmi, *Angew. Chem., Int. Ed.*, **2013**, *52*, 7963−7966; c) D. Canseco-Gonzalez, A. Petronilho, H. Mueller-Bunz, K. Ohmatsu, T. Ooi and M. Albrecht, *J. Am. Chem. Soc.*, **2013**, *135*, 13193−13203; d) A. Gómez-Suárez, Y. Oonishi, S. Meiries and S.P. Nolan, *Organometallics*, **2013**, *32*, 1106−1111; e) M.C. Blanco Jaimes, F. Rominger, M.M. Pereira, R.M.B. Carrilho, S.A.C. Carabineiro and A.S.K. Hashmi, *Chem. Commun.*, **2014**, *50*, 4937−4940; f) R.M.P. Veenboer, S. Dupuy and S.P. Nolan, *ACS Catal.*, **2015**, *5*, 1330−1334; g) X.Z. Shu, S.C. Nguyen, Y. He, F. Oba, Q. Zhang, C. Canlas, G.A. Somorjai, A.P. Alivisatos and F.D. Toste, *J. Am. Chem. Soc.*, **2015**, *137*, 7083–7086; h) C. Vriamont, M. Devillers, O. Riant and S. Hermans, *Chem. Commun.*, **2013**, *49*, 10504; i) S. Dupuy, D. Gasperini and S.P. Nolan, *ACS Catal.*, **2015**, *5*, 6918–6921; l) R.E. Ebule, D. Malhotra, G.B. Hammond and B. Xu, *Adv. Synth. Catal.*, **2016**, *358*, 1478 –1481.

[53] a) L. Hintermann and A. Labonne, *Synthesis*, **2007**, 1121−1150; b) F. Alonso, I.P. Beletskaya and M. Yus, *Chem. Rev.*, **2004**, *104*, 3079−3160.

[54] Schrohe, *Chem. Ber.*, **1875**, *8*, 367.

[55] a) A.Y. Fukuda and K. Utimoto, *J. Org. Chem.*, **1991**, *56*, 3729–3731; b) Y. Fukuda and K. Utimoto, *Bull. Chem. Soc. Jpn.*, **1991**, *64*, 2013–2015.

[56] J.W. Hartman, W.C. Hiscox and P.W. Jennings, *J. Org. Chem.*, **1993**, *58*, 7613-7614.

[57] a) H.T. He, C.R. Qi, X.H. Hu, Y.Q. Guan and H.F. Jiang, *Green Chem.*, **2014**, *16*, 3729–3733; b) M.A. Mann and A. Wagner, *Chem. Commun.*, **2012**, *48*, 434–436.

[58] a) F.X. Zhu, W. Wang W. and H.X. Li, *J. Am. Chem. Soc.*, **2011**, *133*, 11632–11640; b) F. Chevallier and B. Breit, *Angew. Chem. Int. Ed.*, **2006**, *45*, 1599–1602.

[59] Hayashi and Tanaka reported low catalyst loadings (100 ppm) and low amounts of acid promoter (4 mol %) only for the hydration of 1-octyne. For all other alkynes, catalyst loadings typically range from 0.2 to 1 mol % and acid loadings from 25 to 50 mol %.

[60] a) N.A. Romero, B.M. Klepser and C.E. Anderson,*Org. Lett.*, **2012**, *14*, 874–877; b) G.A. Fernandez, A.S. Picco, M.R. Ceolin, A.B. Chopa and G.F. Silbestri, *Organometallics*, **2013**, *32*, 6315–6323; c) X.Y. Xu, S.H. Kim, X. Zhang, A.K. Das, H. Hirao and S.H. Hong, *Organometallics*, **2013**, *32*, 164–171; d) C.E. Czegeni, G. Papp, A.G.; Katho and F. Joo, *J. Mol. Catal. A: Chem.*, **2011**, *340*, 1–8; e) A. Almassy, C.E. Nagy, A.C. Benyei and F. Joo, *Organometallics*, **2010**, *29*, 2484–2490.

[61] Y. Xu, X. Hu, J.J. Shao, G. Yang, Y. Wu and Z. Zhanga, *Green Chem.*, **2015**, *17*, 532-537.

[62] G.A. Carriedo, S. Lopez, S. Suarez, D. Presa-Soto and A. Presa-Soto, *Eur. J. Inorg. Chem.*, **2011**, *9*, 1442–1447.

[63] W. Wang, A. Zheng, P. Zhao, C. Xia and F. Li, *ACS Catal.*, **2014**, *4*, 321-327.

[64] G. Mazzone, N. Russo N. and E. Sicilia, *J. Chem. Theory Comput.*, **2010**, *6*, 2782-2789.

[65] C.M. Krauter, A.S.K. Hashmi and M. Pernpointner, *ChemCatChem*, **2010**, *2*, 1226-1230.

[66] J. Cordón, G. Jiménez-Osés, J.M. López-de-Luzuriaga, M. Monge, M.E. Olmos and D. Pascual, *Organometallics*, **2014**, *33*, 3823-3830.

[67] a) D. Zuccaccia, L. Belpassi, F. Tarantelli and A. Macchioni, *Eur. J. Inorg. Chem.*, **2013**, *24*, 4121−4135 and reference cited therein; b) M. Jia and M. Bandini, *ACS Catal.*, **2015**, *5*, 1638−1652 and reference cited therein.

[68] a) L. Biasiolo, G. Ciancaleoni, L. Belpassi, G. Bistoni, A. Macchioni, F. Tarantelli and D. Zuccaccia, *Catal. Sci. Technol.*, **2015**, *5*, 1558−1567; b) L. Biasiolo, M. Trinchillo, P. Belanzoni, L. Belpassi, V. Busico, G. Ciancaleoni, A. D'Amora, A.

Macchioni, F. Tarantelli and D. Zuccaccia, *Chem. Eur. J.*, **2014**, *20*, 14594−14598; c) M. Trinchillo, P. Belanzoni, L. Belpassi, L. Biasiolo, V. Busico, A. D'Amora, L. D'Amore, A. Del Zotto, F. Tarantelli, A. Tuzi and D. Zuccaccia, *Organometallics*, **2016**, *35*, 641−654.

[69] G. Ciancaleoni, L. Belpassi, D. Zuccaccia, F. Tarantelli and P. Belanzoni, *ACS Catal.*, **2015**, *5*, 803−814.

[70] a) W. Wang, M. Kumar, G.B. Hammond and B. Xu, *Org. Lett.*, **2014**, *16*, 636−639; b) A. Zhdanko and M.M. Maier, *Chem.Eur. J.*, **2014**, *20*, 1918−1930.

[71] a) F. Kerton, *Alternative Solvents for Green Chemistry Green Chemistry Series*, Royal Society of Chemistry, Cambrige, 2009. b) C. J. Clarke, W-C. Tu, O. Levers, A. Bröhl, and J. P. Hallett, *Chem. Rev.,* **2018**, *118*, 747, and references therein. c) C. M. Alder, J. D. Hayler, R. K. Henderson, A. M. Redman, L. Shukla, L. E. Shuster, and H. F. Sneddon, *Green Chem*., **2016**, *18*, 3879. d) D. Prat, A. Wells, J. Hayler, H. Sneddon, C. R. McElroy, S. Abou-Shehada and P. J. Dunn, *Green Chem.,* **2016**, *18*, 288−296.

[72] a) Y. Gu and F. Jèròme, *Chem. Soc. Rev.*, 2013, **42**, 9550. b) S. Santoro, F. Ferlin, L. Luciani, L. Ackermann and L. Vaccaro, *Green Chem.*, **2017**, *19*, 1601.

[73] P.T. Anastas, *Handbook of Green Chemistry*; WILEY-VCH Verlag GmbH & Co. KGaA, Weinheim, Germany, **2010**. Vol. *5*.

[74] a) X. Tian, F. Yang, D. Rasina, M. Bauer, S. Warratz, F. Ferlin, L. Vaccaro and L. Ackermann, *Chem. Commun.*, **2016**, *52*, 9777. b) D. Rasina, A. Kahler-Quesada, S. Ziarelli, S. Warratz, H. Cao, S. Santoro, L. Ackermann and L. Vaccaro, *Green Chem.*, **2016**, *18*, 5025. c) G. Strappaveccia, L. Luciani, E. Bartollini, A. Marrocchi, F. Pizzo and L. Vaccaro, *Green Chem.*, **2015**, *17*, 1071.

[75] a) A. E. Dìaz-Álvarez, J. Francos, B. Lastra-Barreira, P. Crochet and V. Cadierno, *Chem. Commun.*, **2011**, *47*, 6208. b) A. Azua, J. A. Mata, E. Peris, F. Lamaty, J. Martinez and E. Colacino, *Organometallics*, **2012**, *31*, 3911. c) P. K. Khatri and S. L. Jain, *Tetrahedron Lett.*, **2013**, *54*, 2740.

[76] J.-P. Wan, C. Wang, R. Zhou and Y. Liu, *RSC Adv.*, **2012**, *2*, 8789.

[77] a) R. T. Mathers, K. C. McMahon, K. Domodaran, C. J. Retarides, D. J. Kelley, *Macromolecules*, **2006**, *39*, 8982. b) V. Alzari, D. Nuvoli, D. Sanna, A. Ruiu, A. Mariani, *J. Polym. Sci., Part A-1: Polym. Chem.*, **2016**, *54*, 63.

[78] a) M.A. Dubé and S. Salehpour, in *Green Polymerization Methods. Renewable Starting Materials, Catalysis and Waste Reduction*, ed. R.T. Mathers and M. Meier, Wiley-VCH, Weinheim, **2011**, *3*, 143. b) S. Salehpour and M.A. Dubé, *Green Chem.*, **2008**, *10*, 321.

[79] P. T. Anastas, *Handbook of Green Chemistry*, WILEY-VCH Verlag GmbH & Co. KGaA, Weinheim, 2010. Volume 4.

[80] a) I. T. Horwáth and J. Rábai, *Science*, **1994**, *266*, 72. b) K. E. Myers and K. J. Kumar, *Am. Chem. Soc.*, **2000**, *122*, 12025.

[81] a) J. Chen, S. K. Spear, J. G. Huddleston and R. D. Rogers, *Green Chem.*, **2005**, *7*, 64. b) E. Colacinoa, J. Martineza, F. Lamatya, L. S. Patrikeevaa, L. L. Khemchyan, V. P. Ananikov and I. P. Beletskaya, *Coord. Chem. Rev.*, **2012**, *256*, 2893. c) M. J. D. Pires, S. I. Purificação, A. S. Santos and M. M. B. Marques, *Synthesis*, **2017**, *49***,** 2337.

[82] a) Q. Zhang, K. De Oliveira Vigier, S. Royer and F. Jèròme, *Chem. Soc. Rev.*, **2012**, *41*, 7108. b) A. Paiva, R. Craveiro, I. Aroso, M. Martins, R. L. Reis and A. R. C. Duarte, *ACS Sustainable Chem. Eng.*, **2014**, *2*, 1063. c) E. L. Smith, A. P. Abbott and K. S. Ryder, *Chem. Rev*., **2014**, *114*, 11060. d) D. A. Alonso, A. Baeza, R. Chinchilla, G. Guillena, I. M. Pastor and D. J. Ramón, *Eur. J. Org. Chem.*, **2016**, 612 e) P. Liu, J. W. Hao, L. P. Mo and Z. H. Zhang, *RSC Adv.*, **2015**, *5*, 48675.

[83] P. T. Anastas, P. T. *Handbook of Green Chemistry*, WILEY-VCH Verlag GmbH & Co. KGaA, Weinheim, **2010**. Volume 1.

[84] C. Vidal, L. Merz and J. García-Álvarez, *Green Chem.*, **2015**, *17*, 3870.

[85] M. J. Rodrìguez-Álvarez, C. Vidal, S. Schumacher,J. Borge and J. Garcìa-Álvarez, *Chem. Eur. J.*, **2017**, *23*, 3425.

[86] H. Jiang and J. Zhao, *J. Chem. Res.*, **2015**, *39*, 654.

[87] D. Gasperini, A. Collado, A.; Goméz-Suárez, D.B. Cordes, A.M.Z. Slawin and S.P. Nolan, *Chem. Eur. J.*, **2015**, *21*, 5403-5412.

[88] M. Makosza, *Pure Appl. Chem.*, **2000**, *72*, 1399–1403.

[89] A.C. Templeton, W.P. Wuelfing and R.W. Murray, *Acc. Chem. Res.*, **2000**, *33*, 27-36.

[90] It has not been possible to increase the catalyst loading more than 0.2 mol% due to partial precipitation of the catalyst, while the catalysis conducted with 0.5 mol% of NHC-Au-OTf shows no conversion to 3-hexanone.

[91] M. Gòmez-Gallego and M.A. Sierra, *Chem. Rev.*, **2011**, 111, 4857-4963.

[92] In order to better compare the KIE catalytic results entries 1 and 3 are reported again from entry 4 in **Table 4** and entry 3 in **Table 4**, respectively.

[93] S.G. Weber, D. Zahner, F. Rominger and B.F. Straub, *ChemCatChem*, **2013**, *5*, 2330-2335.

[94] J.A. Goodwin, A. Aponick, *Chem. Commun.*, **2015**, *51*, 8730.

[95] Y. Xu, X. Hu, S. Zhang, X. Xi and Y. Wu, *ChemCatChem*, **2016**, *8*, 262 – 267.

[96] S. Attar, W.H. Bearden, N.W. Alcock, E.C. Alyea and J.H. Nelson, *Inorg. Chem.*, **1990**, *29*, 425-433.

[97] a) D. Zuccaccia, L. Belpassi, L. Rocchigiani, F. Tarantelli and A. Macchioni, *Inorg. Chem.*, **2010**, *49*, 3080-3082; b) D. Zuccaccia, L. Belpassi, F. Tarantelli and A. Macchioni, *J. Am. Chem. Soc.*, **2009**, *131*, 3170-3171.

[98] a) J. Cordón, J. López-de-Luzuriaga and M. Monge, *Organometallics*, **2016**, *35*, 732−740; b) M. Kumar, J. Jasinski, G.B. Hammond and B. Xu, *Chem. Eur. J.*, **2014**, *20*, 3113-3119.

[99] a) D. Wang, R. Cai, S. Sharma, J. Jirak, S.K. Thummanapelli, N.G. Akhmedov, H. Zhang, X. Liu, J.L. Petersen and X. Shi, *J. Am. Chem. Soc.*, **2012**, *134*, 9012−9019; b) A. Zhdanko and M.E. Maier, *ACS Catal.*, **2015**, *5*, 5994−6004; c) A. Homs, I. Escofet and A.M. Echavarren, *Org. Lett.*, **2013**, *15*, 5782−5785.

[100] Z. Lu, J. Han, G.B. Hammond and B. Xu, *Org. Lett.*, **2015**, *17*, 4534−4537.

[101] a) M. Preisenberger, A. Schier and H. Schmidbaur, *J. Chem. Soc., Dalton Trans.*, **1999**, 1645-1650.

[102] We studied the JPhos-Au-Cl/AgOTf system (**Table 7**, entry 6) by means of ^{31}P NMR spectra recorded at the end of the reaction (see Experimental part). A main signal at δ 63.9 ppm was observed, indicating that a [JPhos-Au-(3-hexyne)]OTf is prevalently present during the reaction (**ref 126**).

[103] a) A. Leyva and A. Corma, *J. Org. Chem.*, **2009**, *74*, 2067-2074; b) S. Gaillard, J. Bosson, R.S. Ramón, P. Nun, A.M.Z. Slawin and S.P. Nolan, *Chem. Eur. J.*, **2010**, *16*, 13729-13740; c) P. Nun, R.S. Ramón, S. Gaillard, and S.P. Nolan, *J. Organomet. Chem,*, **2011**, *696*, 7-11; d) K.C. Weerasiri, D. Chen, D.I. Wozniak and G.E. Dobereiner, *Adv. Synth. Catal*., **2016**, *258*, 4106-4113; e) A. Collado, S.R. Patrick, D. Gasperini, S. Meiries and S.P. Nolan, *Beilstein J. Org. Chem.*, **2015**, *11*, 1809–1814.

[104] M. Brill, F. Nahra, A. Gjmez-Herrera, C. Zinser, D.B. Cordes, A.M.Z. Slawin and S.P. Nolan, *ChemCatChem*, **2017**, *9*, 117.

[105] M. Gatto, P. Belanzoni, L. Belpassi, L. Biasiolo, A. Del Zotto, F. Tarantelli and D. Zuccaccia, *ACS Catal*., **2016**, *6*, 7363.

[106] P. T. Anastas, *Handbook of Green Chemistry*, WILEY-VCH Verlag GmbH & Co. KGaA, Weinheim, **2010**. Volume 1.

[107] a) F. Kerton, *Alternative Solvents for Green Chemistry Green Chemistry Series*, Royal Society of Chemistry, Cambrige, **2009**. b) C. J. Clarke, W-C. Tu, O. Levers, A. Bröhl, and J. P. Hallett, *Chem. Rev.,* **2018**, *118*, 747, and references therein.

c) C. M. Alder, J. D. Hayler, R. K. Henderson, A. M. Redman, L. Shukla, L. E. Shuster, and H. F. Sneddon, *Green Chem*., **2016**, *18*, 3879. d) D. Prat, A. Wells, J. Hayler, H. Sneddon, C. R. McElroy, S. Abou-Shehada and P. J. Dunn, *Green Chem.,* **2016**, *18*, 288−296.

[108] a) Y. Gu and F. Jèròme, *Chem. Soc. Rev.*, **2013**, *42*, 9550. b) S. Santoro, F. Ferlin, L. Luciani, L. Ackermann and L. Vaccaro, *Green Chem.*, **2017**, *19*, 1601.

[109] P. T. Anastas, *Handbook of Green Chemistry*; WILEY-VCH Verlag GmbH & Co. KGaA, Weinheim, **2010**. Volume 5.

[110] a) X. Tian, F. Yang, D. Rasina, M. Bauer, S. Warratz, F. Ferlin, L. Vaccaro and L. Ackermann, *Chem. Commun.*, **2016**, *52*, 9777. b) D. Rasina, A. Kahler-Quesada, S. Ziarelli, S. Warratz, H. Cao, S. Santoro, L. Ackermann and L. Vaccaro, *Green Chem.*, **2016**, *18*, 5025. c) G. Strappaveccia, L. Luciani, E. Bartollini, A. Marrocchi, F. Pizzo and L. Vaccaro, *Green Chem.*, **2015**, *17*, 1071.

[111] a) A. E. Dìaz-Álvarez, J. Francos, B. Lastra-Barreira, P. Crochet and V. Cadierno, *Chem. Commun.*, **2011**, *47*, 6208. b) A. Azua, J. A. Mata, E. Peris, F. Lamaty, J. Martinez and E. Colacino, *Organometallics*, **2012**, *31*, 3911. c) P. K. Khatri and S. L. Jain, *Tetrahedron Lett.*, **2013**, *54*, 2740.

[112] J.-P. Wan, C. Wang, R. Zhou and Y. Liu, *RSC Adv.*, **2012**, *2*, 8789.

[113] a) R. T. Mathers, K. C. McMahon, K. Domodaran, C. J. Retarides, D. J. Kelley, *Macromolecules*, **2006**, *39*, 8982. b) V. Alzari, D. Nuvoli, D. Sanna, A. Ruiu, A. Mariani, *J. Polym. Sci., Part A-1: Polym. Chem.*, **2016**, *54*, 63

[114] a) M.A. Dubé and S. Salehpour, in *Green Polymerization Methods. Renewable Starting Materials, Catalysis and Waste Reduction*, ed. R.T. Mathers and M. Meier, Wiley-VCH, Weinheim, **2011**, *3*, 143. b) S. Salehpour and M.A. Dubé, *Green Chem.*, **2008**, *10*, 321.

[115] P. T. Anastas, P. T. *Handbook of Green Chemistry*, WILEY-VCH Verlag GmbH & Co. KGaA, Weinheim, **2010**. Volume 4.

[116] a) I. T. Horwáth and J. Rábai, *Science*, **1994**, *266*, 72. b) K. E. Myers and K. J. Kumar, *Am. Chem. Soc.*, **2000**, *122*, 12025.

[117] a) J. Chen, S. K. Spear, J. G. Huddleston and R. D. Rogers, *Green Chem.*, **2005**, ***7***, 64. b) E. Colacinoa, J. Martineza, F. Lamatya, L. S. Patrikeevaa, L. L. Khemchyan, V. P. Ananikov and I. P. Beletskaya, *Coord. Chem. Rev.*, **2012**, *256*, 2893. c) M. J. D. Pires, S. I. Purificação, A. S. Santos and M. M. B. Marques, *Synthesis*, **2017**, *49***,** 2337.

[118] a) Q. Zhang, K. De Oliveira Vigier, S. Royer and F. Jèròme, *Chem. Soc. Rev.*, **2012**, *41*, 7108. b) A. Paiva, R. Craveiro, I. Aroso, M. Martins, R. L. Reis and A. R. C. Duarte, *ACS Sustainable Chem. Eng.*, **2014**, *2*, 1063. c) E. L. Smith, A. P. Abbott and K. S. Ryder, *Chem. Rev*., **2014**, *114*, 11060. d) D. A. Alonso, A. Baeza, R. Chinchilla, G. Guillena, I. M. Pastor and D. J. Ramón, *Eur. J. Org. Chem.*, **2016**, 612 e) P. Liu, J. W. Hao, L. P. Mo and Z. H. Zhang, *RSC Adv.*, **2015**, *5*, 48675.

[119] P. T. Anastas, P. T. *Handbook of Green Chemistry*, WILEY-VCH Verlag GmbH & Co. KGaA, Weinheim, **2010**. Volume *6*.

[120] C. Vidal, L. Merz and J. García-Álvarez, *Green Chem.*, **2015**, *17*, 3870.

[121] M. J. Rodrìguez-Álvarez, C. Vidal, S. Schumacher,J. Borge and J. Garcìa-Álvarez, *Chem. Eur. J.*, **2017**, *23*, 3425.

[122] H. Jiang and J. Zhao, *J. Chem. Res.*, **2015**, *39*, 654.

[123] a) A. A. Maryott and E. R. Smith, *Table of Dielectric costants of pure liquids*, U.S. Government Printing Office, Washington, **1951**. b) I. M. Smallwood, *Handbook of organic solvent properties*, John Wiley & Sons Inc., New York, **1996**. c) C. Wohlfarth, *Landolt-Bornstein: Static dielectric costants of pure liquids and binary liquid mixtures*, Springer-

Verlag Berlin Heidelberg, Germany, **2008**; d) K. D. Rainsford, *Nimesulide - Actions and Uses*, Birkhäuser Basel, Basel, **2006**; e) D. R. Lide, *CRC Handbook of Chemistry and Physics - Internet Version*, Taylor and Francis, Boca Raton, **2006**.

[124] At the beginning of the reaction, two phases are present due to the low miscibility of methanol and solvent, while during the proceeding of the reaction the formation of a single phase is observed owing to the miscibility of the formed acetal.

[125] L. Biasiolo, L. Belpassi, G. Ciancaleoni, A. Macchioni, F. Tarantelli and D. Zuccaccia, *Polyhedron*, **2015**, *92*, 52.

[126] a) G. Ciancaleoni, L. Belpassi, F. Tarantelli, D. Zuccaccia and A. Macchioni, *Dalton Trans.*, **2013**, *42*, 4122. b) D. Zuccaccia, L. Belpassi, L. Rocchigiani, F. Tarantelli and A. Macchioni, *Inorg. Chem.*, **2010**, *49*, 3080. c) N. Salvi, L. Belpassi, D. Zuccaccia, F. Tarantelli and A. Macchioni, *J. Organomet. Chem.*, **2010**, *695*, 2679. d) G. Ciancaleoni, L. Biasiolo, G. Bistoni, A. Macchioni, F. Tarantelli, D. Zuccaccia and L. Belpassi, *Organometallics*, **2013**, *32*, 4444. e) D. Zuccaccia, L. Belpassi, F. Tarantelli and A. Macchioni, *J. Am. Chem. Soc.*, **2009**, *131*, 3170. f) J. A. Akana, K. X. Bhattacharyya, P. Müller and J. P. Sadighi, *J. Am. Chem. Soc.*, **2007**, *129*, 7736. g) S. Flügge, A. Anoop, R. Goddard, W. Thiel and A. Fürstner, A. *Chem. Eur. J.*, **2009**, *15*, 8588. h) T. J. Brown, M. G. Dickens and R. A. Widenhoefer, *J. Am. Chem. Soc.*, **2009**, *131*, 6350. i) T. J. Brown and R. A. Widenhoefer, *J. Organomet. Chem.*, **2011**, *696*, 1216.

[127] We studied the stoichiometric reaction between NHC^{iPr}-Au-(3-hexyne)SbF_6 and DMSO, propionitrile, and GVL in $CDCl_3$. We performed ^1H NMR experiments before and after the addition of the solvent, and the expected variation of the chemical shift of the CH_2 and CH_3 protons of the coordinated 3-hexyne has been always observed, thus indicating that a deco-ordination of the alkyne from the gold fragment does occur when DMSO or propionitrile are added. On the other hand, the addiction of GVL to a solution of NHC-Au-(3-hexyne)SbF_6 in $CDCl_3$ does not change the chemical shift of the CH_2 and CH_3 protons of 3-hexyne, thus indicating that 3-hexyne remains co-ordinated to gold (see the Experimental part).

[128] P. de Frèmont, E. D. Stevens, M. R. Fructos, M. M. Dìaz-Requejo, P.J. Pérez and S. P. Nolan, *Chem. Commun.*, **2006**, *0*, 2045.

[129] A. Pandey, R. Rai, M. Pal and S. Pandey, *Phys.Chem.Chem.Phys.*, **2014**, *16*, 1559.

[130] G. Bistoni, P. Belanzoni, L. Belpassi and F. Tarantelli, *J. Phys. Chem. A*, 2016, **120**, 5239.

[131] a) F. M. Bickelhaupt, N. J. R. van Eikema Hommes, C. Fonseca Guerra and E. J. Baerends, *Organometallics*, **1996**, *15*, 2923. b) C. Fonseca Guerra, J. W. Handgraaf, E. J. Baerends and F. M. Bickelhaupt, *J. Comput. Chem.*, **2004**, *25*, 189.

[132] a) K.K.Y. Kung, V.K.Y. Lo, H.M. Ko, G.L. Li, P.Y. Chan, K.C. Leung, Z. Zhou, M.Z. Wang, C.M. Che and M.K. Wong, *Adv. Synth. Catal.*, **2013**, *355*, 2055-2070; b) J. Cordòn, G. Jiménez-Osés, J.M. Lòpez-de-Luzuriaga, M. Monge, M.E. Olmos and D. Pascual, *Organometallics*, **2014**, *33*, 3823-3830; c) M. Joost, L. Estévez, K. Miqueu, A. Amgoune and D. Bourissou, *Angew. Chem. Int. Ed.*, **2015**, *54*, 5236-5240; d) R. Kumar and C. Nevado, *Angew. Chem. Int. Ed.* **2017**, *56*, 1994-2015; e) A.G. Nair, R.T. McBurney, M.R.D. Gatus, S.C. Binding and B.A. Messerle, *Inorg. Chem.*, **2017**, *56*, 12067-12075.

[133] R.Uson, A. Laguna, M. Laguna, D.A. Briggs, H.H. Murray and J.P. Fackler, *Inorganic Syntheses*, Jhon Wiley & Son, Inc: Hoboken, NJ, **2007**.

[134] T.E. Mueller, J.C. Green, D.M.P. Migos, C.M. McPartlin, C. Whittingham, D.J. Williams and T.M. Woodroffe, *J. Organomet. Chem.*, **1998**, *551*, 313-330.

[135] R. Usòn, A. Laguna, J. Vicente, J. Garcìa, B. Bergarache, *Inorg. Chim. Acta*, **1978**, *29*, 951-956.

[136] A.S. Hashmi, T. Hengst, C. Lothschultz and F. Rominger, *Adv. Synth. Catal.*, **2010**, *352*, 1315–1337.

[137] A.J. Arduengo, K. Roland and R. Schmutzler, *Tetrahedron*, **1999**, *55*, 14523-14532

[138] L. Hintermann, *Beilstein Journal of Organic Chemistry,* **2007**, *3*, No. 22.

[139] A. Collado, A. Gómez-Suárez, A.R. Martin, A.M.Z. Slawin and S.P. Nolan, *Chem. Commun.*, **2013**, *49*, 5541-5543.

[140] D. Gasperini, A. Collado, A. Goméz-Suárez, D.B. Cordes, A.M.Z. Slawin and S.P. Nolan, *Chem. Eur. J.*, **2015**, *21*, 5403-5412.

[141] A. Apulovicova, U. El-Ayaan, K. Shibayama, T. Morita and Y. Fukuda, *Eur. J. Inorg. Cham.*, **2001**, *10*¸2641-2646**.**

[142] K.V. Vasudevan, R.R. Butorac, C.D. Abernethy and A.H. Cowley, *Dalton Trans.*, **2010**, *39*, 7401-7408.

[143] L. Biasiolo, M. Trinchillo, P. Belanzoni, L. Belpassi, V. Busico, G. Ciancaleoni, A. D'amore, A. Macchioni, F. Tarantelli and D. Zuccaccia, *Chem. Eur. J.*, **2014**, *20*, 14594-14598.

[144] Gatto, M.; Belanzoni, P.; Belpassi, L.; Biasiolo, L.; Del Zotto, A.; Tarantelli F.; Zuccaccia, D. *ACS Catal*., **2016**, *6*, 7363.

[145] Ciancaleoni G.; Belpassi L.; Tarantelli F.; Zuccaccia D.; Macchioni A. *Dalton Trans.* **2013**, *42*, 4122-4131

[146] Biasiolo, L.; Del Zotto, A.; Zuccaccia, D. *Organometallics*, **2015**, *34*, 1759–1765

[147] a) Baerends, E. J.; Ellis, D. E.; Ros, P. *Chem. Phys.* **1973**, *2*, 41-51; b) Te Velde, G.; Bickelhaupt, F. M.; Baerends, E. J.; Guerra, C. F.; van Gisbergen, S. J. A. *J. Comput. Chem* **2001**, *22*, 931-967; c) ADF2014.05, SCM, Theoretical Chemistry, Vrije Universiteit, Amsterdam, The Netherlands, 2014, http://www.scm.com.

[148] a) Becke, A. D. *Phys. Rev. A* **1988**, *38*, 3098-3100; b) Perdew, J. P. *Phys. Rev. B*, **1986**, *33*, 8822-8824.

[149] a) van Lenthe, E.; Baerends, E. J.; Snijders, J. G. *J. Chem. Phys.* **1994**, *101*, 9783-9792; b) Van Lenthe, E.; Van Leeuwen, R.; Baerends, E. J. *Int. J. Quantum Chem.* **1996**, *57*, 281-293.

[150] a) A. Klamt and G. J. Schüürmann, *Chem. Soc. Perkin Trans.*¸1993, **2**, 799; b) A. J. Klamt, *Phys. Chem.*, 1995, **99**, 2224; c) A. Klamt and V. J. Jones, *Chem. Phys.*, ***1996***, **105**, 9972.

[151] a) F. Neese, The ORCA program system, *Wiley Interdiscip. Rev.: Comput. Mol. Sci.*, **2012**, *2*, 73-78; https://orcaforum.cec.mpg.de

[152] Grimme, S. *J. Chem. Phys.* **2006**, *124*, 034108.

[153] Ciancaleoni, G.; Rampino, S.; Zuccaccia, D.; Tarantelli, F.; Belanzoni, P.; Belpassi, L. *J. Chem. Theory Comput.* **2014**, *10*, 1021-1034.